POLITECNICO DI TORINO

Corso di Laurea Magistrale

in Ingegneria Meccanica

Tesi di Laurea Magistrale

Simulation and Control Of a Through-The-Road-Parallel Hybrid Electric Vehicle

Relatori

Prof. Alessandro Vigliani

Prof. Enrico Galvagno

Prof. Aldo Sorniotti

Candidato

Francesco Soldano

Matr. s241969

ANNO ACCADEMICO 2018/2019

SOMMARIO

List of figures

List of tables

ABSTRACT

In the last years, the research concerning hybrid electric vehicles (HEV) has been developing greatly because of some dangerous natural phenomena such as global warming, directly linked to vehicles exhaust emissions. The hybrid electric vehicles are characterized by an improved fuel economy thanks to extra degrees of freedom provided by battery energy storage and one or more electric machines which allow running a smaller combustion engine in a higher efficiency region.

The aim of this thesis is to demonstrate the viability both in terms of fuel economy and performance of a powertrain downsizing when coupled with modern electrical traction motors.

In this regard, at the beginning of this research work, the capability of the baseline conventional powertrain, represented by a front-wheel-drive Opel Insignia with a 2.0 l diesel engine, performed numerically. Successively, the electrification of the rear axle via an electric motor has allowed the implementation of through-the-road-parallel (TTRP) hybrid architecture. Different gearshift strategies and an energy management controller have been implemented.

Indeed, to guarantee an additional improvement in terms of fuel economy a well-defined energy management strategy is required, the aim of all those strategies is to find the optimal power-split between the electrical and thermal source and these results can be achieved only through actions that the controller must take at each time instant. For this reason, the interest in energy management strategies has increased and a lot of different controllers have been proposed. However, this work focuses on the Adaptive-Equivalent Consumption minimization strategy (A-ECMS), used to analyse the behaviour of the hybrid vehicle. A-ECMS is characterized by a cost function that must be minimized at each time in order to reduce fuel consumption and it only depends on instantaneous variables. The whole powertrain has been implemented in Amesim while the control strategy in Simulink and the two software have been run in co-simulation.

In this thesis, an upgrade of the strategy mentioned before is proposed, thus together with the A-ECMS another control logic is introduce in order to find online the optimal gear engaged by the transmission, that according to the information from the A-ECMS and the knowledge of the actual gearbox efficiency, can make the

optimal choice for the purpose of obtain the minimum break specific fuel consumption (BSFC).

Different simulation scenarios have been utilised in co-simulation to assess the controller' performance.

Eventually, the results show that the through-the-road-parallel hybrid electric vehicle do manage to reduce total fuel consumption over standard drive cycles with respect to the baseline vehicle. Nevertheless, some issues might be identified regarding the actual vehicle's driveability, especially concerning the high number of gearshifts that occur along a drive mission, which could make the implementation of this controller more difficult on a real vehicle. For that reason, the driver could be subjected to frequent fluctuations. Therefore, the development of a filter to add could be a good prosecution of this work.

1. Introduction

Decreasing fuel consumption and emissions in automobiles has been an active research topic in recent years. For this reason, vehicles with alternative powertrain systems, especially hybrid-electric vehicles (HEVs), have shown significant interest in fuel consumption and emissions. This kind of vehicle provide improved fuel economy due to extra degrees of freedom provided by battery energy storage and one or more electric machines which allow running a smaller combustion engine in a higher efficiency region.

To guarantee an improvement in terms of fuel economy a well-defined energy management strategy is required, the aim of all these strategies is to find the optimal power split between the electrical and thermal source and these results can be achieved only through actions that the controller must take at each time instant.

In recent years the interest in energy management strategies has increased and a lot of different controller has been proposed. This work focuses on Adaptive-Equivalent Consumption minimization strategy (A-ECMS) used to analyse the behaviour of a through-the-road-parallel hybrid vehicle (TTRP-HEV). The A-ECMS is characterized by a cost function that must be minimized at each sample time, which depends only to instantaneous variables. Together with the A-ECMS another control logic is introduce in order to find online the optimal gear engaged by the transmission, that according to the information from the A-ECMS and the knowledge of the actual gearbox efficiency, can make the optimal choice for the purpose of obtain the minimum break specific fuel consumption (BSFC).

The vehicle is modelled in Amesim environment while the control logic is implemented in Matlab/Simulink.

The next chapter, the second one of this work, provides an overview of hybrid electric vehicle architectures and gives some information about the energy management, examining the most important strategies.

In the third chapter a description of vehicle characteristics is provided, highlighting the main features of internal combustion engine, electric motors, gearbox and battery. The fourth chapter focus on the powertrain implemented in Amesim, explaining the most important components of the model and providing some results obtained with the baseline vehicle equipped with a downsized ICE, start-stop strategy, and optimal gearshift map.

The fifth chapter provides a detailed explanation of the energy management strategy adopted to obtain a well-defined power split between the thermal and electric source, focusing especially on the mathematic equations.

In the sixth chapter all results obtained are shown, making a comparison between the baseline vehicle and the hybrid vehicle characterized by a through-the-road-parallel architecture.

Eventually in the final chapter an overview of the results obtained is done with also some considerations concerning the possible future works.

2. Hybrid Vehicles

Nowadays because of the great problem linked to emissions, responsible for the growing environmental concerns, the hybrid electric vehicles are the first fundamental step to follow in order to achieve the main target, concerning the reduction of fuel consumption and pollutant emissions.

The main characteristic of hybrid electric vehicles is to combine the use of the internal combustion engine with an electric machine to optimize the operation of the engine itself. In fact, the powertrain is designed in order to isolate the engine from the vehicle operating conditions, allowing the engine to operate more efficiently. In the hybrid electric vehicles, the engine could be downsized because it has the chance to work to operating points characterized by a higher efficiency, this means that there is a reduction in terms of fuel consumption, although it already can provide the power request. Though the most important feature is the regenerative braking. In vehicle with internal combustion engine only, during a brake phase kinetic energy is loss as heat dissipation; this situation changes in hybrid vehicle because this waste energy could be recovered thanks to electric motor, which has a reverse motion, and stored in a battery. Thus, the battery can release the energy when it needed, and another advantage is linked to the reduction of the wear of the brakes.

In this chapter an overview of all hybrid electric vehicles possible architecture is made in order to focus on advantages and disadvantages of each configuration.

2.1 Powertrain structures

Controlling the energy transfer from sources to the loads with minimum loss of energy is the main issue for HEV design and this depends on the driving cycles. HEVs include more electrical apparatus compared to the conventional vehicles such as advanced energy storage devices and energy converters and powertrain configuration can be divided into four types:

a) Series hybrids
b) Parallel hybrids
c) Series/parallel hybrids
d) Through-the-road-parallel hybrids

2.1.1 Series Hybrid electric vehicle

Series hybrid electric vehicles (SHEV) are made up by internal combustion engine, generator, battery packs, converters and electric motors. In SHEV the internal combustion engine is decoupled by the wheels, so it is not directly able to drive the vehicle, it is connected to a generator, so the only function is to generate the electric energy, stored in the battery, when the battery state of charge drops under a specific threshold.

ICE is turned off when the battery packs feed the system in urban driving and it is turned on when the battery energy is low in country driving. As mentioned in [1] the battery charge or discharge is influenced by the power demand. Since the ICE is decoupled by the speed of the wheel, so it is not influenced

Consequently, the main characteristic of this structure is that engine can operates at its maximum efficiency point because of the engine operating point that is completely decoupled with respect to the velocity of the vehicle, so the fuel efficiency improves, and the carbon emissions is less than the other vehicle configurations. At the same time the fact that only the electric motor can provide the needed traction to the vehicle is the main disadvantage of this configuration because the electric machine must be oversized in order to satisfy the maximum power request, as consequence also battery dimension would be significant if an acceptable range in terms of kilometres would be guarantee.

Series hybrids have a good behaviour in urban drive cycles where there are frequent start and stop events [2].

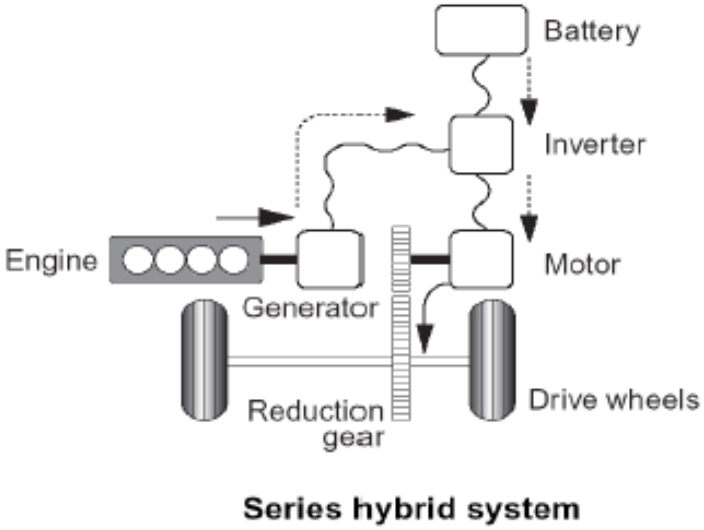

Figure 1: Series hybrid system

2.1.2 Parallel Hybrid electric vehicle

As shown in Fig.2, in this type of architecture, the electrical and mechanical path are connected in parallel.

In this configuration both the electrical and thermal path could be directly link to the wheels, so through a device called planetary gear the power request is split between the two energy sources. This means that in parallel hybrid vehicles both the engine and the electric motor could be downsized, which is an advance compared to series configuration. On the other hand, the internal combustion engine is coupled with the driveline, so along a drive mission its operating point could be not fixed, this is reflected in a lower global drivetrain efficiency respect to the previous configuration.

In the most common strategy ICE is always on and the electric motor is turn on only when the power request by the vehicle is higher than the internal combustion engine one. On the contrary when the road load is not so high ICE can exploit part of its power to recharge the battery, so it is possible to avoid that SOC battery drops to much. However as claimed in [3] through clutch system also the only electric mode is possible.

Eventually parallel structure is more complex than series hybrid vehicle and therefore it is usually used in small vehicle.

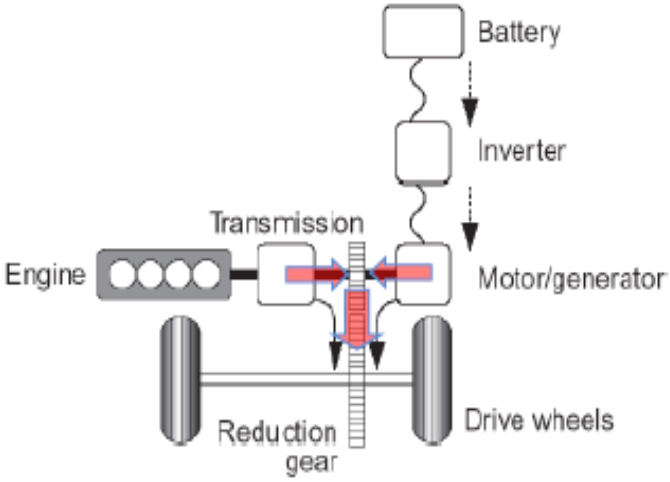

Figure 2: Parallel hybrid system

2.1.3 Combination of parallel and series HEVs

Quickly the previous configurations have been replaced by series-parallel system in order to combine the advantages of both.

This configuration required another electric machine and a planetary gear unit. Especially the last device gives the chance to decouple the engine from vehicle speed, so ICE can work at a fixed operating point that means an improvement in efficiency as in series vehicles. Obviously, the architecture is very complex as also the strategy control, that means the vehicle prize should be high, since also the future maintenance should be very hard.

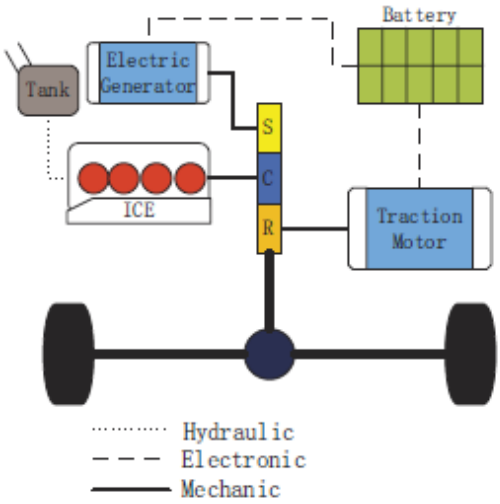

Figure 3: Serie/parallel hybrid system [4]

2.1.4 Through-the-road-parallel hybrid

Through-the-road-parallel architecture is composed of an internal combustion engine mounted on the front axle and an electric motor powering the rear one. These two powertrains are not directly connected to each other, as the parallel configuration is implemented through the road-tyre force interaction [5]. For this reason, both axles will move at the same speed. The heat engine provides power to the front wheels, while the electric motors drive the rear wheels, or absorb power from them during the regenerative braking. This kind of architecture is spreading out because the reconversion of the actual vehicle fleet to hybrid is gaining interest and this is could be a short-term solution.

It is reasonable to expect that the benefits in terms of fuel savings would be lower respect of a native hybrid, as mentioned in [6].

2.2 Levels of hybridization

Level of hybridization is another way to classify electric vehicles, in this respect it could be identify three different categories:

a) Start and Stop
b) Hybrid
c) Mild Hybrid
d) Full Hybrid

2.2.1 Start and Stop

In vehicles with *Start and Stop* architecture the energy provides by the battery is not used to drive the vehicle but only to turn on/off the internal combustion engine. Battery recharge takes place during breaking thanks to vehicle kinetic energy, converted in electric energy thorough the reversible electric machine.

Anyway, *Start and Stop* technology enables a reduction of fuel consumption because it is possible to turn off the engine during vehicle stopped. This is very useful when vehicle stop at traffic lights. A well-defined control logic in these vehicles is very important to avoid frequent on/off.

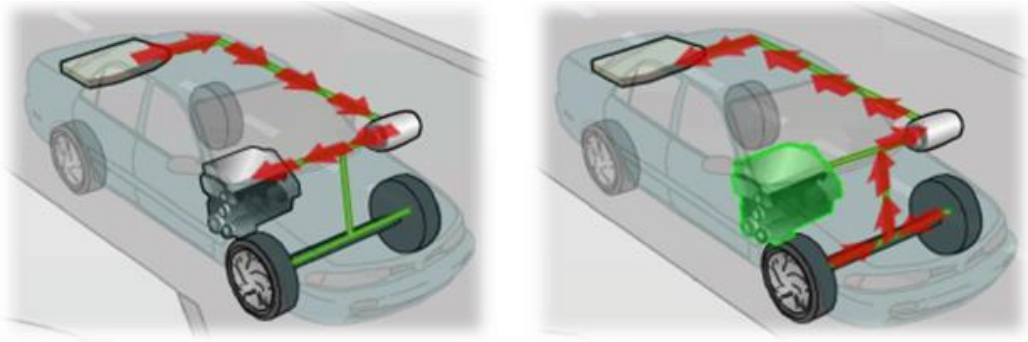

Figure 4: a) Power direction during traction, b) battery recharge during breaking

2.2.2 Hybrid

In this architecture the reversible electric machine is not only used to start the engine but also to give traction during acceleration phases. Since the motor or generator is mechanically bound to the ICE thorough a belt drive, the pure electric mode is not possible.

The internal combustion engine is downsized respect to conventional vehicles.

Electric motor supplies the engine when the power request is high; it works also as generator converting energy from the engine or brakes and stored it in the battery.

Thus, the battery must provide power to vehicle and it is more powerful and much bigger than a traditional one.

During the starting phase the internal combustion engine turn on and meanwhile the electric motor convert part of the mechanical energy in electric energy and it charges the battery. After that during the cruising phase the ICE provides all the power request to the traction and the electric motor only turns on during the acceleration phases when the power request rises. Instead when vehicle stops the battery feeds the auxiliaries while the motors are off.

2.2.3 Mild hybrid

The challenge about the reduction of emissions in 2020 has encouraged the development of other solutions in terms of hybrid vehicles layout. One of this is represent by mild hybrid electric vehicles (MHEV) because of their advantages in terms of costs compared to fully hybrid vehicles. This kind of architecture is characterized by a belt driven motor connected in series to an engine crank-shaft. As claimed in [7], replacing the belt with an alternator the fuel efficiency of the powertrain increased and it is one of the main features of this configuration.

Furthermore, mild hybrid electric vehicles are very similar to traditional ones equipped with start-stop technology, the difference is that the electric motor is bigger and more powerful because it must speed up the engine when vehicle starts. Finally, these vehicles are equipped also with another battery over the traditional auxiliary battery in order to recover the wasted energy during the braking phase.

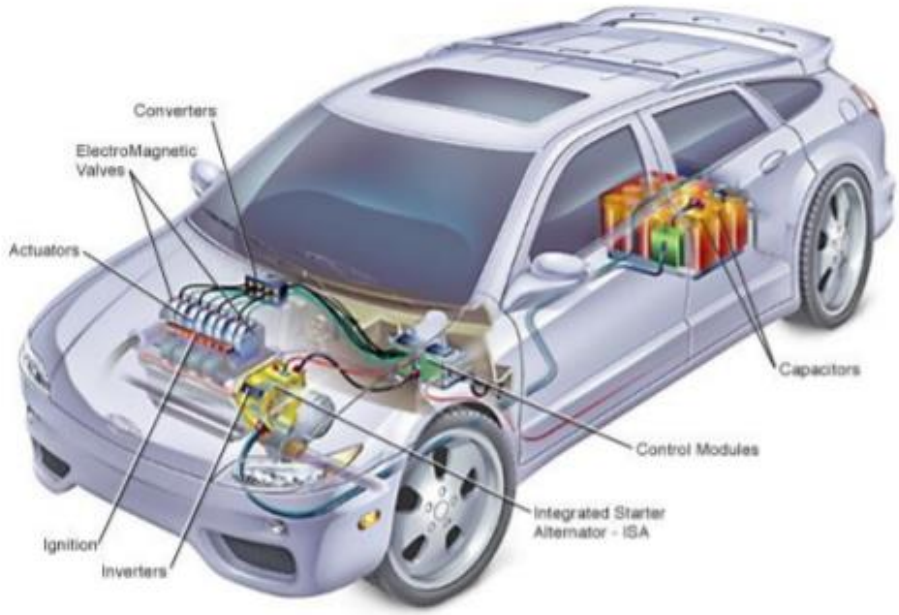

Figure 5: Powertrain in a Mild HEV

2.2.4 Full electric

Full electric vehicles can provide traction to the transmission only thanks to the electric motors when the speed or acceleration are low, so the battery is the only source of energy. At the same time this kind or vehicles can decoupled kinematic conditions of the ICE from the drivetrain so the engine can work with a minimum specific fuel consumption. The full electric mode guarantee so an important improvement in terms of fuel consumption but also in terms of emissions reduction. Obviously in this structure a generator and a power split device are needed.

The generator has the function to convert the ICE energy in electricity and then electric energy could be used to provide power to the vehicle or to recharge the battery.

In the following figure the power flow during the driving mode is represented.

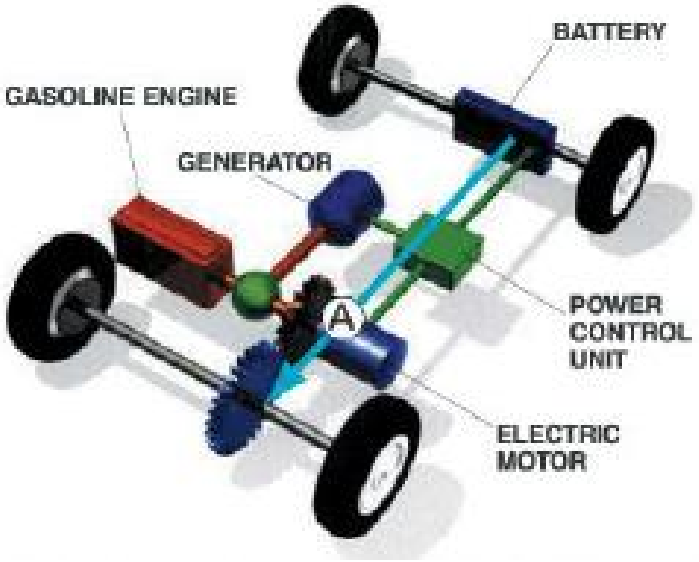

Figure 6: Full electric layout [2].

2.3 Energy management in hybrid electric vehicles

Energy management involve a lot of variables in electric vehicles and in the last years different type of these strategies have been presented by researchers, so a general description is not possible. However, some features are usually common.

The main idea in the heuristic strategies is that the engine must work only when its efficiency is very high, so if this condition does not occur the engine is turned off and the electric path is favourite.

A second principle, that represents also another degree of freedom, is that the battery is characterized by an upper and lower bound. Thus, in real-time the control strategy must focus on these parameters and makes the better decision in order to aim the target, usually represented by the reduction of fuel consumption. The choice taken by the controller is reflected in a well-defined split ratio between the electric and thermal source. In fact, if SOC drops below a certain threshold the regenerative mode is preferred, while when its level is near the upper bound the electric motor is exploited to provide vehicle propulsion instead of the engine.

It is important to underline that when the controller manage to engine works at high efficiency, if the torque request is low the engine can provide more power than the required one, thus part of this energy could use to recharge the battery. In this way when the power demand rise electric motor can support the engine. Obviously in order to develop a controller with an optimal behaviour the complex of the vehicle will increase.

Generally, all control strategies concerning energy management try achieving the same targets, which are:

- Maximum fuel economy
- Minimum emissions
- Minimum system costs
- Good driving performance

Thus, the design of power control strategies for HEVs involves different considerations. Some key considerations are summarized in [8].

2.3.1 Energy management as an optimum of a function

One of the issues that encouraged a lot of researches along the years is the need to turn the energy management problem in a mathematical one. To achieve that the main features of this problem are analysed. Fuel economy and reduction of pollutions are the target that each controller try achieving along a drive mission.
This highlight how the solutions shall be global, in terms that, for example, the fuel consumption must be minimized from the beginning of the driving cycle until the end of it. At the same time the control actions required to get the final goal are local, which means all variables involved in the strategy must change every time in order to match some conditions such as the torque request by the wheel.
Therefore mathematically, the problem can be formulated as show in [2]:

$$J = \varphi(SOC_f) + \int_0^T \dot{m}_f(x,u,t)dt = \varphi(x,u,v,t) \tag{1}$$

Obviously, the problem shown in Eq.1 must consider also the fact that all the components in a powertrain have some limitations regarding their operating points. For example, the battery state of charge has a lower and an upper bound that represents two different scenarios: the battery could be fully charge or fully discharge.

2.3.2 Energy management algorithms

In short, al strategies concerning energy management can be divided as claimed in [9]:

a) Rule based strategies
b) Optimization based strategies

Another classification is based on optimization methods:

a) In this first method all the information regarding the driving cycle such as speed, slope road or number of gearshifts must to be known in advance. Dynamic programming is an example of this methods.
b) The second one is about a local optimization that means during a driving mission the controller knows all the past conditions while the future ones are unknown. In this case an ECMS controller could be use.

2.3.2.1 Optimal control strategy – dynamic programming

The globally optimal solution could be achieved through the dynamic programming strategy as shown in [10], [11], [12].If the system is not subject to external disturbances this strategy guarantee and optimal solution. This is possible only if

the whole driving cycle is known in advance, in this way the controller is sure to make the best decision in order to achieve the main target of the strategy, that could be the reduction of fuel consumption, emissions or the fact that the battery state of charge should be close to a threshold value along the driving cycle. Therefore, a real time implementation on a vehicle is impossible because the drive cycle is not known in advance, even if this kind of problem could be overcome through new GPS technology that provide information about, traffic and slope road an example of this is present in [13].

Another limitation that makes impossible the implementation on a real vehicle is linked to the high computational time due to the relatively large grid density required [14]. The actual electronic indeed cannot dealing with this type of effort yet because the processing time should be so fast that each control actions should be instantly. Any way thanks to optimal results that this strategy can achieve as shown in some works [15]

In any case these limitations underline another major drawback of DP that is its poor flexibility [16].

Nevertheless, dynamic programming remains the strategy that is better to achieve the optimum, so it is usually used as a benchmark compared with other strategies.

2.3.2.2 Sub-optimal control strategy- equivalent consumption minimisation strategy

According to previous section DP is not suitable for real-time implementation due to remarkable computational effort. Therefore, some researches moved on a local optimization problem such as Equivalent Consumption Minimization Strategy (ECMS) in which the cost function, that must be evaluated each sample time depends only by the current variables. Thus, only past conditions regarding the drive mission are needed, while the future information could be unknown. Therefore the most important thing is to find a factor that convert electric power in fuel power [14], so it is possible to evaluate each quantities at the same time and in the same domain.

In this way according to the cost function value determined in real-time the controller makes the best decision in terms of power split between the electric and thermal paths in order to minimize the instantaneous fuel consumption. Thus, this strategy can handle a good charge-sustaining operation along a driving cycle, because based on current information regarding the battery state of charge and

current fuel consumption it can decide to exploit much more the engine or the electric motor. The previous considerations are well summarized in the following equation claimed in [9].

$$\dot{m}_f^{total} = \dot{m}_f + \dot{m}_f^{eq} = \dot{m}_f + \frac{s}{Q_{lhv}} P_{el} \tag{2}$$

As the Eq.2 shows the ECMS calculates the total fuel consumption given by the sum of the real ICE fuel consumption and the equivalent fuel consumption of the electric motors. $\dot{m}_f$ is the consumption of the engine, while $\dot{m}_f^{eq}$ is the equivalent fuel consumption of the electric energy source. Certainly, one of the most interesting things of this strategy is that the only parameter that should be tune is the equivalent factor *s*, which allows the conversion between two different kind of energy. At first the calibration of this parameter was possible only if the driving cycle was known in advance but later some other solution has been proposed. In this respect the solution in [17] is very interesting where the tuning parameter is updated each time instant, so it is possible to adapt it according to the current driving cycle.

3. Vehicle parameters

Scope of this thesis is to demonstrate the viability in terms of fuel economy and performance of a powertrain downsizing when coupled with modern electrical traction motors. As preliminary step the capability of the baseline conventional powertrain (2.0l Turbo Diesel Engine) has been performed numerically; the fuel economy improvement of the smaller combustion engine (1.6l Turbo Diesel Engine) has been proved ad validated with several gearshift patterns and thanks to the introduction of the energy management controller A-ECMS.

The main vehicle characteristics are reported in Table 1 for:

a) The baseline vehicle, the FWD Opel Insignia with a 2.0 l diesel engine
b) The electrified version of the vehicle, the mild-hybrid Opel Insignia with a 1.6 l diesel engine.

The baseline vehicle is equipped with a transversal diesel 2.0 l internal combustion engine (ICE) propelling the front axle, through an 8-speed automatic transmission. The main modifications associated with the electrified layout are:

1) The ICE downsizing, with the adoption of a 1.6L diesel engine;
2) The introduction of a motor generator unit (MGU) in P0 position;
3) The electrification of the rear axle via an electric motor according to a P4 layout, which allows the implementation of through-the road-parallel architecture.

The schematic of the resulting TTRP-HEV is reported in Figure 7.

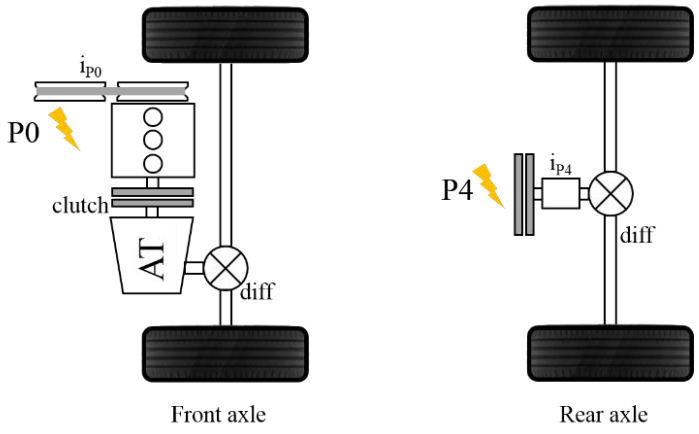

Figure 7: TTRP HEV driveline layout

Table 1: Main vehicle parameters

Parameter	Unit	Opel Insignia 2.0L FWD	Opel Insignia 1.6L AWD Mild-Hybrid
Total vehicle mass	kg	1696	1647
Rolling resistance	-	0.009	0.008
Coefficient of viscous friction (from coastdown tests)	N/(m/s)	4.89	2.74
Windage coefficient (from coastdown tests)	$N/(m/s)^2$	0.30	0.372
Wheel rim diameter	in	17	17
Tyre width	mm	225	215
Tyre height	%	55	55
Wheel radius	m	0.34	0.33

In the following sections the main characteristics of the main components are presented.

3.1 Engine characteristics

The main ICE parameters are reported in Table 2. It is important to underline that for each ICE the efficiency characteristics are provided as brake specific fuel consumption (BSFC) maps in g/kWh, as functions of crankshaft torque and speed, as it stands in Fig. 9.

Table 2: Internal combustion engine parameters

Description	Unit	2.0 l FWD	1.6 l AWD Mild-Hybrid
Total displacement	l	1.956	1.598
Number of cylinders	-	4	4
Idle speed for hot engine	rpm	750	730
Response time for torque decrease without turbo effect	s	0.01	0.01
Response time for torque decrease	s	0.01	0.01
Fuel to CO2 conversion factor	gCO_2/ g fuel	3.15	3.15
Fuel consumption for hot engine at idle speed	g/h	216	136.8
Engine coolant temperature	°C	90	90
Oil sump temperature	°C	100	100

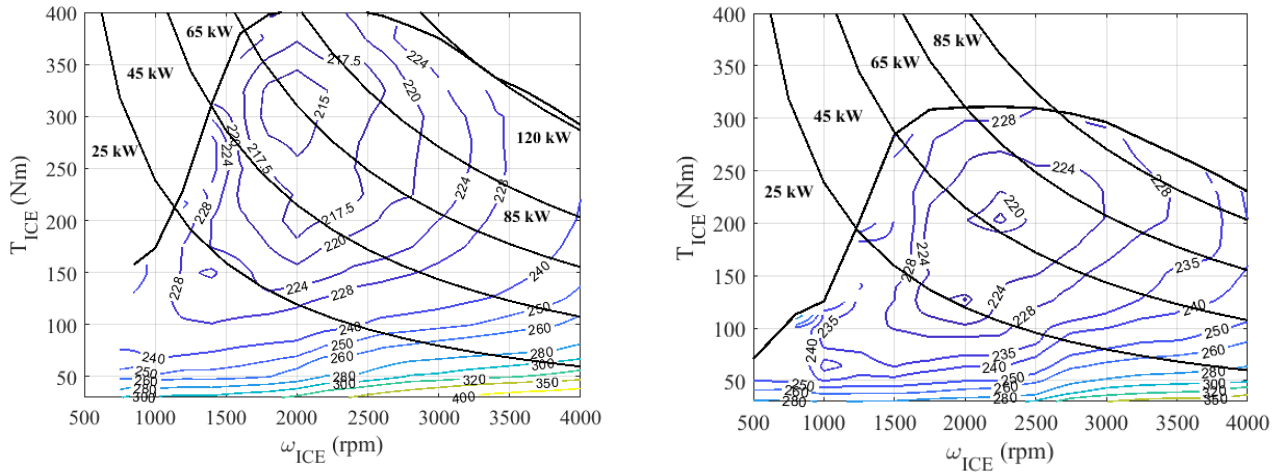

a)2.0 l Diesel ICE

b)1.6 l Diesel ICE

Figure 8: BSFC maps provided for the two considered ICEs

3.2 Transmission

Automatic transmissions (ATs) are used on both the baseline and the electrified vehicle demonstrators. The gearbox performance is expressed in term of maps providing the torque loss for each gear. For instance, for the 8-speed transmission a series of eight 3-dimensional lookup tables were provided for each gear, which output the torque loss T_{loss} as a function of the primary shaft torque and speed. The mechanical efficiency (η_{AT}) associated with each gear can be derived through the following formula:

$$\eta_{AT} = \frac{(T_{PS} i_{AT} - T_{loss})\omega_{SS}}{T_{PS}\omega_{PS}}$$

Where:

- T_{PS} is the primary shaft torque [N/m]
- i_{AT} is the gearbox torque ratio
- ω_{SS} second shaft speed [rad/s]
- ω_{PS} primary shaft speed [rad/s]

Examples of gearbox mechanical efficiencies are shown in Fig. 9 and Fig. 10

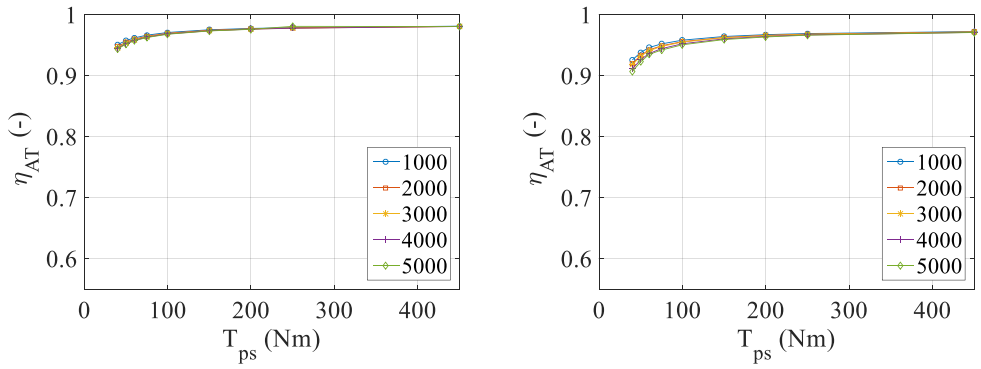

a)

b)

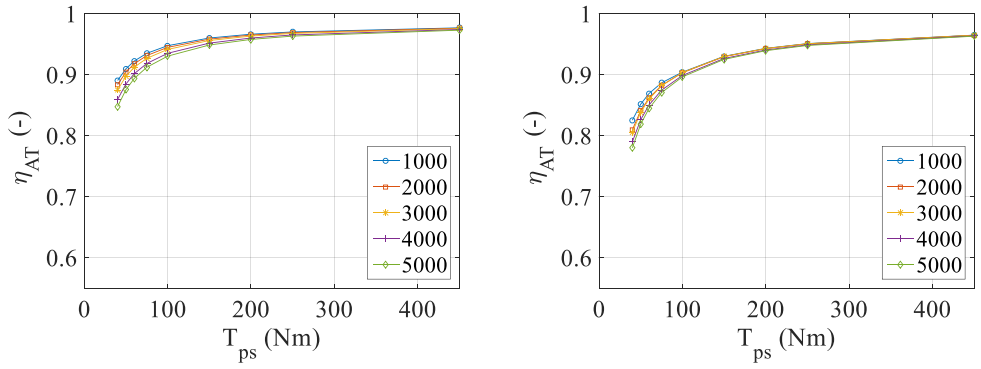

c)

d)

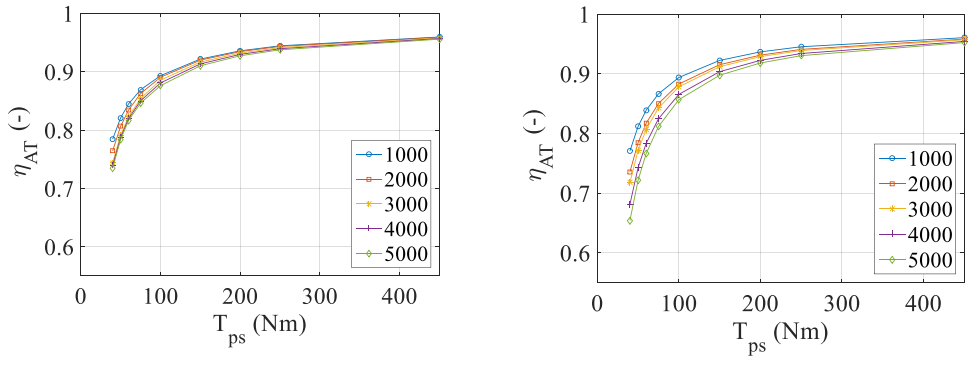

e)

f)

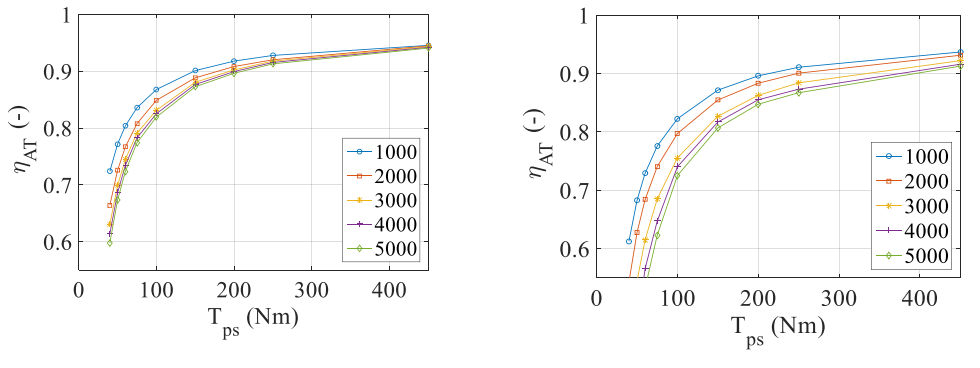

g)

h)

Figure 9: 8–speed gearbox efficiency for different primary shaft speeds and gears: a) 1st gear; b) 2nd gear; c) 3rd gear; d) 4th gear; e) 5th gear; f) 6th gear; g) 7th gear and h) 8th gear

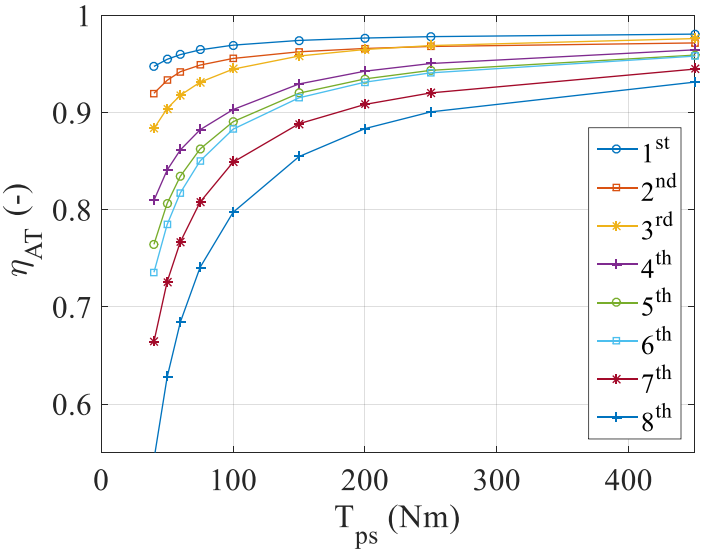

Figure 10: 8-speed gearbox efficiency as a function of the input torque at 2000 rpm input speed

Similarity, for the 6-speed gearbox efficiency maps have been considered. These are reported in Fig. 11 and Fig. 12

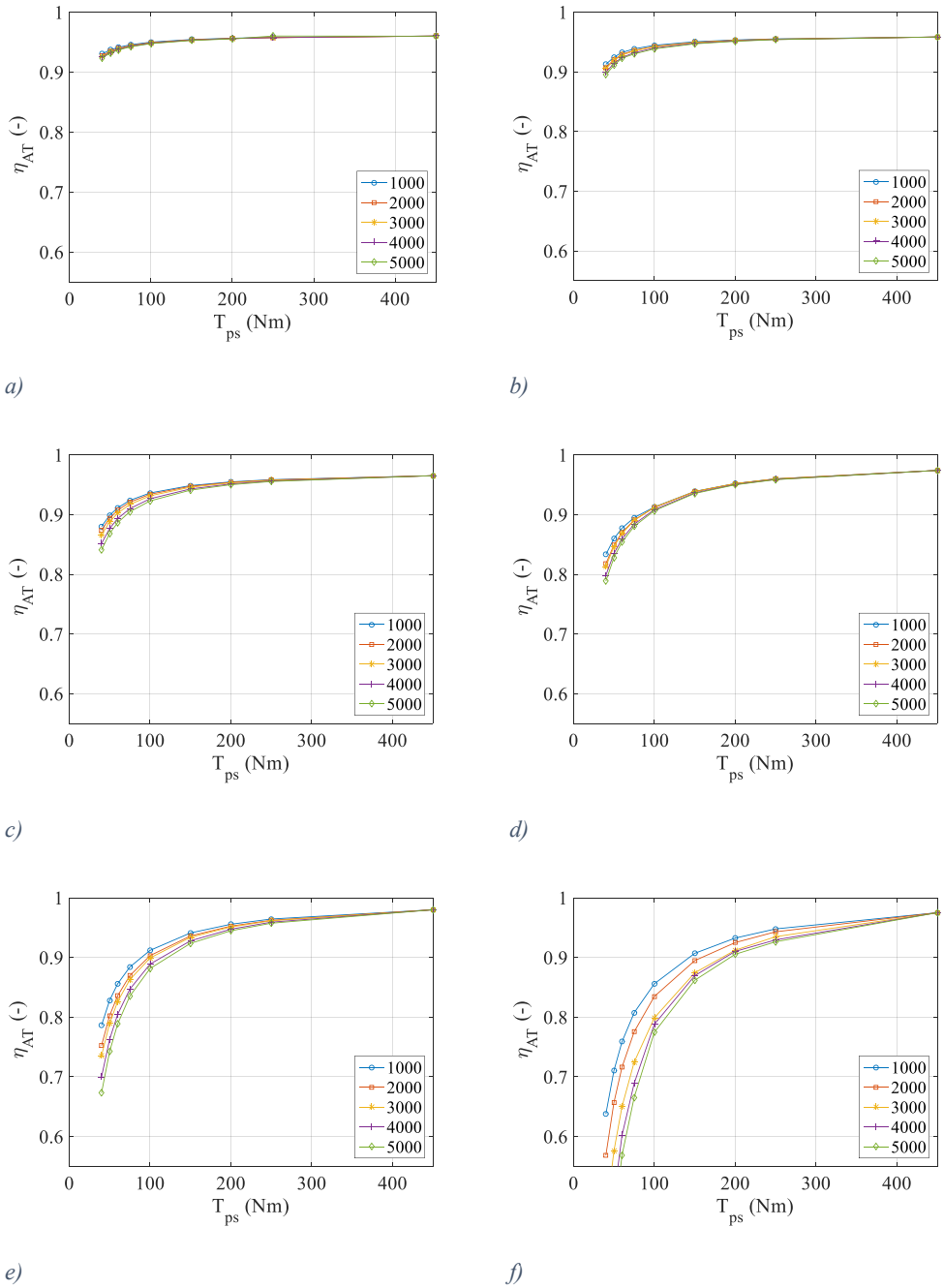

Figure 11: 6-speed gearbox efficiency for different primary shaft speeds and gears: a) 1^{st}gear; b) 2^{nd}gear; c) 3^{rd}gear; d) 4^{th}gear; e) 5^{th}gear; f) 6^{th}gear.

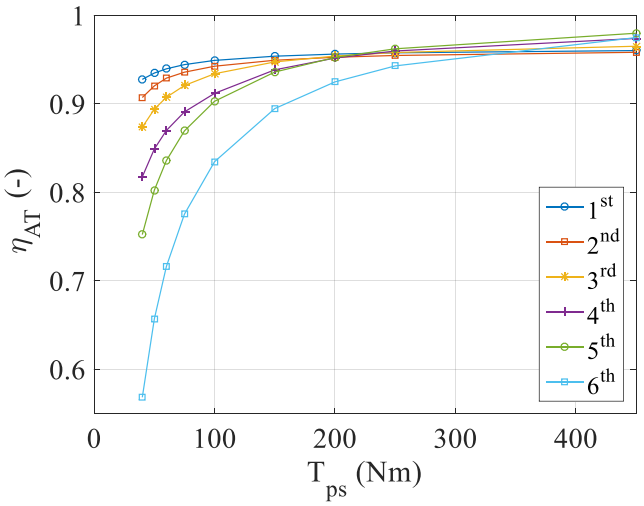

Figure 12: 6-speed gearbox efficiency as a function of the input torque at 2000 rpm input speed

In both configurations the efficiency for low values of primary shaft torque is high in low engaged gears, while it decreases in high speed gear

3.3 Electric motors

The characteristics of the P4 and P0 electric motors for the electrified vehicle demonstrator are reported in Tab.3 and in Tab.4. Based on the data provided in terms of maximum EM power and torque, it is possible to generate the maximum and minimum EM torque characteristics as function of speed (ω_{P4} and ω_{P0}), which are reported in Fig.13. The EM efficiency values were provided as constants.

Table 3: Motor generator unit (MGU) P0 electric motor and installation parameters

Parameter	Unit	Value
Torque time constant	s	0.1
Constant efficiency	-	0.95
Maximum power	W	12000
Maximum torque	Nm	35
Maximum speed	rpm	~12000
Reduction ratio	-	2.7

Table 4: P4 electric motor installation parameters

Parameter	Unit	Value
Torque time constant	s	0.1
Constant efficiency	-	0.94
Maximum power	W	31000
Maximum torque	Nm	134
Maximum speed	rpm	10500
Reduction ratio	-	9.5

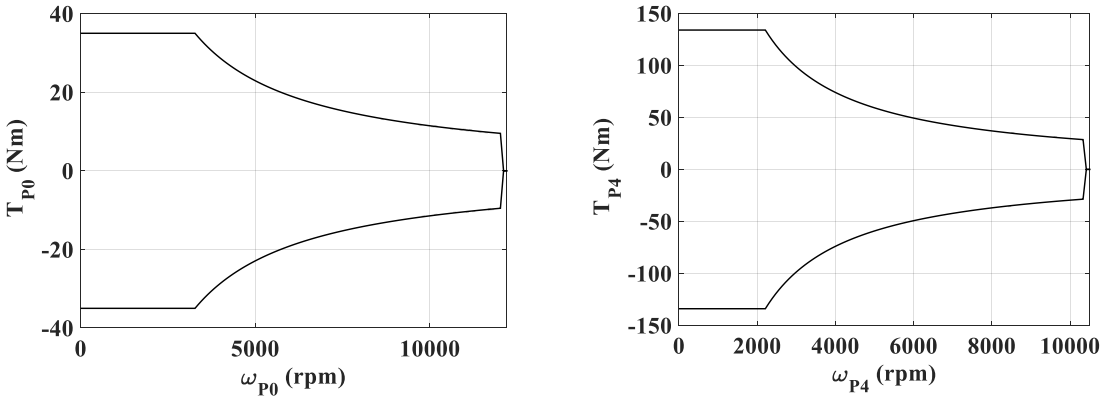

a) P0 electric motor *b) P4 electric motor*

Figure 13: Electric motor torque characteristics

3.4 Battery characteristics

In a hybrid vehicle battery is one of the main components and most common kind of battery pack used are NiMH and Li-Ion which advantages and disadvantage are exposed in [18]

48V battery is used in this vehicle because of its rated power capabilities on the order of 8-16 kW, which are rapidly becoming a new standard in the automotive industry. Indeed, 48V Mild Hybrid Electric Vehicles (MEHV) allow to extend start-stop and regenerative braking functionalities, providing fuel economy benefits of up to 10-15 % in standard passengers vehicles [19].The rapid spread of this technology is explained because of the rise in demand for computing power, control electronics, mechatronics and real-time software that will increase the electrical loading on the vehicles' architecture. Since the word moves towards the complexities of autonomous driving, this power demands will continue to

accelerate and therefore 48V battery is an essential near to mid-term building block for these technologies.

Indeed, unlike a conventional vehicle where the electric machine is a conventional 12V alternator then it able only to provide low negative torque generating electric current, the hybrid version needs a system able to control high negative and high positive torque. For this reason, a bi-directional belt is needed.

In this work an alternative hybrid architecture is proposed compared to powertrain architecture of a conventional MHEV vehicle, that can facilitate high power loads and high currents at low voltage, as shown in the following pictures.

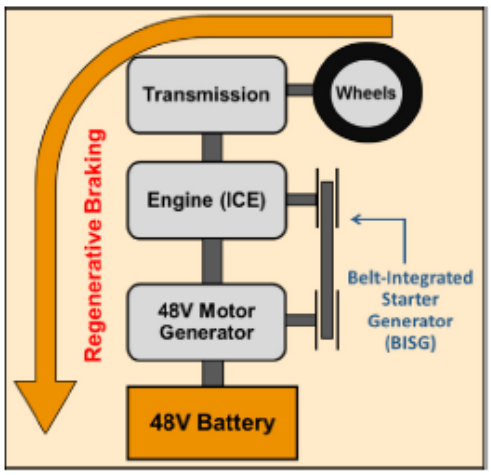

Figure 14: Powertrain architecture of a conventional MHEV vehicle [20]

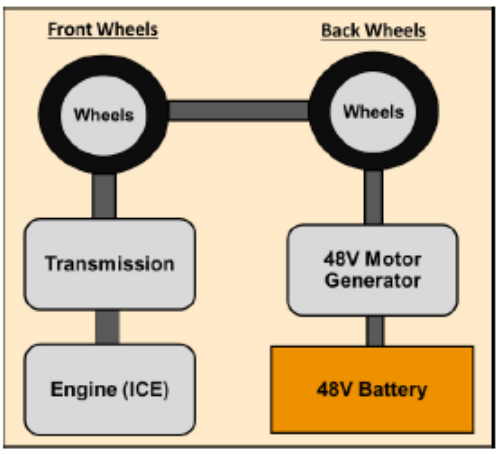

Figure 15:Through the road parallel MEHV vehicle [20]

The 48V battery characteristics used in the vehicle model are reported in the following table.

Table 5: Main parameters of the 48V battery

Parameter	Unit	Value
Temperature influence	-	no
Number of cell in series per battery pack	-	N/A
Number of cells in parallel	-	N/A
Number of battery bank in series	-	N/A
Battery capacity	Ah	242
Total battery capacity	kWh	11.6

4. Simulation model

The chapter provides an overview of the AMESim models which were provided by Siemens.

By the way the activity and results described in this report were obtained through such models. In particular, the simulations targeted the assessment of the fuel consumption and CO_2 emission reductions along WLTP cycle, achievable through an optimal gearshift map generation and an energy-efficient torque split between the internal combustion engine and electric motor.

The vehicle layouts covered by AMESim simulations are:

1) Baseline vehicle, the conventional vehicle demonstrator equipped with 2.0 l Diesel engine, 8-speed AT, and STOP/START technology. The respective AMESm model is in Fig.16.

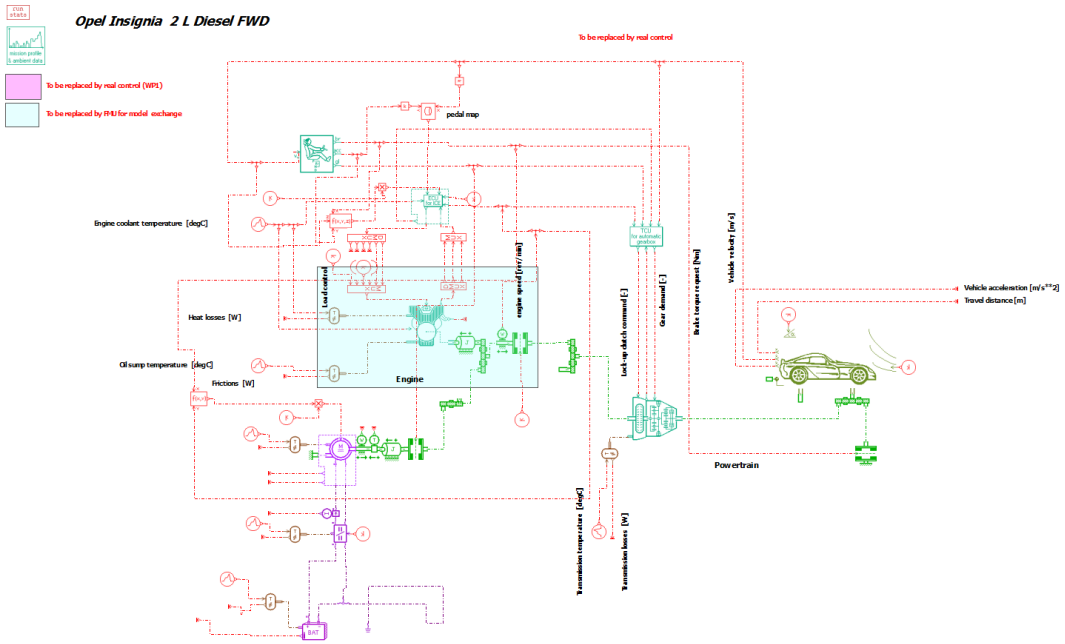

Figure 16:AMESim simulation model of the baseline vehicle

2) Vehicle demonstrator with downsized ICE, the front-wheel-drive (FWD) conventional vehicle equipped with 1.6 l Diesel ICE, 6-speed AT and STOP/START technology; in this case, the simulations have been performed with the AMEsim model of the mild hybrid vehicle by disconnecting the electric motors from the drivetrain. The respective AMESim model is in Fig.17.

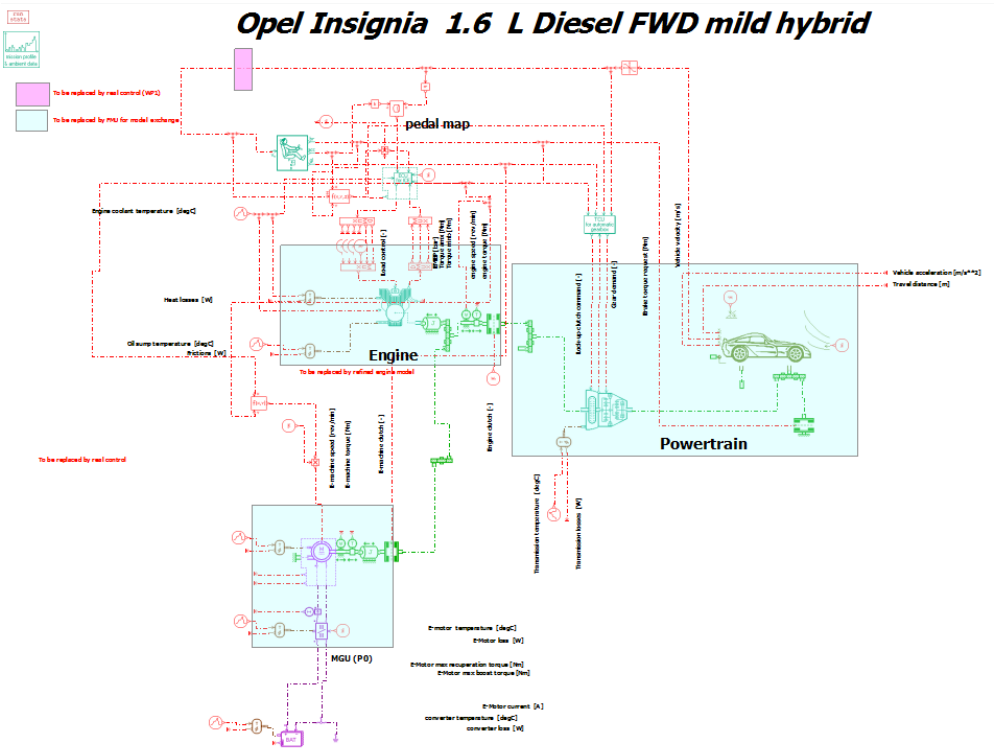

Figure 17: AMESim simulation model of the conventional vehicle equipped with 1.6 l Diesel ICE

3) Electrified vehicle demonstrator, the hybridised vehicle with a through-the-road-parallel (TTRP) layout, equipped with a downsized 1.6 l Diesel ICE connected to a belt driven motor generator unit (MGU), and a P4 electric motor (EM) connected to the rear axle by means of a reduction ratio of 9.5. Because of the hybrid architecture, which needs the implementation of a control strategy, a co-simulation framework has been implemented to run the AMESim model together with MATLAB\Simulink. This meant that AMESim and Simulink use their own solver for the co-simulation interface. This interface is represented by the white block, which has as input the variables from the Amesim components that are also the input of the Simulink model. At the same time the outputs of the white block are the variables come from the output of the Simulink model.

The respective AMESim model is in Fig.18, while the flowchart representing the signals exchanged between the two simulation environments are reported in Fig.19.

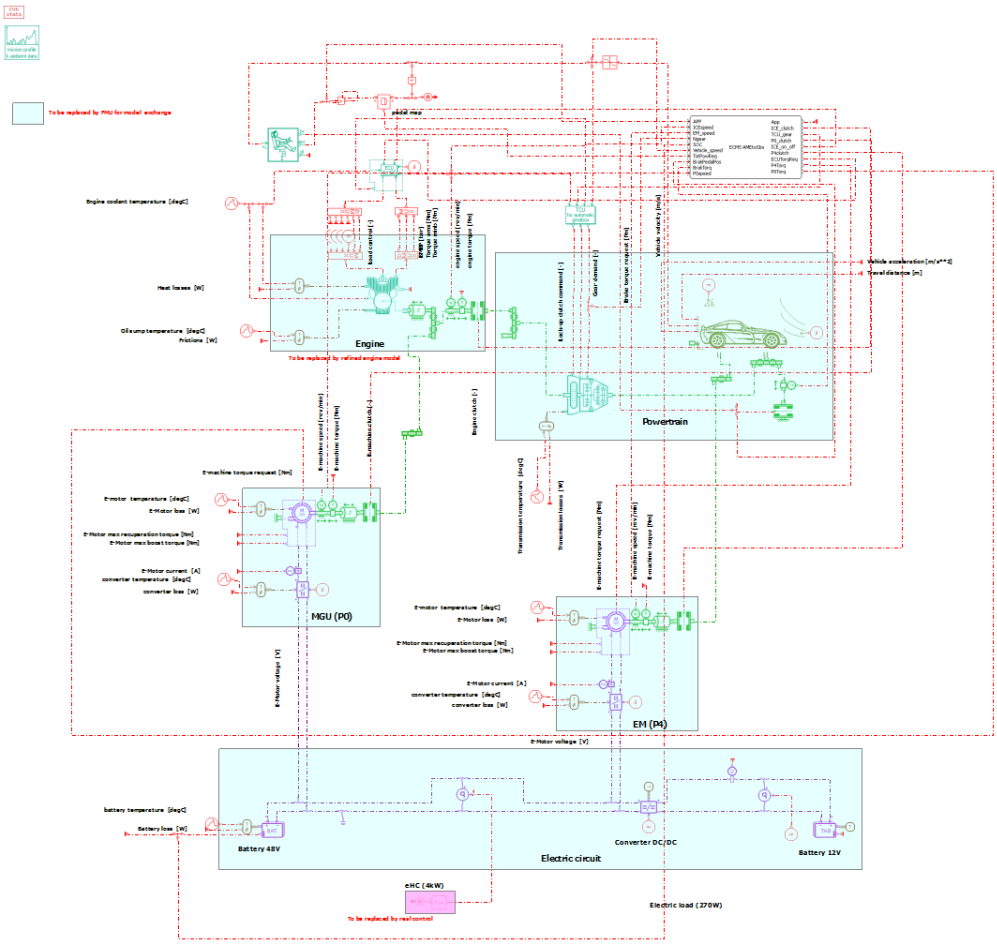

Figure 18: AMESim simulation model of the hybridized vehicle

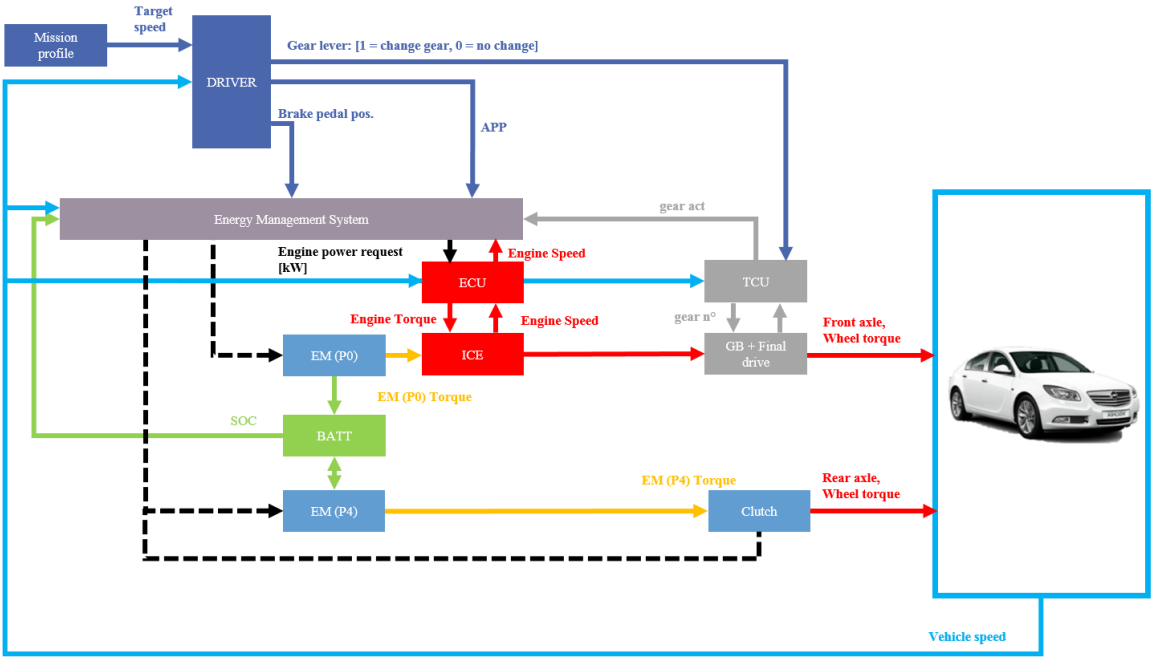

Figure 19: Signals flow chart utilised of the co-simulation framework

All three AMESim models include:

1) A driver model, based on a PID controller, used to follow the reference vehicle speed coming from the mission profile (driving cycle)
2) An internal combustion engine (ICE) model with the dynamic and performance characteristics described in the previous chapter.
3) An engine control unit ECU model
4) An automatic gearbox model.
5) A transmission control unit (TCU) model
6) A vehicle model emulating the longitudinal dynamics of the car.
7) START/STOP strategies

4.1 Engine control unit ECU

The engine control unit is one of the most important components in the model because several regulations are performed by the ECU such as: engine idle speed, maximum engine speed and fuel resume speed. Therefore, in the Amesim model there is a direct connection between the control unit and the engine because they usually exchange feedbacks with each other. Indeed, the ECU receive from the engine the value of maximum engine torque, minimum engine torque and current break mean effective pressure (BMEP) while the ECU sent to engine other signals such as engine load, number of deactivated cylinder and the signal concerning the overconsumption during engine start.

4.2 Transmission control unit (TCU)

Transmission control unit is another fundamental component in the Amesim model since it must be used to determine the gear ratio and the lockup clutch controls with different strategies. This units needs some information such as engine rotary velocity, vehicle speed and the engaged gear ratio to develop the choice in order to choose the value of actual gear engaged. This value will be sent to the automatic gearbox model. It is important to underline how the strategies used in this control unit are various possible and they could be function of engine speed, vehicle speed or other custom strategies like a specific gearshift map.

4.3 Automatic gearbox model

Automatic gearbox model is equipped with six gears that are engaged according to the signal coming from the TCU. One of the most important components of gearbox is the torque converter, which is made by an impeller, turbine and stator. The fluid flows from the impeller and it is directed over the blades of turbine, so the turbine can rotate, but between the impeller and the turbine a stator must be interposed because of the blades of the stator, that through their shape can deflect the fluid flow at an angle of almost 90 degrees. The result is a multiplication in torque because the fluid flows back more slowly. The last component of the torque converter is the lock-up clutch that is used to lock the turbine to the impeller. In this way both elements can rotate at same speed and the losses associated with fluid drive are eliminated. Even though a well-defined control of this clutch is needed because of the problem concerning vibration and noise that could be occur at low speeds, as underline in [21].

4.4 START/STOP strategy

Nowadays most of vehicles are equipped with stop-start strategy that turn off the engine when the vehicle stops, for example in proximity of traffic lights. In this way there is a reduction in terms of fuel consumption, because engine idle consumption is removed. It is straightforward that this technology could be very useful in urban areas. The system uses a computer that manages to recognize when the vehicle is stationary, instead when the brake pedal is released the starter can speed up the engine until its idle speed. Usually there is a button in the cars and thanks to it driver can enabled or disabled the stop-start function.

A conventional electric starter motor works by engaging a small pinion gear with a large ring gear fitted around the outside of the engine flywheel. For this reason, to make simulation faithful to the reality a start-stop strategy has been implemented in AMESim.

In this model the starter is represented by an electric motor, that through a clutch is linked to the engine. So, when the clutch is engaged the electric motor is capable to transfer torque to the engine and start it.

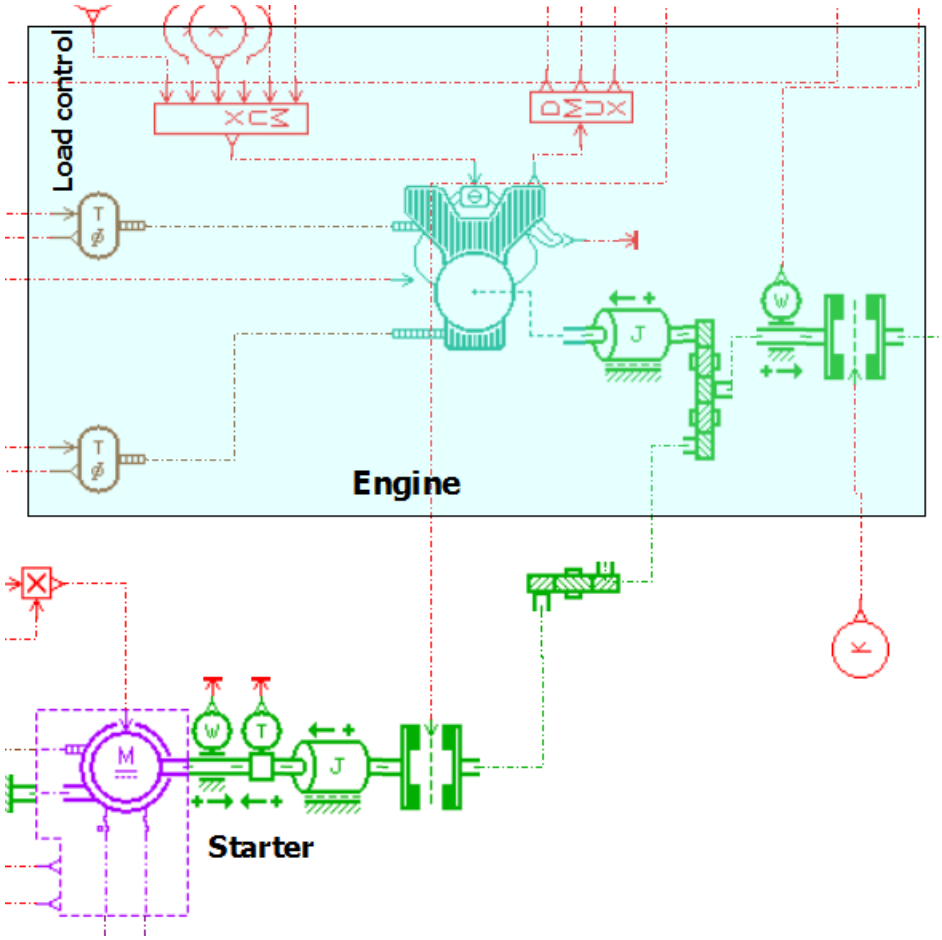

Figure 20:Starter plus Engine in AMESim model

Indeed, the control strategy has been made through two f(x,y,z) block from AMESim library, where one is linked to the engine control unit (ECU) and the other to the electric motor (STARTER), as shown in Fig.21 and Fig.22. The function block in Fig.21 contains an expression that is equal to 1 if the expression is satisfied and it is equal to 0 if it is not satisfied.

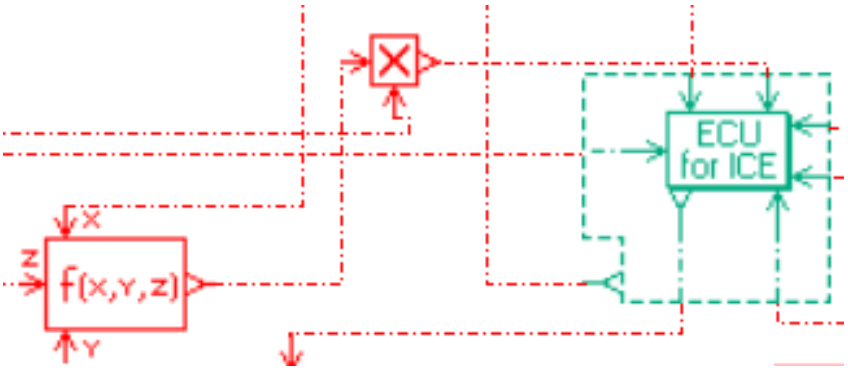

Figure 21: Start-stop strategy

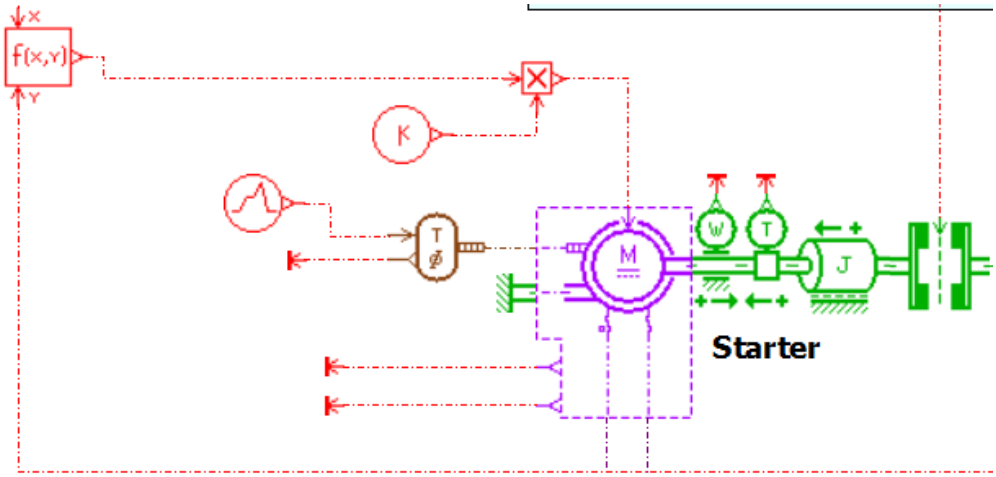

Figure 22: Control strategy concerning the starter torque

The ECU receiving as input the value 1 or 0 and turn on or turn off the engine respectively. In this case x, y and z are:

- x is the brake pedal position and its value ranges from 0 to 1;
- y is the vehicle acceleration;
- z is the vehicle control speed in feedback from PID control

So, when brake pedal position is equal to 0.8, vehicle acceleration is equal to 0 and vehicle control speed is less than 0.5 m/s expression in the function block is equal to zero and ECU turn off the engine. Otherwise if previous conditions are not satisfied the expression is equal to zero and the ECU turn on the engine.

At the same time when the clutch between starter and engine is closed, the starter must be handling to transfer the needed torque to start the ICE. This control is manage by another function block, f(x,y), shown in Fig.22.

In this block:

- x is the brake pedal position
- y is the ICE rotor speed [rpm]

So when the value of brake pedal position is less than 0.8 and the ICE rotor speed is less than 730 rpm, that is engine idle speed, means that the engine should be started, therefore the logic expression in the function block is equal to 1 and this value is multiplied by a constant value (maximum electric motor torque) through the block “k” as shown in Fig.22.

4.5 Model formulation

The simulation models do not have a tyre model; therefore, the saturation of the maximum wheel torque is achieved by setting the maximum Coulomb friction torque in the AMESim transmission model on the front axle, and the maximum P4 EM torque on the rear axle.

Fig.20 shows the 1D vehicle model block used to calculate the longitudinal acceleration, speed and travelled distance.

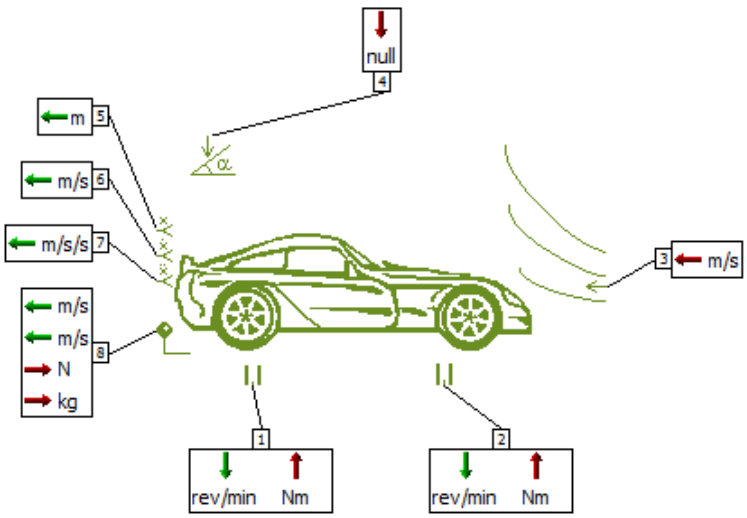

Figure 23: 1D AMESim vehicle model

The model formulation is expressed through the following equations. The equivalent force of the engine at the driven wheels (F_{engine}) is:

$$F_{engine} = \frac{T_{ICE,w,r}}{R_{w,r}} + \frac{T_{ICE,w,f}}{R_{w,f}} \tag{3}$$

Where:

- $T_{ICE,w,r}$ is the ICE torque at the rear axle;
- $T_{ICE,w,f}$ is the ICE torque at the front axle;
- $R_{w,r}$ is the rear wheel radius;
- $R_{w,f}$ is the front wheel radius.

$$F_{slope} = M_{car} * g * \sin(\alpha_{slope}) \quad (4)$$

Where:

- F_{slope} is the force due to the longitudinal road gradient;
- M_{car} is the mass of vehicle:
- g is the gravitational acceleration;
- α_{slope} is the slope angle [rad] that in this study has been considered zero.

$$F_{friction} = r_{veh} * V + F_{roll} * sign(V) \quad (5)$$

Where:

- $F_{friction}$ is the equivalent friction force of the vehicle, which can be obtained from coast down tests;
- r_{veh} is the coefficient of viscous friction;
- V is the longitudinal velocity of the vehicle;
- F_{roll} is the rolling resistance force expressed in eq.6.

$$F_{roll} = R_{roll} * (M_{car} * g * \cos(\alpha_{slope}) - W_z * V_c) \quad (6)$$

In which:

- R_{roll} is the rolling friction coefficient;
- W_z is the windage coefficient in the vertical direction that in this study it is considered zero;
- V_c is expressed in eq.7.

$$V_c = (V + V_{wind}) * |V + V_{wind}| \quad (7)$$

$$F_{aer} = W_x * V_c \quad (8)$$

Where:

- F_{aer} is the aerodynamic drag force;
- W_x is the windage coefficient in the longitudinal direction;

The windage coefficient are deduced from the aerodynamic coefficients as follows:

$$W_x = \frac{1}{2} * \rho_{air} * S_x * C_x \quad (9)$$

$$W_z = \frac{1}{2} * \rho_{air} * S_x * C_z \quad (10)$$

In which:

- ρ_{air} is the air density;
- S_x is the vehicle active area for air resistance;
- C_x is the aerodynamic coefficient along longitudinal axe;
- C_z is the aerodynamic coefficient along vertical axe.

The sum of all forces applied to the vehicle is divided by the body mass, including wheel inertias, to get the vehicle acceleration:

$$A_{acc} = \frac{1}{M_{car} + \frac{J_{w,r}}{{R_{w,r}}^2} + \frac{J_{w,f}}{{R_{w,f}}^2}} * \left(F_{engine} - F_{slope} - F_{aer} - F_{friction}\right) \quad (11)$$

Where:

- $J_{w,r}$ is the rear wheel inertia;
- $J_{w,f}$ is the front wheel inertia.

In this study both the inertia are considered to be equal.

4.6 Simulation with optimal gearshift map and stop/start strategy

This subchapter illustrates the results obtained with the electrified vehicle only in ICE mode, and with an optimal gearshift map. This procedure has been developed in another thesis [22] but results in term of fuel consumption obtained in the current work are a little different thanks to two upgrades made in the simulation model:

1. Gearbox efficiency maps for 6-speed automatic transmission instead of a constant efficiency for each gear;
2. START-STOP technology.

4.6.1 Gearshift maps for the baseline vehicle

For the evaluation of the performance along the driving cycle, the time range between 1400 s and 1600 s has been chosen to help the readability of the plots; The main reasons to choose this interval are explained as follows:

1. At the beginning there is a deceleration followed by several acceleration/deceleration manoeuvres;
2. There is a vehicle stop phase;
3. The acceleration of the vehicle within such interval is one of the highest along the whole driving cycle.

In this way all vehicle performances are analysed.

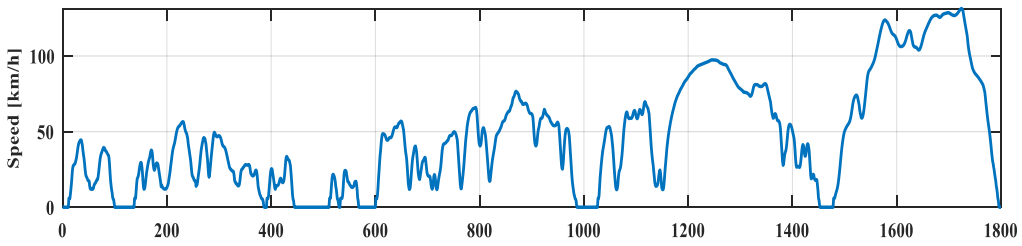

Figure 24: Vehicle speed during the WLTP driving cycle

In the following tables a comparison in terms of performance and fuel consumption is done on baseline vehicle with different gearshift strategies.

Tab.6 show how in full-performance mode there is an increase both in fuel consumption and emissions, while the vehicle performances improve in terms of acceleration as shown in Tab.8. Instead, in fuel-economy mode it is clear the advantages concerning emissions and fuel consumption

Table 6: Fuel consumption and CO_2 emissions results along WLTP for the baseline vehicle

Baseline vehicle model	Fuel consumption (l/100km)	CO_2 emissions (g/km)
Standard	6.00	159
Full performance	6.91	183
Fuel economy	5.69	151

Table 7: Percentage variations with respect to the standard gearshift logic

Baseline vehicle model	Fuel consumption variation (%)	CO_2 emissions variation (%)
Full performance	+15.17%	+15.01%
Fuel economy	-5.17 %	-5.03 %

Table 8: Acceleration test results for the baseline vehicle

Baseline vehicle model	0-100 km/h (s)	40-100 km/h in 4th (s)	80-120 km/h in 5th (s)	0-1000 m (s)
Standard	9.1	6.2	6.0	30
Full performance	8.5	-	-	29.4
Fuel economy	9.3	-	-	30.1

Table 9: Percentage variation with respect to standard gearshift logic

Baseline vehicle model	0-100 km/h acceleration time variation (%)	0-1000 m acceleration time variation (%)
Full performance	-6.59 %	-2.00 %
Fuel economy	+2.20 %	+0.33 %

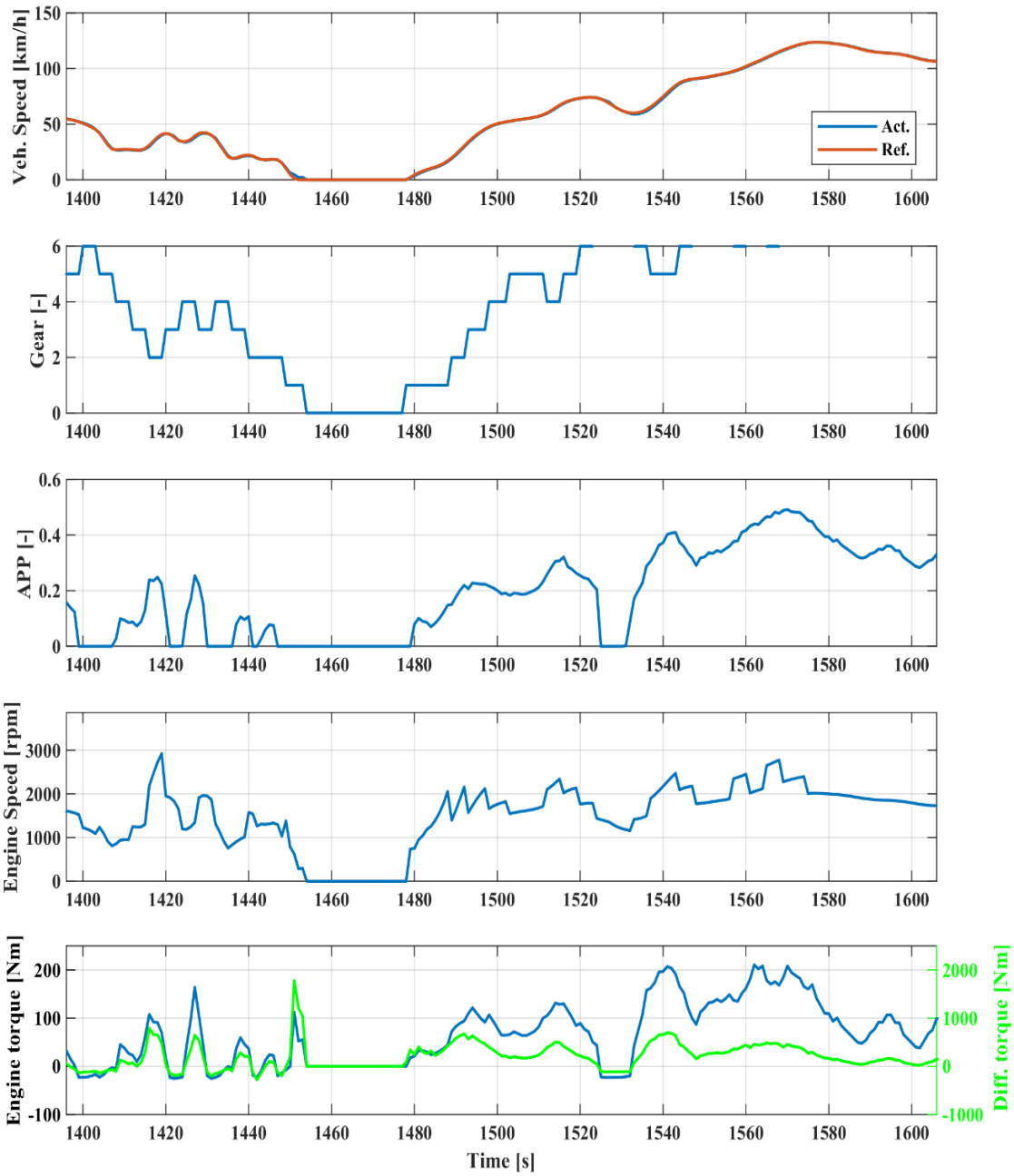

Figure 25: Example of results with fuel economy gearshift map applied to the baseline vehicle with stop start

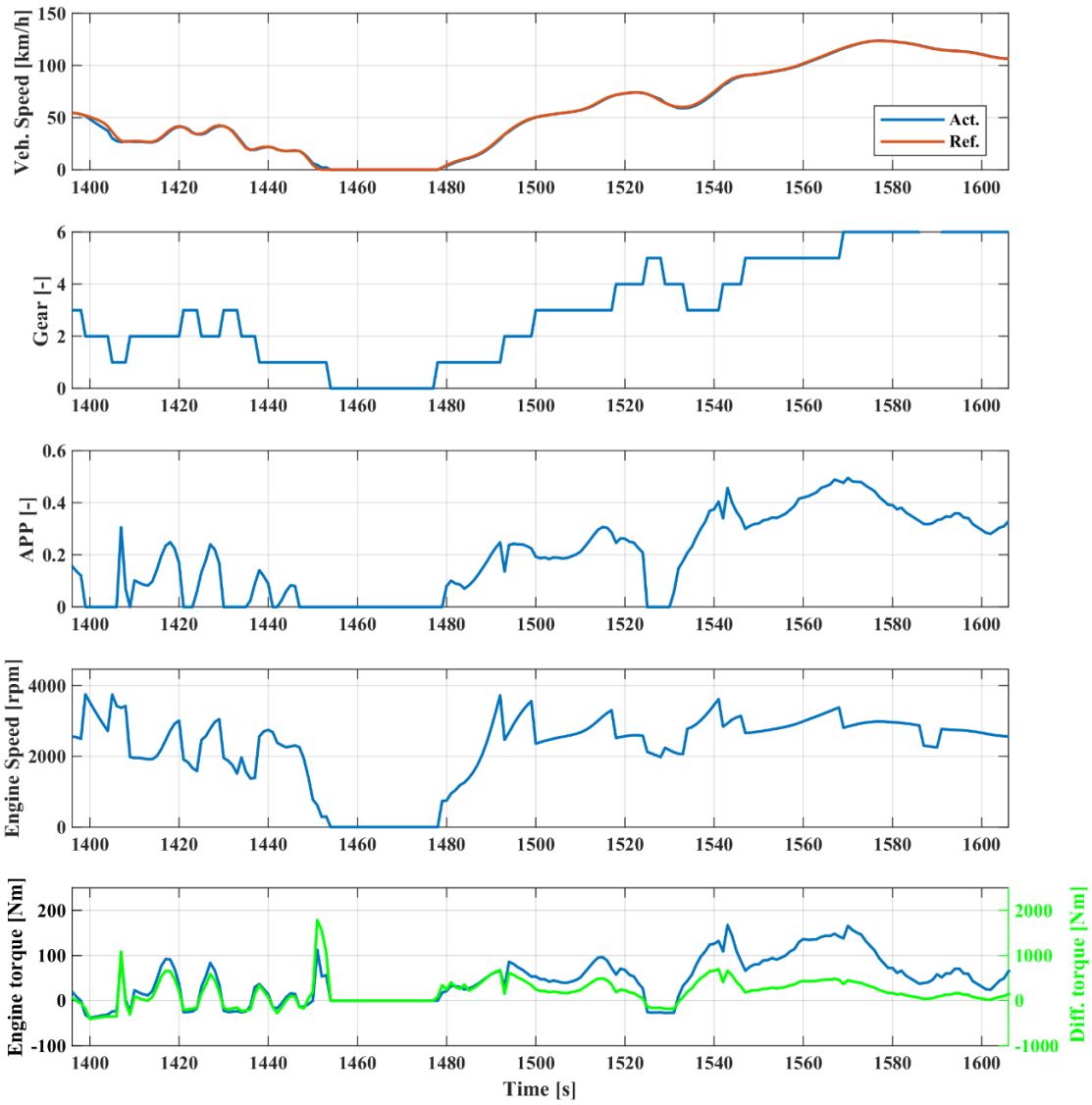

Figure 26: Example of results with fuel economy gearshift map applied to the baseline vehicle with stop start

Through Fig. 27 and Fig.28 it is possible to analyse how the implemented *start-stop* works. Indeed, when the vehicle is stationary (vehicle speed is equal to zero) engine speed is equal to zero and as consequence also the torque applied by the engine is zero. When the vehicle must restart the electric motor (starter) applies the needed torque to the engine, that reaches its idle speed and gives the request power to the car.

In this way ICE idle consumption is removed and this is reflected by a global reduction of fuel consumption.

4.6.2 Gearshift map for the electrified vehicle demonstrator in ICE mode

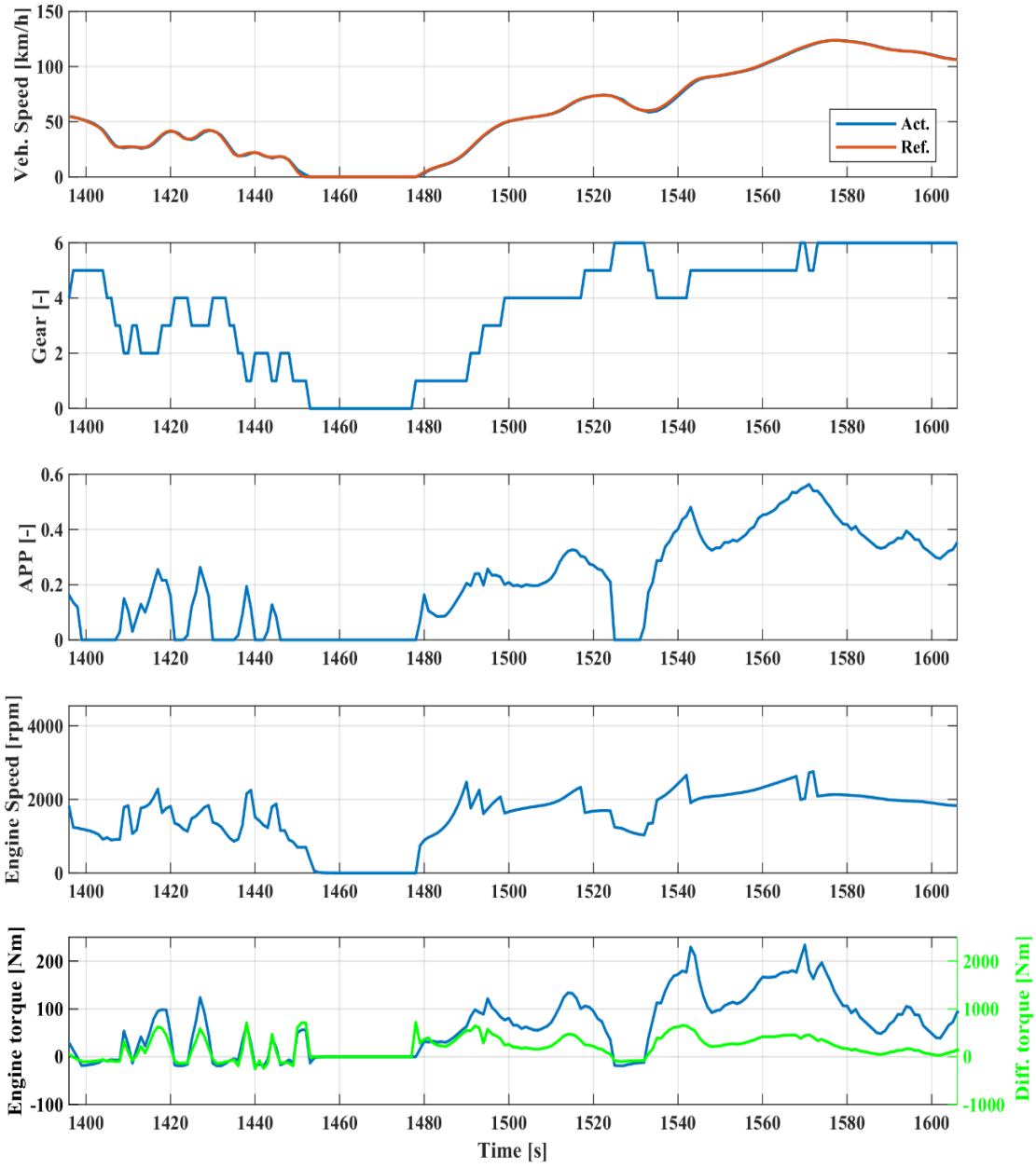

Figure 27:Example of results with the optimized gearshift map applied to the electrified vehicle with stop start

In the following tables the results in terms of fuel consumption, CO_2 emissions and vehicle acceleration are reported, where Custom 2 is the strategy used in [22] to find an optimal compromise between fuel economy and full performance.

Table 10: Fuel consumption and CO_2 emission results along the WLTP for the electrified vehicle in ICE mode with efficiency gearbox and start-stop strategy

Electrified vehicle in thermal mode	Fuel consumption (l/100km)	CO_2 emissions (g/km)
Standard	5.92	157
Full performance	6.74	178.2
Custom 2	5.82	154.1

Table 11: Percentage variations with respect to the standard gearshift algorithm

Electrified vehicle in thermal mode	Fuel consumption variation (%)	CO_2 emissions variation (%)
Full performance	+16.6%	+16.9%
Custom 2	-1.69%	-1.85%

Obviously since in the model the variable efficiency of the transmission is considered, instead that a constant value, the fuel consumption increases compared with the previous version. In the following table the percentage variation is reported

Table 12: Percentage variation with respect of the model without gearbox efficiency and start/stop strategy

Electrified vehicle in thermal mode	Fuel consumption variation (%)	CO_2 emissions variation (%)
Full performance	+13.85%	+14.0%
standard	+12.7%	+12.9%
Custom 2	+12.37%	+12.4%

Table 13: Acceleration test results for the electrified vehicle thermal mode.

Electrified vehicle in thermal mode	0-100 km/h (s)	40-100 km/h in 4^{th} (s)	80-120 km/h in 5^{th} (s)	0-1000 m (s)
Standard strategy	12.6	-	-	33.36
Full performance	9.94	-	-	31.17
Custom 2	9.94	-	-	31.17

Table 14: Percentage variations with respect to the standard gearshift algorithm

Electrified vehicle in thermal mode	0-100 km/h acceletaion time variation (%)	0-1000 m acceletaion time variation (%)
Full performance	-27.71%	-11.27%
Custom 2	-27.71%	-11.27%

After this evaluation the optimal gearshift maps obtained by the compromise between full performance and fuel economy has been modified because the high number of gearshifts that occur especially at high speed. Indeed, the simulations showed frequent fluctuations of the 5^{th} and 6^{th} gear. The fluctuations are triggered by the frequent variations of accelerator pedal position and by the slanted gearshift map at high speed in correspondence of this gears. Therefore, a modified gearshift map has been used. In the next figures the previous and the new gearshift map are reported.

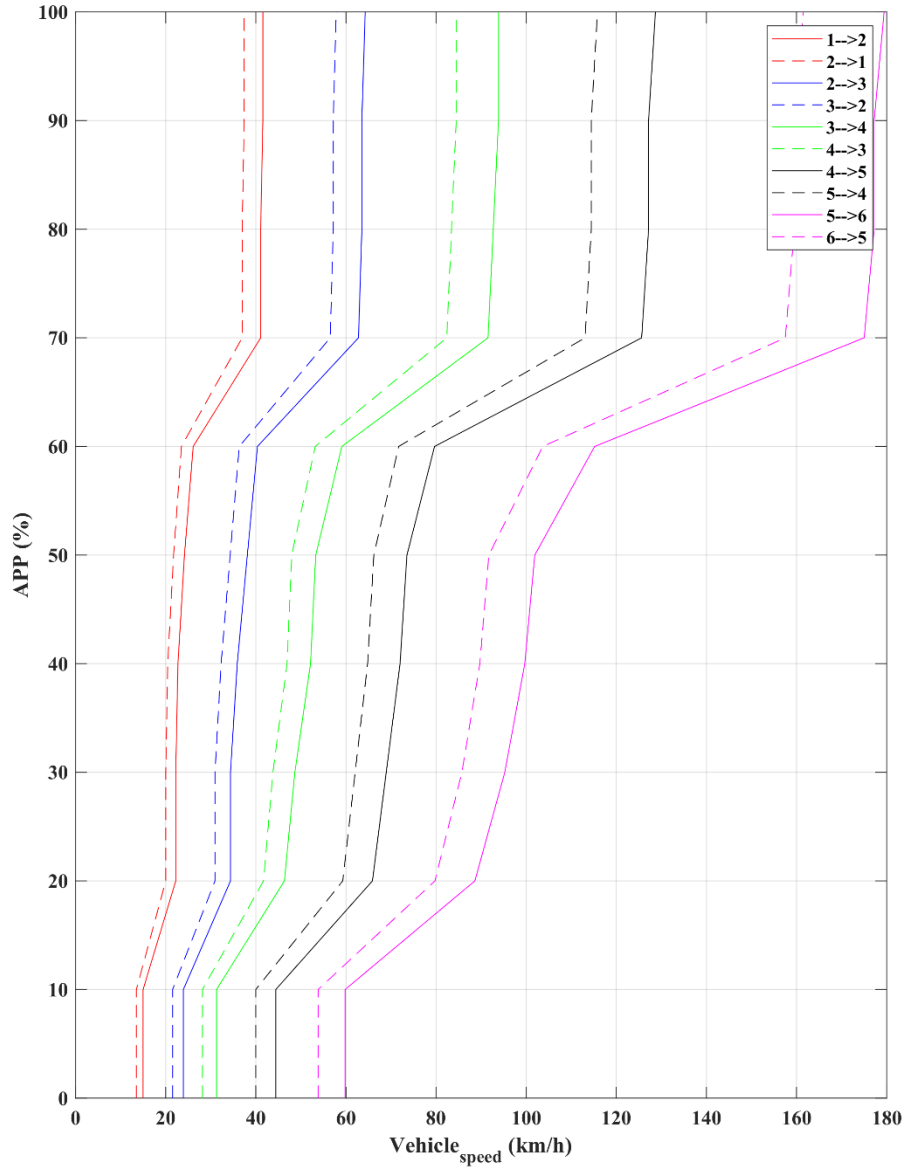

Figure 28: Gearshift map obtained from the compromise between full performance and fuel economy

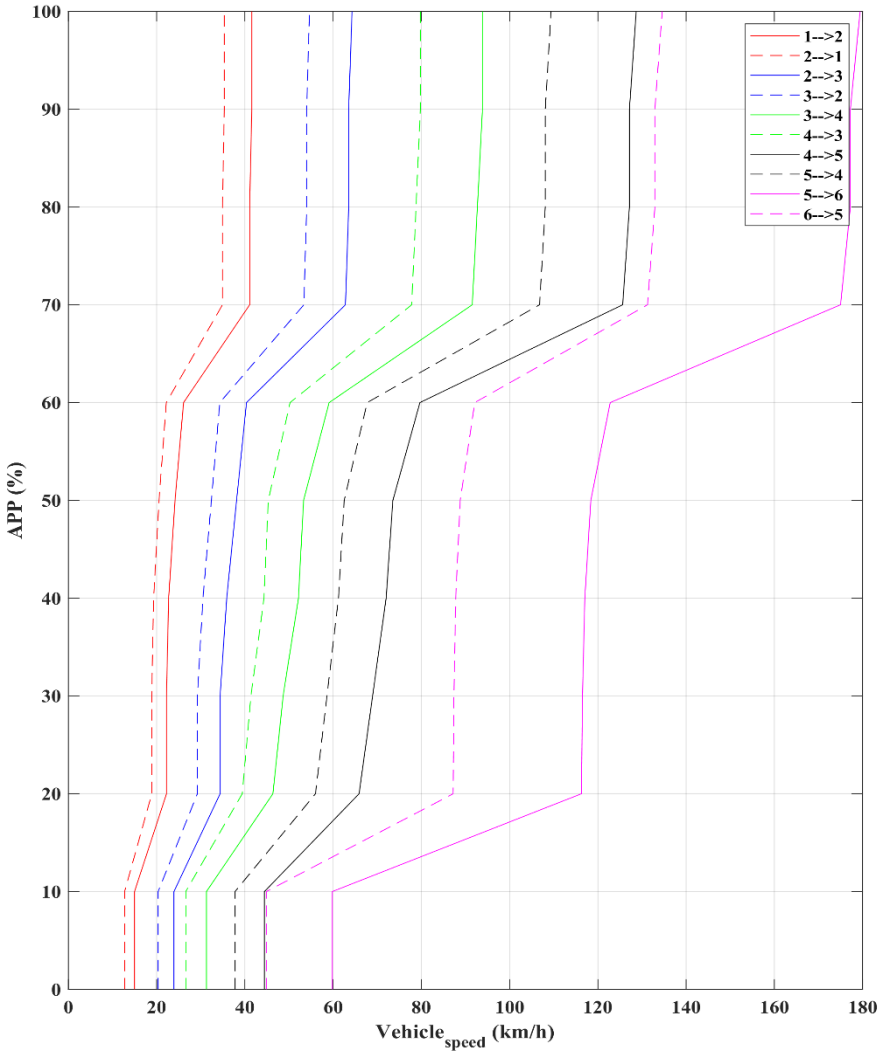

Figure 29: Gearshift map modified

As shown in Fig. 31 in order to reduce the frequent fluctuations of the gears the hysteresis between the upshift (solid line) and the downshift (dashed line) has been increased. The hysteresis value used in the previous version of the gearshift map is 90 % for each gear, while in this version 85 % is chosen for the 1st, 2nd, 3rd, 4th and 75 % between the 5th and 6th, since the simulations showed that in this range problems regarding fluctuations occur.

5. The A-ECMS control strategy

The decision regarding the amount of power delivered by each energy source installed on the HEV is managed by the energy management system (EMS). This is affected by several constraints, such as the system configuration and the components characteristics.

The control of an HEV can be summarized in the following tasks:

a) Low-level control task, which is based on classical feedback control methods applied to each component of the drivetrain.

b) High-level control, namely the Energy Management System (EMS), which supervises the overall system and optimizes the energy flow through the drivetrain while meeting given constraints.

The inputs are established by the interaction between the driver and the vehicle (i.e., actual vehicle speed and accelerator pedal position) so that the ECMS receives and process information, and outputs the optimal set-points sent to the actuators and achieved by low-level control layers.

All inputs that ECMS controller (developed in Simulink environment) receive come from AMESim because this software work in co-simulation.

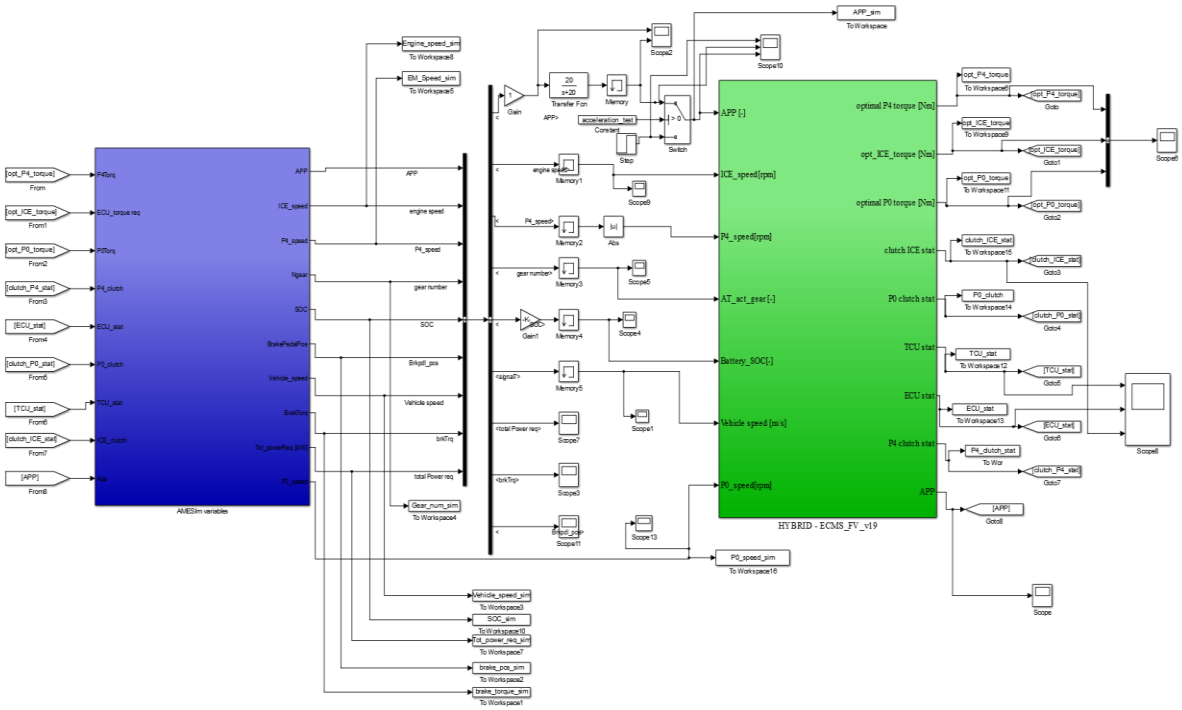

Figure 30: ECMS controller

In Fig.32 the blue block contains all AMESim variables that go to the ECMS controller block (the green one).

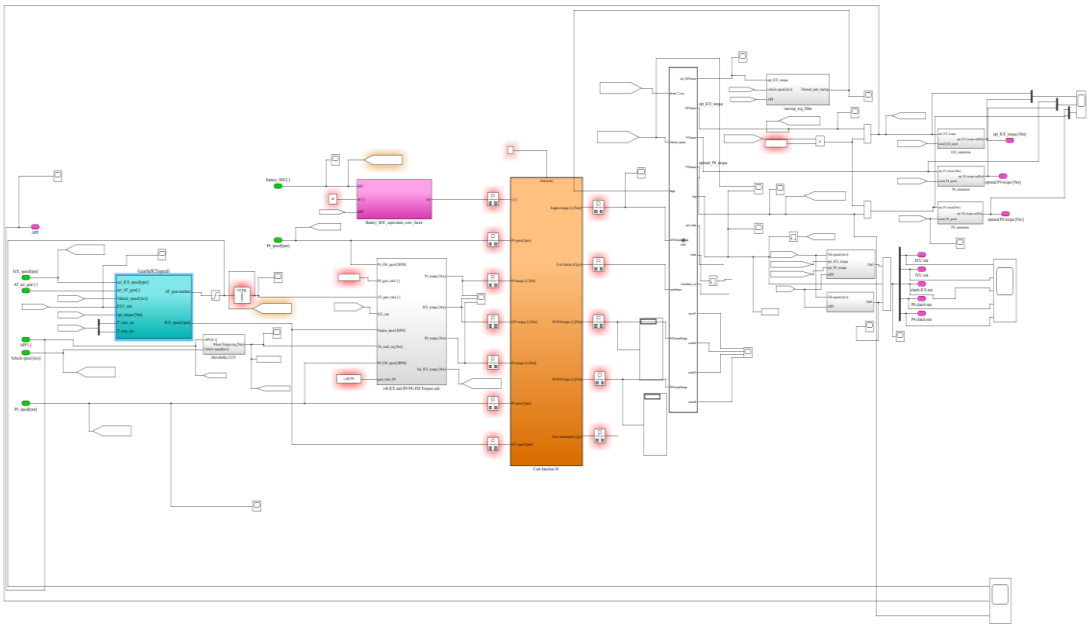

Figure 31:ECMS controller

In Fig. 33 an overview of ECMS controller is shown in which the pink, grey and orange blocks handle the power split and the reduction of fuel consumption thanks to the strategy explained in the next subchapter.

ECMS control strategy needs the actual gear engaged during the simulation and so e gearshift logic is implemented in the blue block.

5.1 Gearshift logic

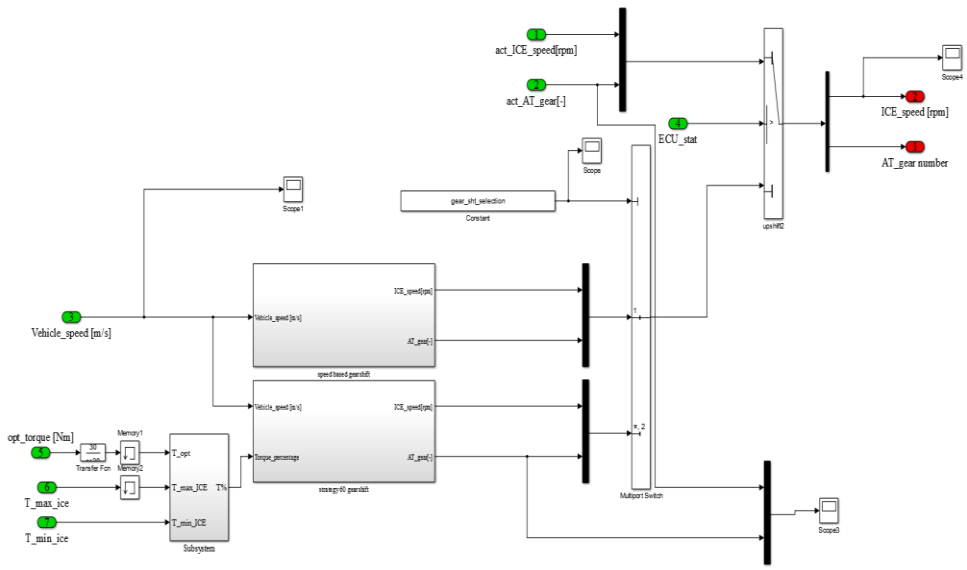

Figure 32:Gearshift logic block

The engine speed and gear number current value are chosen through a switch, which value depends on ECU state that could be 1 or 0. If ECU state is equal to 1 the controller used the variables originating from AMESim, otherwise the values of engines speed and gear number come from one of two different gearshift strategy.

5.1.1 Basic gearshift logic

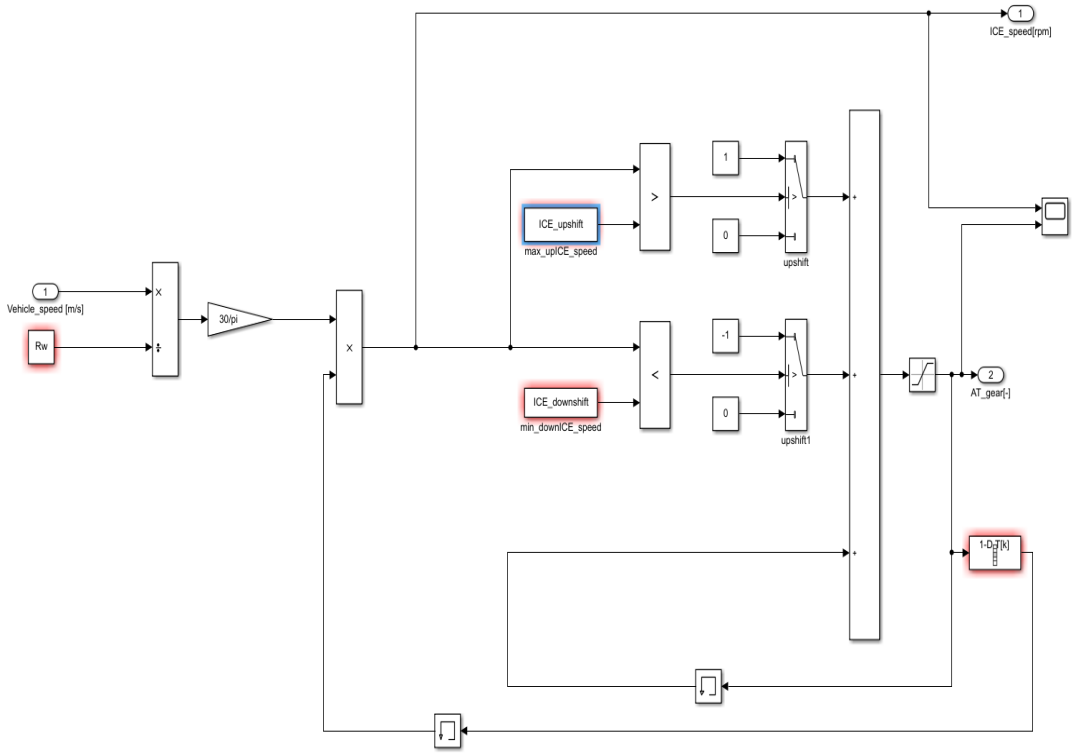

Figure 33: Basic gearshift logic

This kind of strategy is based on a simple comparison between the current value of engine speed, evaluated from vehicle current speed, and two thresholds in accordance with which the upshift or the downshift happen. Thus, if engine speed is higher than the upshift threshold the gear goes up. On the other hand, if engine speed is lower than downshift threshold the gear goes down. Otherwise, when the engine speed is including between the two thresholds the gear number remains constant.

5.1.2 Alternative gearshift logic

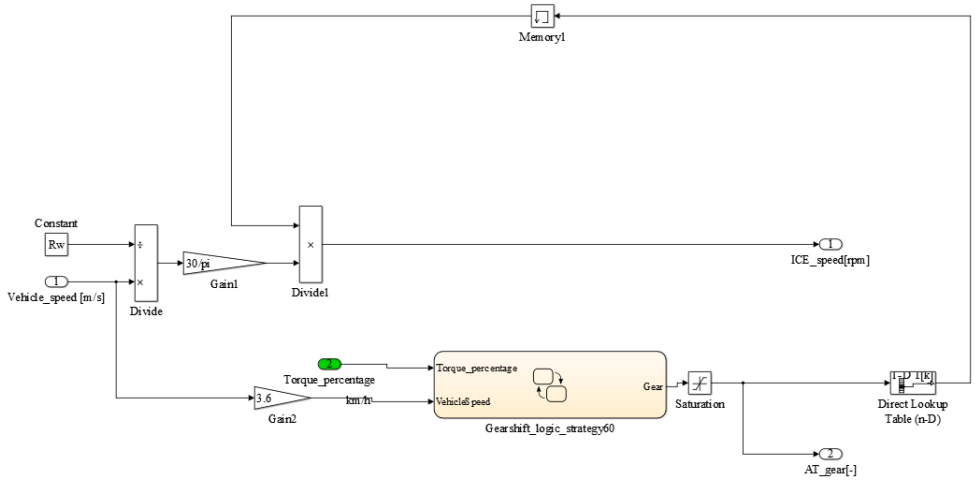

Figure 34: Alternative gearshift block

In this strategy the decision regarding an upshift or downshift is more complex, and it is summarized in Fig.34. The most important parameters in this control strategies are the actual vehicle speed and the accelerator pedal position (APP), in fact at each time, according to these values, there is only a vehicle speed for which a gearshift could happen.

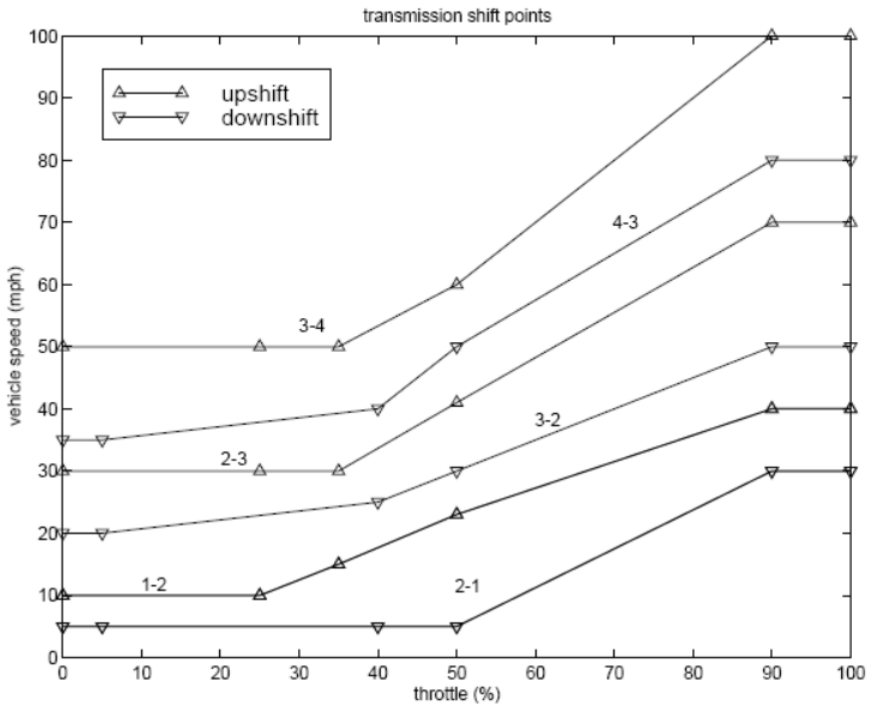

Figure 35:Schedule for gearshift

Since the problem concerning the engaged gear is a decision-making problem a Stateflow block from Simulink library is needed as shown in Fog.36. Obviously in this block the vehicle speed and the APP enter as input while the engaged gear is the output of the block.

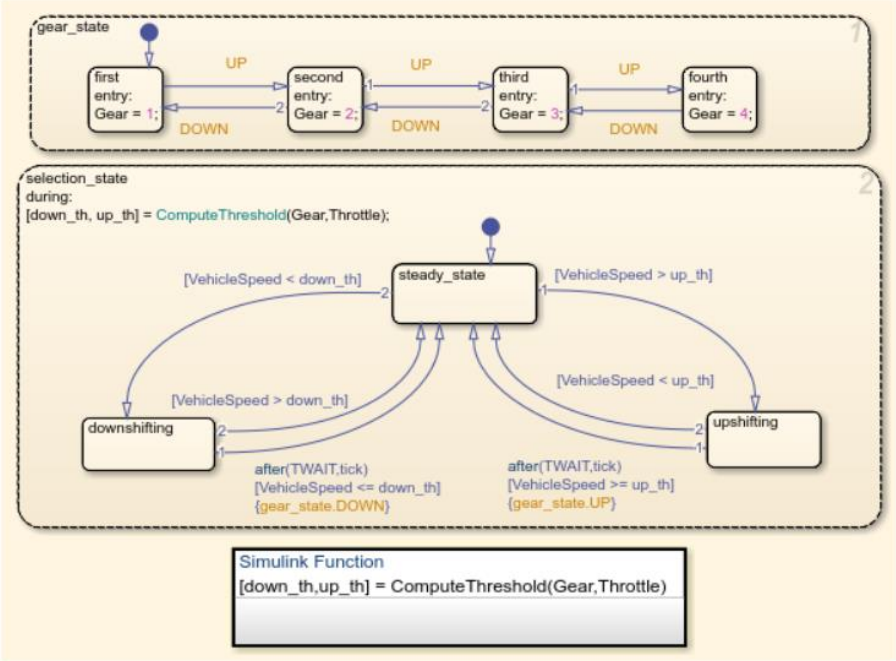

Figure 36:Stateflow diagram of the transmission shift logic

Following the gearshift logic behind this model is explained.

During the simulations at every time steps through the knowledge of the input of vehicle speed and APP from the driver, the Stateflow block can evaluate the value of downshift and upshift threshold. So, the model compares this thresholds value with the actual vehicle speed, and it decide if a gearshift is needed. In order to avoid frequent gearshift, that could be originated by a noise, the shift condition must remain for a time equal to “TWAIT”, and only if this condition is provided the gearshift takes place. After that when the shift condition goes away the system return un steady-state.

5.2 ECMS formulation

The Equivalent Consumption Minimisation Strategy (ECMS) is used as supervisory controller in the Hybrid Electric Vehicle (HEV). It selects the instantaneously optimal control action to obtain the power split between the electrical and thermal power sources installed on the vehicle while meeting appropriate constraints. The optimal solution is normally related to a cost function to be minimized. The cost function consists of the instantaneous mass fuel rate of the ICE and an equivalent fuel consumption associated with the electrical components of the powertrain.

The ECMS calculates the total fuel consumption given by the sum of the real ICE fuel consumption and the equivalent fuel consumption of the electric motors. At each sample time, a cost function depending only on the system states at the current time is minimised. It is an instantaneous optimisation problem which can be summarised in two scenarios:

1. The battery is in discharge: the electrical part is working in traction mode and P_{el} >0. A recharge will be required in the future, through regenerative braking or an additional positive torque, and therefore fuel consumption, by the internal combustion engine;
2. The battery is in charge: the electrical part is currently working in generation mode and P_{el}< 0. In future the energy stored in the battery will be used so that a fuel saving will be achieved

The instantaneous equivalent fuel consumption, which is also the cost function of the problem, is:

$$J_t = \dot{m}_{fuel} + \dot{m}_{equiv} = \dot{m}_{fuel} + \frac{s}{H_{LHV}} P_{elec} \tag{12}$$

Where:

- $\dot{m}_{fuel}$ is the engine fuel consumption;
- $\dot{m}_{equiv}$ is the equivalent fuel consumption of the electric part;
- H_{LHV} is the lower fuel heating values;
- s is the equivalence factor to convert electric power into equivalent fuel consumption;
- P_{elec} is the power which flows from/to the electric motors.

The fuel consumption is:

$$\dot{m}_{fuel} = BSFC \cdot P_{ICE} \tag{13}$$

In which $BSFC$ is the brake specific fuel consumption of the engine, provided the $BSFC$ map.

To evaluate the equivalent electric motor fuel consumption, the average efficiency of the components is generally used. In discharge mode it is:

$$P_{el}(t) = \frac{P_{EM}(t)}{\eta_{batt}(P_{EM})\,\eta_{EM}(P_{EM})} \tag{14}$$

Where η_{EM} is the EM efficiency and η_{batt} is the battery efficiency.

In this mode a recharge will be needed in future, and it is impossible to know beforehand the efficiency values. Usually, the tank-to-battery energy conversion efficiency is used to evaluate the equivalence factor.

$$s_{dis} = \frac{1}{\bar{\eta}_{tank \to batt}} \tag{15}$$

Thus, the equivalent fuel consumption in discharge mode is:

$$\dot{m}_{equiv,dis} = s_{dis} \frac{1}{\eta_{EM}\eta_{batt}} \frac{P_{EM}}{H_{LHV}} \tag{16}$$

In charge mode, the following is used:

$$P_{el}(t) = P_{EM}(t)\,\eta_{batt}(P_{EM})\,\eta_{EM}(P_{EM}) \tag{17}$$

In this mode, the electrical part works in traction in the future time steps, and it is impossible to know a priori the efficiency values. Similarly, the battery-to-tank energy conversion efficiency is used to evaluate the equivalence factor

$$s_{ch} = \bar{\eta}_{batt \to tank} \tag{18}$$

The equivalent fuel consumption in charge mode is:

$$\dot{m}_{equiv,ch} = s_{ch}\,\eta_{EM}\,\eta_{batt} \frac{P_{EM}}{H_{LHV}} \tag{19}$$

(20) and (23) are combined to obtain a formulation of $\dot{m}_{equiv}$:

$$\dot{m}_{equiv} = \gamma\, s_{dis} \frac{1}{\eta_{EM}\eta_{batt}} \frac{P_{EM}}{H_{LHV}} + (1-\gamma)\, s_{ch}\,\eta_{EM}\,\eta_{batt} \frac{P_{EM}}{H_{LHV}} \tag{20}$$

Where γ is given by the following relation:

$$\gamma = \frac{1 + sign(P_{EM})}{2} \tag{21}$$

The ECMS behaviour strongly depends on the equivalence factors (s_{dis}, s_{ch}), which can be obtained with a numerical optimization routine along a set of driving cycles.

5.3 Equivalence factors

In order to avoid the dependence by the average efficiencies another analysis has shown [23] that the two equivalent factors can be evaluated through energy considerations, thus assumption on the path efficiencies are not needed.

This analysis requires collecting data on the electrical and fuel energy used by the car along a specific driving cycle of duration *t*.

Considering the wheel axle in a vehicle the main relationship about torques balance is:

$$T_{w,req} = T_{w,ICE} + T_{w,el} \tag{22}$$

Based on eq.26 the control variable that regulates the torques split is u, defined as follow:

$$u = \frac{T_{w,el}}{T_{w,req}} \tag{23}$$

It is important to underline that in this work only the P4 contribution has been considered because it is possible to neglected P0 contribution as it will show in the results chapter.

In all simulations $u \in [-u_l, u_r]$,where u_l and u_{ur} are respectively the lower and the upper bounds for the battery state of charge during the driving cycles.

If $u = 0$ the vehicle is in pure thermal mode and all torque needed at the wheels is provided by the internal combustion engine. In this case $E_{fuel,0}$ is al the energy needed to drive the cycle. At the same time $E_{el,0}$ is not zero due to regenerative braking power, thus in the simulations it has been evaluated as the sum of the total energy loss during the brake phases. On the other hand, when $u = 1$ all the power request is provided by the electrical path.

The pure thermal case divided the curve $E_{fuel} = f(E_{el})$ in two branches that are characterized by a linearity in the region of interest, as shown in the following figure.

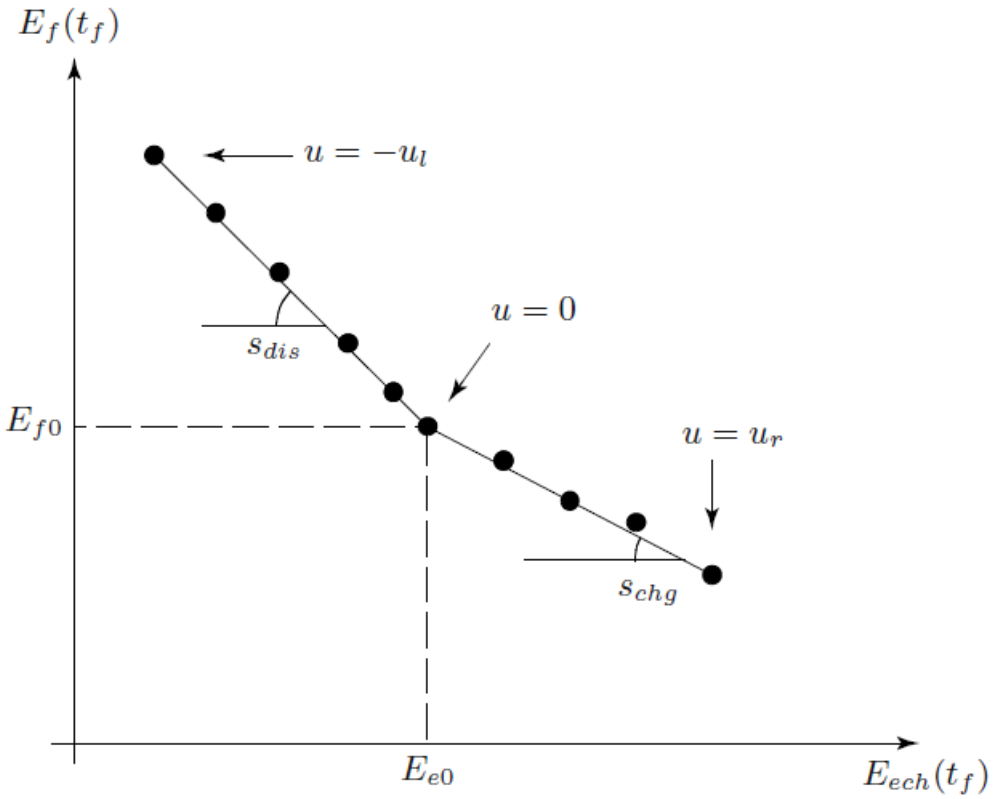

Figure 37: Dependency between fuel and electric energy in hybrid vehicle

The slopes of the two lines that fit the data are s_{dis} and s_{ch}. Once it is found these two values the mean value is considered in the implemented model, because of the adaptive method that used in this works. Indeed, the variation of s_{dis} and s_{ch}during a specific driving missions should be function of a variable parameter shown in Eq.30. Anyway, the previous analysis led to the following results:

Table 15: Equivalence factors value

s_{dis}	s_{ch}
3	3

Some simulations have been run for different u values and the electric and thermal energy are evaluated thanks to the following formula.

$$E_{fuel}(t) = \int_0^{\tau} H_{LHV}(\tau) * \dot{m}_{fuel}(\tau)\, d\tau \tag{24}$$

$$E_{el}(t) = \int_0^{\tau} I_{batt}(\tau) * V_{batt,OC}(\tau)\, d\tau \tag{25}$$

Where:

- $I_{batt}(\tau)$ is the instantaneous value of battery current;
- $V_{batt,OC}(\tau)$= is the instantaneous value of battery open circuit voltage.

Anyway, these factors vary according to the driving cycle. In general, a pair of equivalence factors that minimize the fuel consumption for a given driving cycle might not minimize it in another one. This means that ECMS provides good results if the driving cycle is like the one for which the strategy has been tuned.

Adaptive ECMS (A-ECMS) is an ECMS typology that evaluates the equivalence factor while considering two of the principal constraints of the problem, i.e., the lower and upper limits of the battery SOC. By means of the A-ECMS, the equivalence factor is changed dynamically along the driving cycle to control the SOC variation. In particular, the use of the electric components must be discouraged when the state of charge is close to the lower limit, SOC_{min}, and must be encouraged when the state of charge is close to the upper limit, SOC_{max}.

Several methods based on SOC feedback are available in the literature, among of which the simplest is represented by:

$$s = s_0 + K_P(SOC_{ref} - SOC(t)) \tag{26}$$

Where s is proportional to the difference between the actual state of charge $SOC(t)$ and the reference state of charge set a priori, i.e., SOC_{ref}. The value of the proportional gain (K_P) is a tuning parameter.

5.3.1 A-ECMS implementation for the P0+P4 HEV without gearbox efficiency in the controller

The assumption is that the vehicle speed (V_{Veh}) is known at each time instant. The following kinematic relationship hold:

$$\omega_w = \frac{\omega_{P4}}{i_{P4}} = \frac{\omega_{ICE}}{i_{AT}} = \frac{\omega_{P0}}{i_{P0} i_{AT}} \tag{27}$$

Where:

- i_{AT} is the actual ICE gear;
- i_{P0} is the transmission ratio of the belt driven transmission ratio of the motor generator unit (MGU);
- i_{P4} is the transmission ratio of the rear electric motor;

The wheel torque ($T_{w,req}$) requested by the driver is given by superposition of the effects of the ICE ($T_{w,ICE}$) and the electrical components ($T_{w,el}$):

$$T_{w,req} = T_{w,ICE} + T_{w,el} \tag{28}$$

Where the electrical part where the electrical part ($T_{w,el}$) is given by the P0 and P4 contributions:

$$T_{w,el} = T_{w,P4} + T_{w,P0} = T_{P4} i_{P4} + T_{P0} i_{P0} i_{AT} \tag{29}$$

It is possible to identify electrical torque limitations based on the characteristics of the electric machines and their position along the driveline:

$$T_{w,el(min)} = T_{P4,min} i_{P4} + T_{P0,min} i_{P0} i_{AT} \tag{30}$$

$$T_{w,el(max)} = T_{P4,max} i_{P4} + T_{P0,max} i_{P0} i_{AT} \tag{31}$$

Hence, knowing the actual vehicle speed and the torque requested by the driver, it is possible to determine the minimum and maximum torque that the ICE can provide:

$$\begin{aligned} T_{ICE,min} &= max\left(\frac{T_{w,req} - T_{w,el\ (min)}}{i_{el}}, T_{ICE,min}\right) \\ &= max\left(\frac{T_{w,req} - T_{w,el(min)}}{i_{el}}, 0^*\right) \end{aligned} \tag{32}$$

$$T_{ICE,max} = min\left(\frac{T_{w,req} - T_{w,el(max)}}{i_{el}}, T_{ICE,max}\right) \tag{33}$$

If the braking ICE torque is neglected.

A vector $[T_{ICE,min}, \dots, T_{ICE,max}]$ is generated, which contains a set of n discretised value of torque that the ICE can provide to satisfy the torque request.

Consequently, the two vectors are obtained:

$$\left[T_{w,req}\right]_{n\times 1} = T_{w,req} \cdot (1, \dots, 1)_{n\times 1} \tag{34}$$

$$\left[T_{w,el}\right]_{nx1} = [T_{w,req} - T_{ICE,} i_{AT}] \tag{35}$$

The last one is the vector containing the set of n electric torques within the interval $[T_{w,el(min)}, \dots, T_{w,el(max)}]$.

Obviously n is another tuning parameter because for high value of this constant the A-ECMS controller is more accurate because the number of the possible torques that the ICE can provide is higher, therefore the algorithm can make a better choice. On the other hand, if n rises the computational cost increase so also the simulation

time. Based on the above, since the analysis of this controller is projected to a real-time implementation n=10 is chosen in order to obtain acceptable simulation times. With respect to $T_{w,el}$, the torque split between the P0 and P4 motors is managed as follows:

If $0 \leq [T_{w,el}] \leq T_{w,P4(max)}$

$$T_{P4} = \frac{T_{w,req} - T_{ICE} i_{AT}}{i_{P4}} \qquad (36)$$

$$T_{P0} = 0$$

If $[T_{w,el}] > T_{w,P4(max)}$

$$T_{P4} = T_{P4(max)} \qquad (37)$$

$$T_{P0} = \frac{T_{w,req} - T_{ICE} i_{AT} - T_{P4,max} i_{P4}}{i_{P0} i_{AT}}$$

If $T_{w,P4(min)} \leq [T_{w,el}] < 0$

$$T_{P4} = \frac{T_{w,req} - T_{ICE} i_{AT}}{i_{P4}} \qquad (38)$$

$$T_{P0} = 0$$

If $[T_{w,el}] < T_{w,P4(min)}$

$$T_{P4} = T_{P4(min)} \qquad (39)$$

$$T_{P0} = \frac{T_{w,req} - T_{ICE} i_{AT} - T_{P4,min} i_{P4}}{i_{P0} i_{AT}}$$

This electrical split algorithm is justified by the fact that the P4 motor provides power to the wheel along a shorter path (hence more efficient) than the P0 motor, and thus it is used as much as possible.

Once all the vectors are known, the cost associated to each combination of $(T_{P4}, T_{P0}, T_{ICE},)$ is evaluated:

$$[J]_{n\times 1} = \left[\dot{m}_{fuel}\right]_{n\times 1} + \left[\dot{m}_{eq,P4}\right]_{n\times 1} + \left[\dot{m}_{eq,P0}\right]_{n\times 1} \qquad (40)$$

Finally, the optimal torque split is chosen such that J is minimized.

5.3.2 A-ECMS implementation for the P0+P4 HEV with online gearshift logic and efficiency

In this thesis an upgrade of the previous controller algorithm is proposed. In the previous controller the gearshift logic, under which the decision about upshifts or downshifts was taken, was based on an optimal gearshift map generated offline in order to follow some specifications such as performance and fuel consumption. In

order to reduce the fuel consumption and sometimes also the total number of gearshifts during a driving cycle the online gearshift logic is proposed.
As explain previous the A-ECMS controller carries out to generate the optimal split torque between the engine and the two electric motors. Just the P0 and P4 torque represent some of the input of the gearshift block.

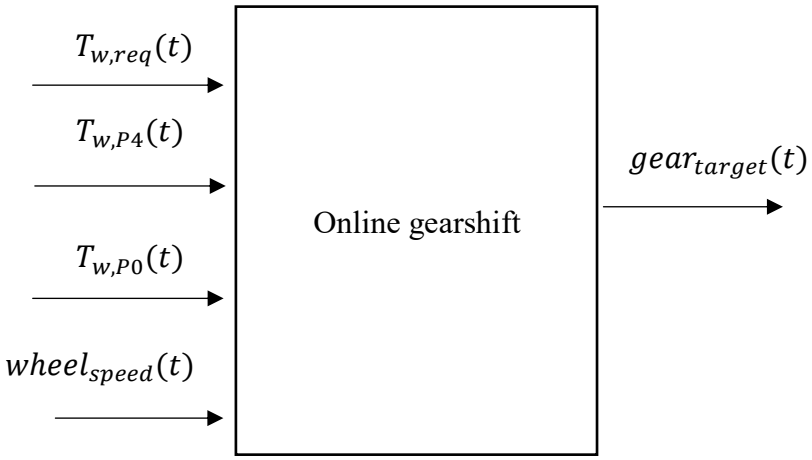

Figure 38: Online gearshift logic

The first step is to find the ICE torque contribution at wheels, and it is possible thanks to the knowledge of the actual total torque request by the vehicles and the torque contributions, provided by the energy management controller. So, the following expression can be evaluated.

$$T_{w,ICE} = T_{w,req} - T_{P4} i_{P4} - T_{P0} i_{P0} i_{AT} \tag{41}$$

Find $T_{w,ICE}$, this value is saturated thanks to ICE characteristics and the knowledge of all gear ratios. Hence two vectors $[\, T_{ICE,1^{st}\,gear}, \dots, T_{ICE,6^{th}\,gear}]$ and $[ICE_{\,speed,1^{st}\,gear}, \dots, ICE_{speed,6^{th}\,gear}]$ are generated:

$$[T_{ICE}]_{6\times1} = T_{w,ICE} / [i_{AT}]_{6\times1} \tag{42}$$

$$\left[ICE_{speed}\right]_{6\times1} = Wheel_{speed} * [i_{AT}]_{6\times1} \tag{43}$$

In this way all possible torques and speeds generated by internal combustion engine, as function of the six engaged gears, are available. Despite of everything some conditions must be verified in order to understand which gears is feasible. Since the following check is needed:

$$[T_{ICE}]_{6\times1} \leq \left[T_{ICE,max}\right]_{6\times1} \tag{44}$$

$$\left[ICE_{speed}\right]_{6\times1} \leq \left[ICE_{speed,max}\right]_{6\times1} \tag{45}$$

$$ICE_{idle\ speed} < \left[ICE_{speed}\right]_{6\times1} \tag{46}$$

The $T_{ICE,max}$ and $ICE_{speed,max}$ values for each gear are evaluated interpolating the ICE characteristic.

After that thanks to the engine break specific fuel consumption map provided by manufacturers the BSCF associated with each feasible gear is estimated, the minimum one is taken ad as consequence the gear associated with it is chosen as the actual gear engaged by the transmission. This logic is summarized as follow.

$$BSFC_{operative} = \min(\left[BSFC_{feasible}\right]_{6\times1}) \tag{47}$$

$$Gear_{actual} = \left[Gear_{feasible}(BSFC_{operative})\right]_{6\times1} \tag{48}$$

The aim of this strategies is to minimize fuel consumption, so the controller makes every possible decision even at the cost of driveability because if the final target is to reduce the fuel consumption also fluctuations of gears are possible. Since to overcome this issue the gearshift block runs at different frequency from the model itself, so this frequency becomes a tuning parameter as explained after. For this reason, the AMESIM model receives in input the gear from the gearshift logic block, while the optimal ICE torque comes from the A-ECMS block.

$$time_{gearshift} = time_{step} * constant \tag{49}$$

In the above equation $time_{step}$ is the simulation time of the Matlab/Simulink model, while $time_{gearshift}$ is the processing time of the gearshift logic. The $constant$ term has the task of modify the computational time in order to contain frequent gearshifts. For this reason, a systematic approach has been used to find the optimal compromise between fuel consumption and driveability as shown in the next chapter.

Furthermore, the use of an online gearshift logic involves bypassing the TCU component in the vehicle model because now the signal of the engaged gear in the gearbox comes from Simulink environment.

However, another feature is added because 6-speed AT gearbox efficiency is neglected in the first implementation of the controller. Next step has been incorporated transmission and differential efficiency in the power split between

engine and electric motors. Since the ICE is linked to the AT transmission the following equations has been considered.

The first one in traction mode when $T_{ICE} > 0$.

$$P_{ICE}^{PS} = P_{ICE}^{SS} * \eta_{AT} * \eta_{diff} \tag{50}$$

Where:

- P_{ICE}^{FS} is the ICE power evaluated on the first shaft of the transmission;
- P_{ICE}^{SS} is the ICE power evaluated on the second shaft of the transmission;
- η_{AT} is the transmission efficiency;
- η_{diff} is the differential efficiency

As consequence the vector [$T_{ICE,1^{st}\,gear}, \dots, T_{ICE,6^{th}\,gear}$] which contains a set of six discretised value of torque that the ICE can provide to satisfy the torque request is divided by η_{AT} and η_{diff}.

The second equation is applied during the breaking.

$$\eta_{AT} * \eta_{diff} * P_{ICE}^{PS} = P_{ICE}^{SS} \tag{51}$$

In this case the vector containing the ICE torques is multiplied by the two efficiencies.

The efficiencies have been included in the algorithm thanks to six look-up table, in which the values of efficiency are known, for each gear, as function of the primary shaft speed and engine torque.

$$\eta_{AT} = \eta_{AT}(T_{ICE}, PS_{speed}) \tag{52}$$

Since the efficiency matrix are provided through well-defined dimension an interpolation is necessary.

$$\eta_{AT,i} = f([T_{ICE,i}]_{k\times1}, [ICE_{speed}]_{k\times1}, [T_{ICE}]_{6\times1}, [ICE_{speed}]_{6\times1}) \tag{53}$$

In this way the efficiency for each feasible gear is available at each instant.

5.3.3 ICE on/off condition

To effectively switch on the ICE a moving average with a sliding window of 2 s has been adopted. The ICE is switched on as soon as the moving average $\bar{T}_{ICE,opt}$ reaches a value greater of 60 Nm. This is to avoid sudden peaks of ICE torque requests and to allow the ICE operation within its efficient region.

$$ICE_{ON} = \frac{T_{ICE,opt}(t) + T_{ICE,opt}(t-1) + \cdots + T_{ICE,opt}(t-N)}{N+1} \tag{54}$$

However, this condition is bypassed whenever the torque requested by the driver is greater than the maximum torque the P4 EM can provide.
On the other hand, the ICE is switched off if the vehicle speed is lower than 2 m/s.

6. Results and discussion

This chapter deals with the results obtained through the implementation of the co-simulation model. More specifically, the electrified vehicle demonstrator model (with the 1.6 l diesel engine equipped with a 6-speed AT, a 11 kW MGU-P0 and a 31 kW P4 electric motor) in AMESim has been connected to the ECMS strategy implemented in Matlab/Simulink. The New European Driving cycle (NEDC), the Worldwide harmonized Light vehicles test Procedure (WLTP) and the ARTEMIS motorway have been selected to evaluate the performance of the EMS for fuel consumption reduction. At the beginning NEDC was chosen for tuning procedure of the controller because it presents a simpler vehicle speed profile with respect of the WLTP, allowing easier interpretation of the results. After, to guarantee a reasonable behaviour of the controller also on other kind of driving cycles WLTP has been chosen for the upgrade procedure.
Later, the same EMS has been tested along acceleration tests in order to assess the acceleration performance of the mild-hybrid vehicle and get the 0-100 km/h, 40-80 km/h, and 80-120 km/h acceleration times. Lastly, the results obtained have been compared against the original vehicle equipped with the 2.0 l diesel internal combustion engine and 8-speed AT.

6.1 Tuning of A-ECMS controller with online gearshift

As explained in the previous chapter A-ECMS algorithm and gearshift logic runs at different constant time. The transition rate between these two controllers is found through a tuning done with simulations at different frequencies. The results obtained are shown in function of the frequency f expressed in the following equation:

$$f = \frac{1}{time_{step} * constant} \tag{55}$$

The frequencies values used in the simulations are:

Table 16: frequency values for gearshift control strategy

f [Hz]	0.333	0.400	0.444	0.500	0.571	0.667	0.800	0.889	1	1.33	2	4	10

Following results concerning fuel consumption are presented:

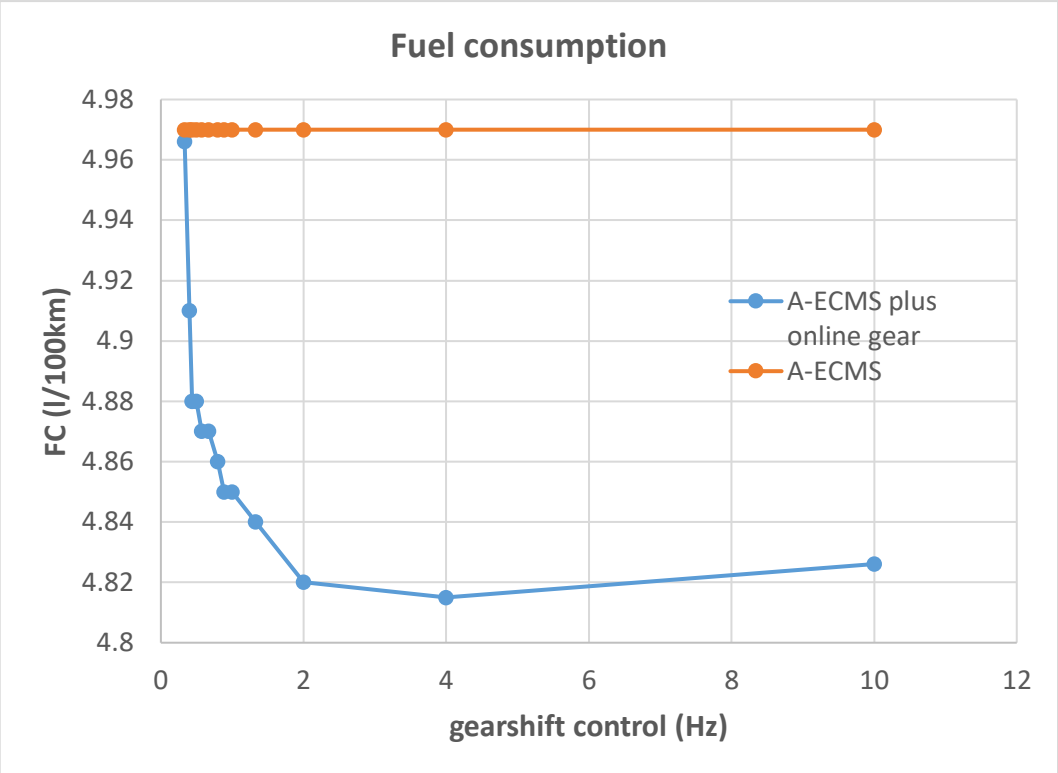

Figure 39:Comparison concerning fuel consumption between two controllers along WLTP

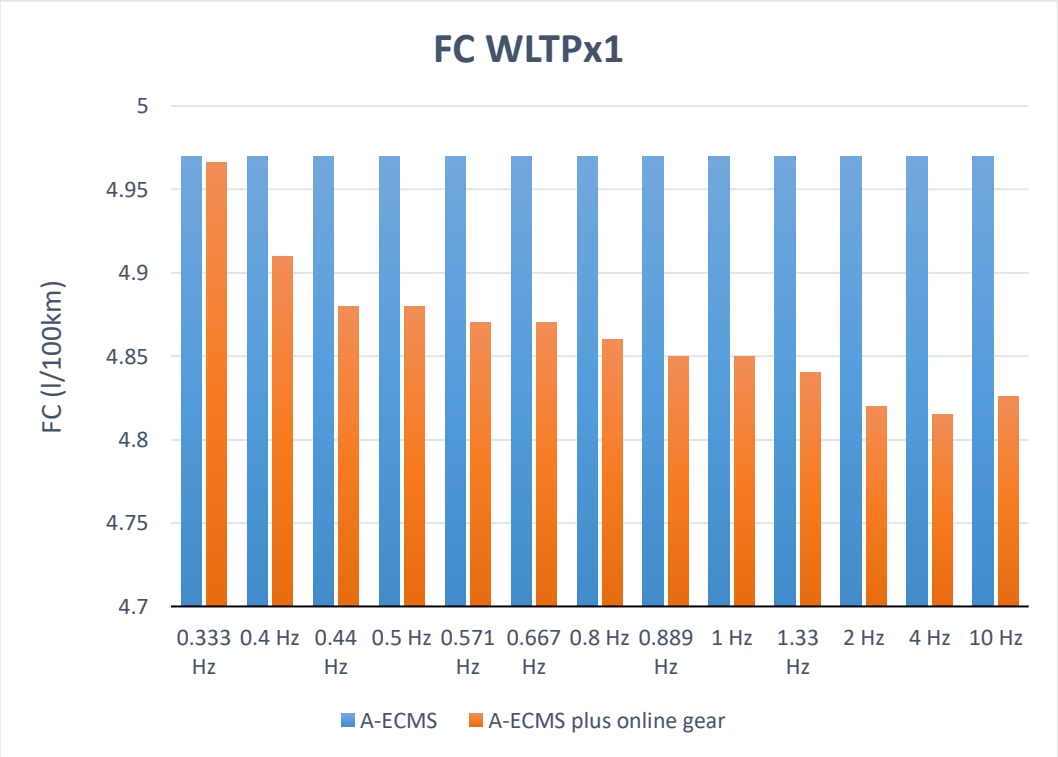

Figure 40: Histogram concerning fuel consumption along WLTP

Fig.40 and Fig.41 show how in A-ECMS with online gearshift and efficiency there is always a reduction in fuel consumption for all frequency values. How it was

expected with increased value of frequency the reduction of fuel consumption rises, but this happens until the value $f = 4\ Hz$. After that the fluctuations of the gears become too significant, so they compromise the good behaviour of the controller. Clearly in order to consider also the driveability a detailed analysis has been done, considering some characteristic parameters as described in [24] , [25], [26] . Concerning the gearbox this analysis focus on the total number of gearshifts and the mean value of time for each engaged gear along WLTP mission, while concerning the engine the total number of events where the ICE is on or off are considered.

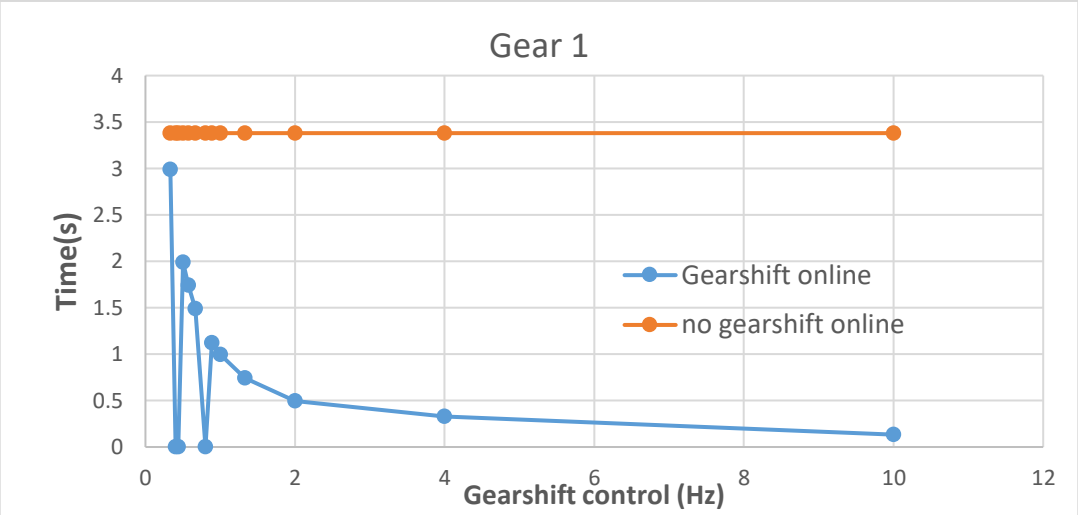

Figure 41:Comparison between two controllers for 1st gear

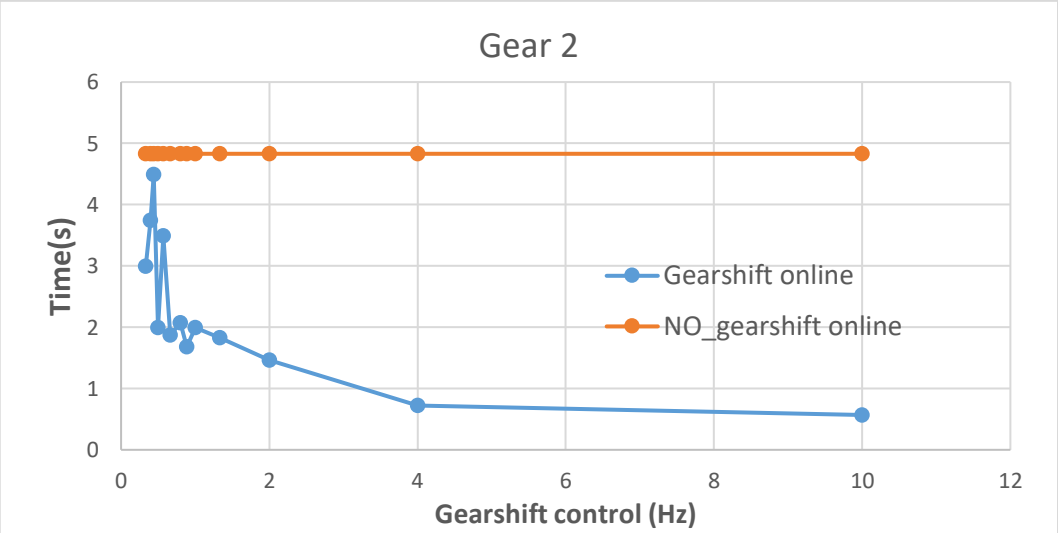

Figure 42:Comparison between two controllers for 2nd gear

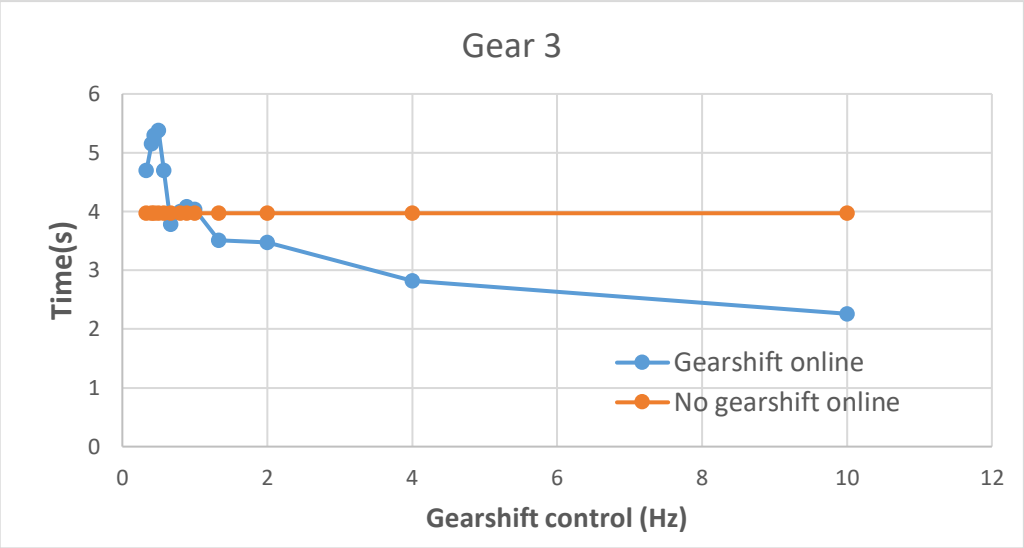

Figure 43:Comparison between two controllers for 3rd gear

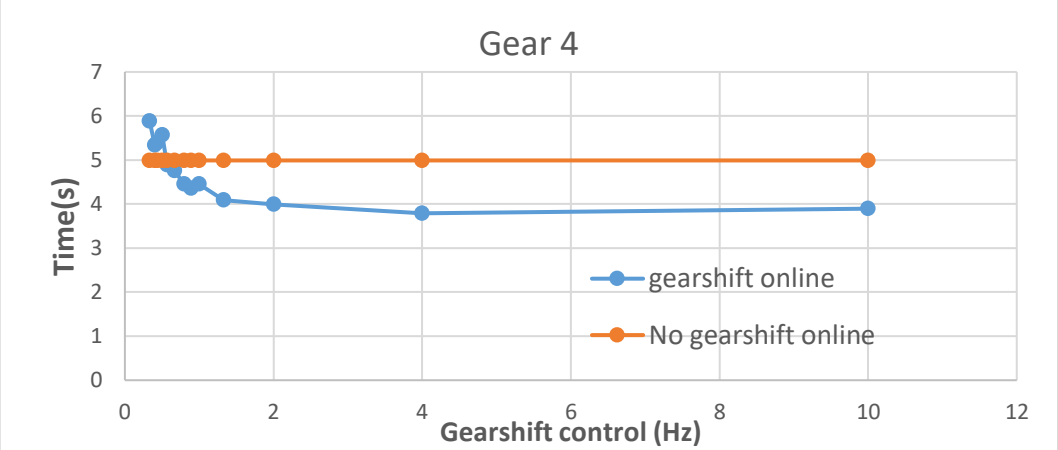

Figure 44: Comparison between two controllers for 4th gear

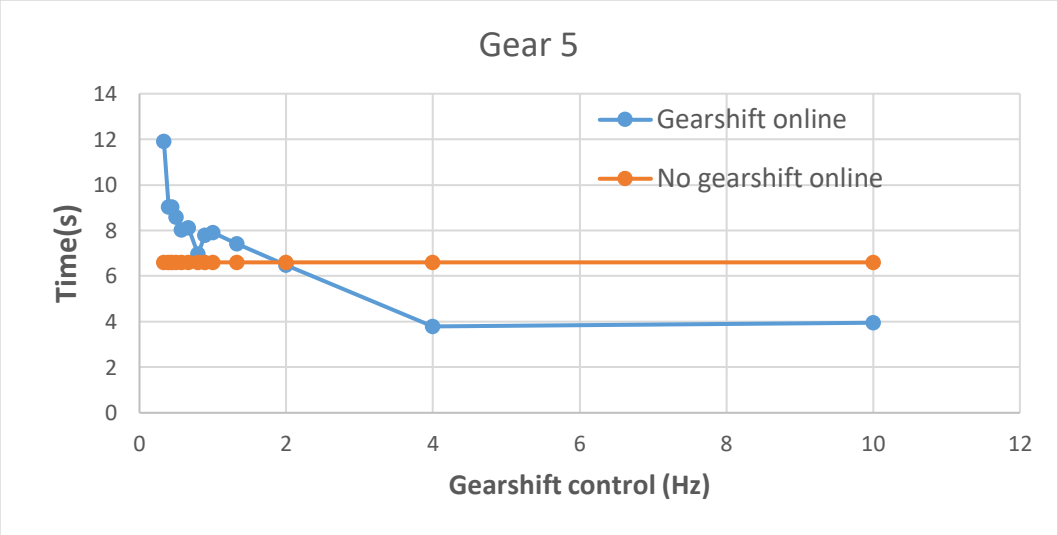

Figure 45: Comparison between two controllers for 5th gear

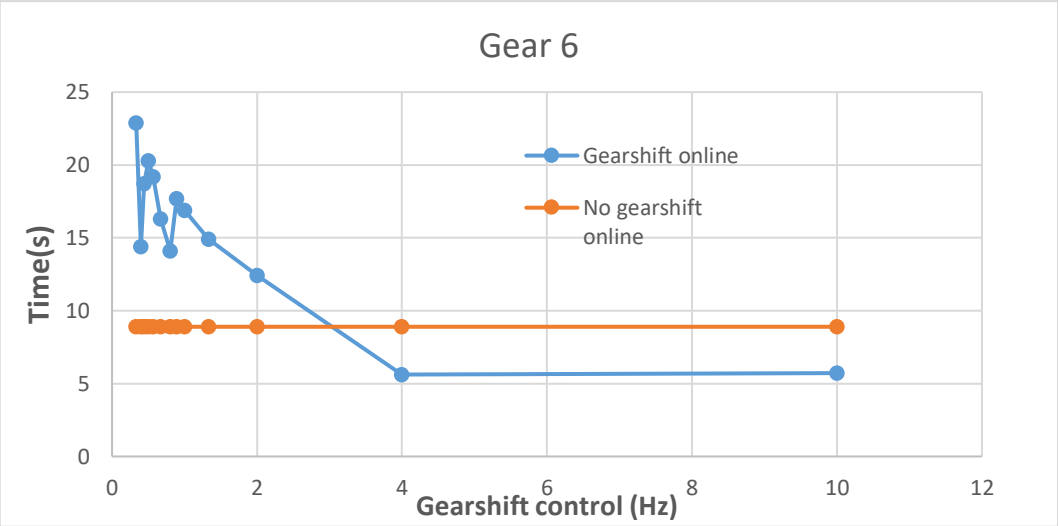

Figure 46: Comparison between two controllers for 6th gear

Analysing fig.42-fig.47 1st and 2nd gear is engaged for a very short time during the driving mission, indeed for all the frequencies the mean values is lower than the mean value related to the strategy with only the A-ECMS. One of the problems related to the gearshift map strategy com was the high number of gearshifts that occur at high speed and it largely reflected in great fluctuations especially of the 5th and 6th gear.

Obviously, frequency influence also the total number of gearshifts along the driving mission as shown in fig.48

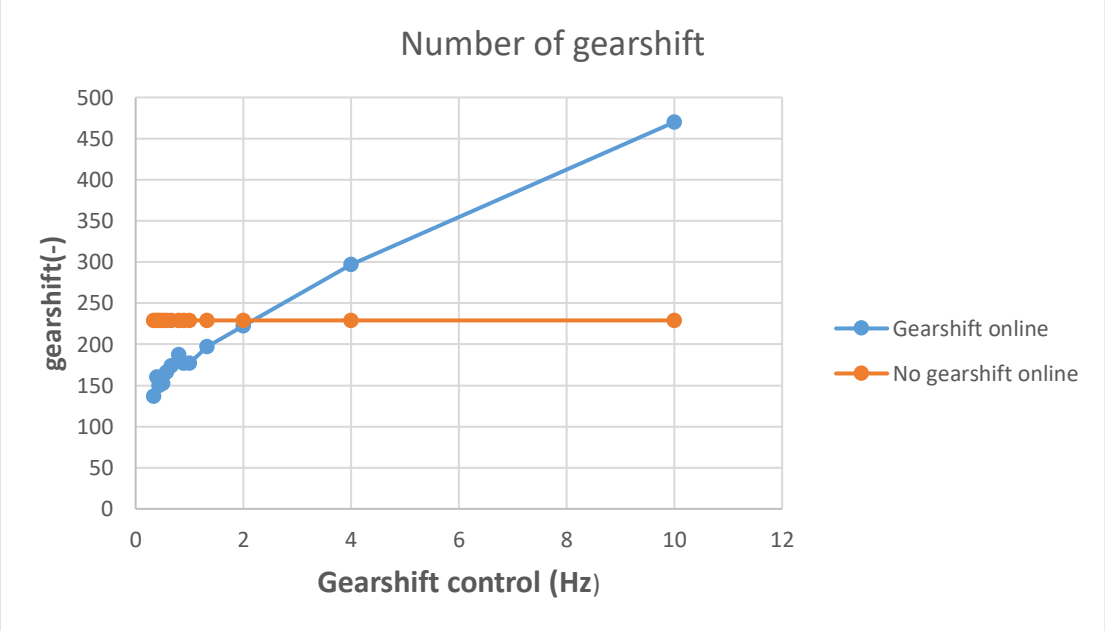

Figure 47: Total gearshift along WLTP for different value of gearshift frequency

The above plot shows that for high frequency values the total number of gearshifts increase because of the achievement of the final target concerning the reduction of

fuel consumption. Instead when the rate transition rises, the evaluation of the actual gear engaged by the motor is delayed so the total number of gearshifts is reduced. As consequence the driveability increase at the cost of fuel consumption. Obviously, the numbers of gearshift along a drive mission is still high, but this situation usually occurs because of the coexistence of a gearshift logic and an energy management controller as underline in [27].

Anyway the best compromise found to satisfy the reduction of fuel consumption and in order to have some benefits also in terms of driveability the value $f = 4\ Hz$ is chosen

6.2 Driveability map

In the energy management controller, a driveability map is implemented, that according to actual vehicle speed and accelerator pedal position evaluates every time the torque request by the vehicle.

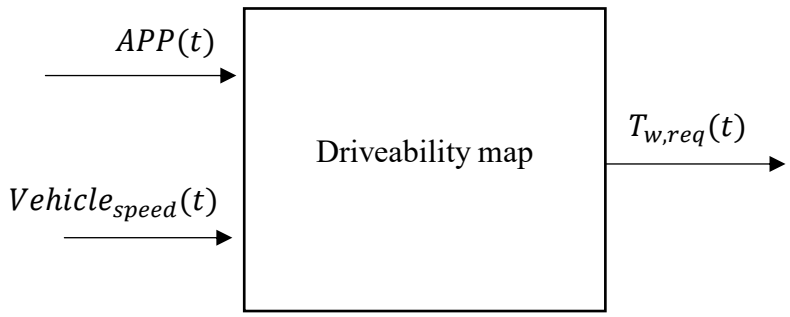

Figure 48:Driveability map

In this hybrid vehicle the wheels torque request is provided by the thermal source and electric one, represented by the P_0 and P_4 motors.

$$T_{w,req} = T_{ICE} i_{AT} + T_{P4} i_{P4} + T_{P0} i_{P0} i_{AT} \quad (56)$$

Concerning the internal combustion engine thanks to the ICE characteristic and the knowledge of gearbox ratios is it possible to find the $T_{w,ICE}$ as function of the vehicle speed and gear, as shown in the following 3D graph.

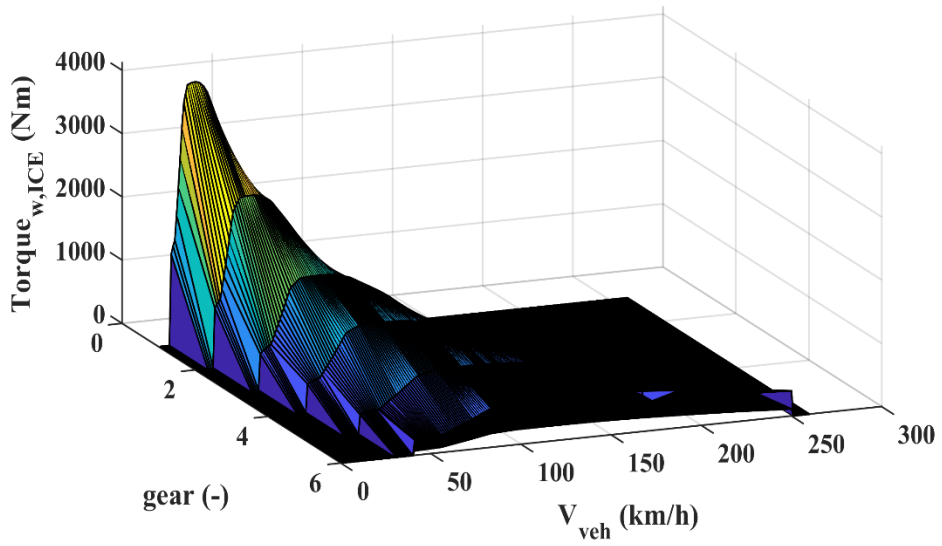

Figure 49:Wheels ICE torque as function of the gear and vehicle speed

The resulting envelope curve has been found considering the maximum and minimum torque that the motors can provided as function of the vehicle speed, so that the torque available at wheels is always known. As consequence:

$$T_{w,ICEmax}(v) = T_{ICEmax}(v)\, i_{AT}$$
$$T_{w,ICEmin}(v) = T_{ICEmin}(v)\, i_{AT} \quad (57)$$

$$T_{w,P4max}(v) = T_{P4max}(v)\, i_{P4}$$
$$T_{w,P4min}(v) = T_{P4min}(v)\, i_{P4} \quad (58)$$

$$T_{w,P0max}(v) = T_{P0max}(v)\, i_{P0} i_{AT}$$
$$T_{w,P0min}(v) = T_{P0min}(v)\, i_{P0} i_{AT} \quad (59)$$

So, the result is:

$$T_{w,reqmax}(v) = T_{w,ICEmax} + T_{w,P4max} + T_{w,P0max} \quad (60)$$

$$T_{w,reqmin}(v) = T_{w,ICEmin} + T_{w,P4min} + T_{w,P0min} \quad (61)$$

Based on the above the following plot is derived that shown the $T_{w,req}$ as function of the accelerator pedal position. Reducing this value, expressed as percentage, the available torque decreases and for APP equal to zero it is possible to find the regeneration curve. This latter condition occurs when the driver release the accelerator pedal and the vehicle starts to break.

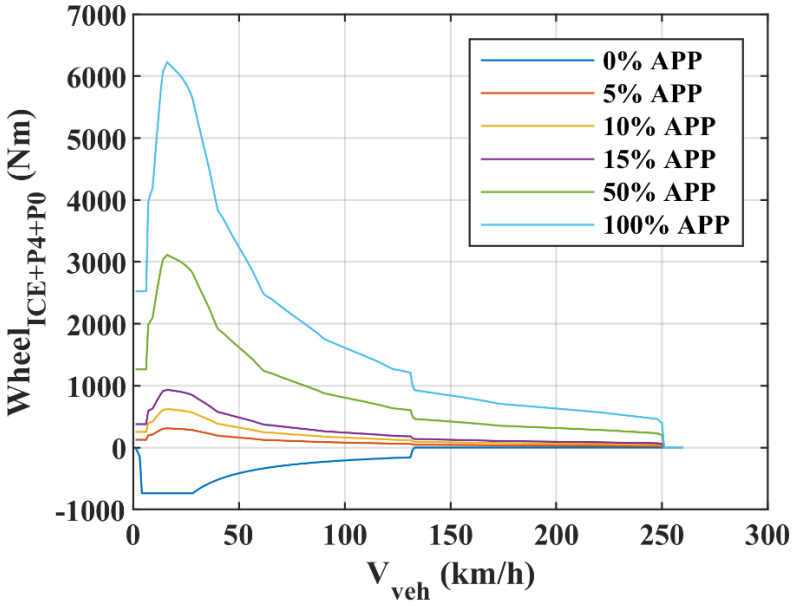

Figure 50: Wheel torque request for different values of accelerator pedal position

6.3 Fuel consumption results

The performance of the ECMS is highly influenced by the s_{chg} and s_{dis} coefficients, as well as the K_{prop} gain, which are used to evaluate the battery SOC equivalent factor, $s(t)$. The tuning, made for NEDC and WLTP, carried out via the co-simulation environment allowed to determine the following values.

Cycle	K_{prop}	s_{chg}	s_{dis}
NEDC	10	2.8	2.8
WLTP	3.6	3.0	3.0

These have been used for all the driving cycles performed in this task. They are the result of a compromise between charge sustainability and performance. WLTP set of values is chosen in al simulations along different type of driving cycles. In this section all results with A-ECMS strategy has been obtained through two different controllers:

- Controller 1= This controller adopts only the A-ECMS algorithm with off-line gearshift map;
- Controller 2= This controller adopts the A-ECMS algorithm with online gearshift logic and actual gearbox efficiency.

At first some significant plots obtained with controller 1 are presented for three different driving cycles

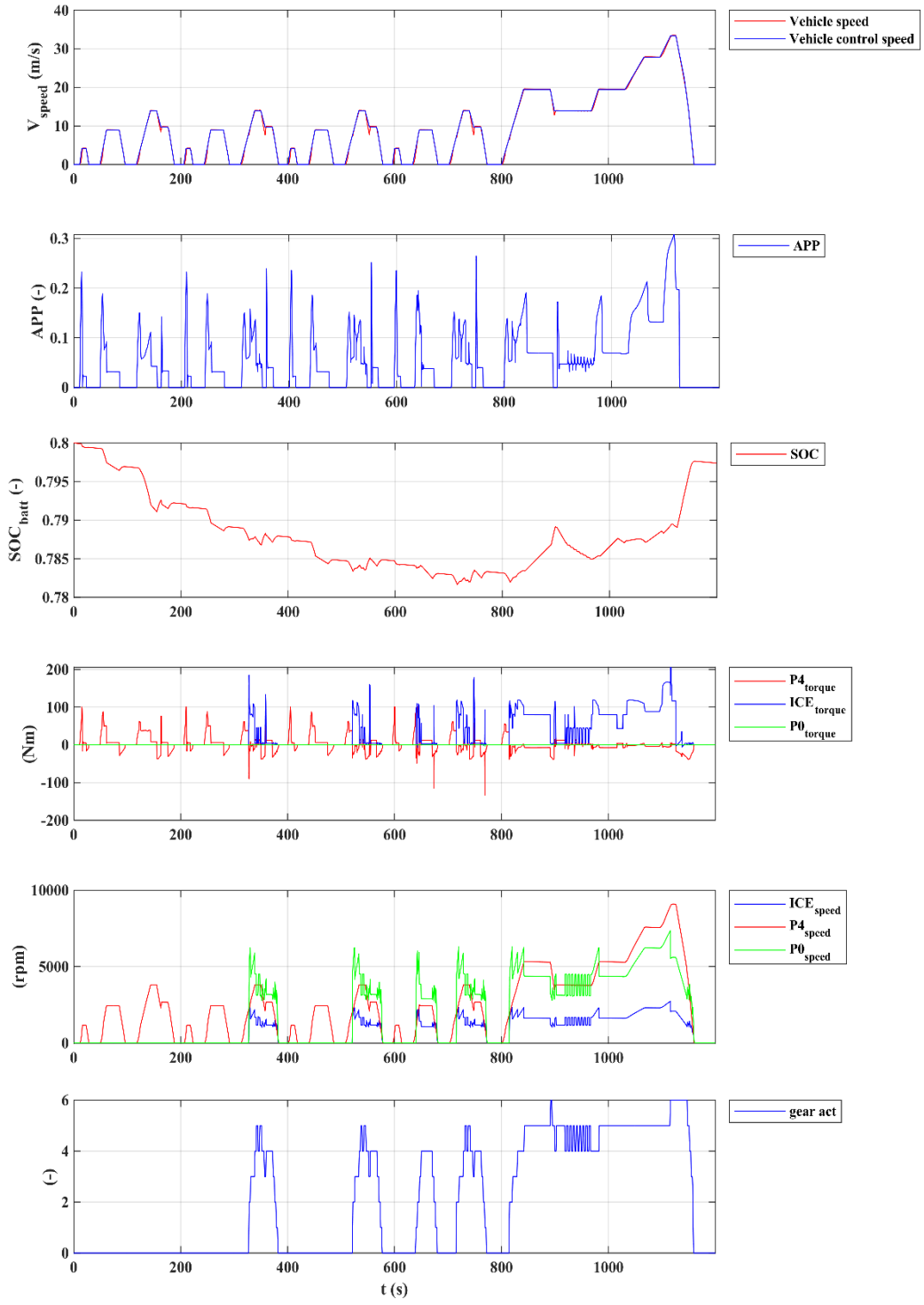

Figure 51:Simulation results of the electrified vehicle demonstrator along the NEDC

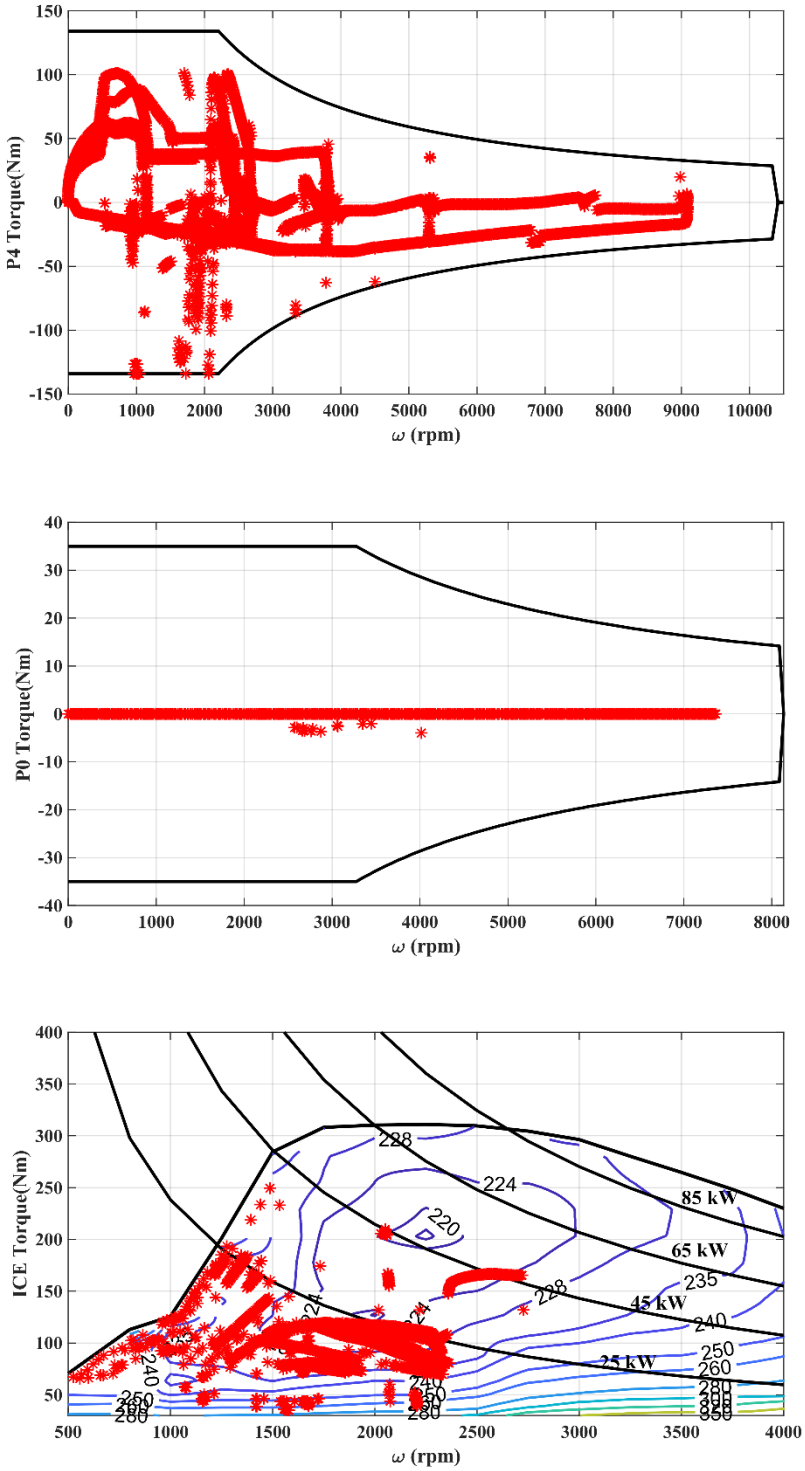

Figure 52: Operating points of a) P4 b) P0 and c) ICE of the electrified vehicle demonstrator along the NEDC

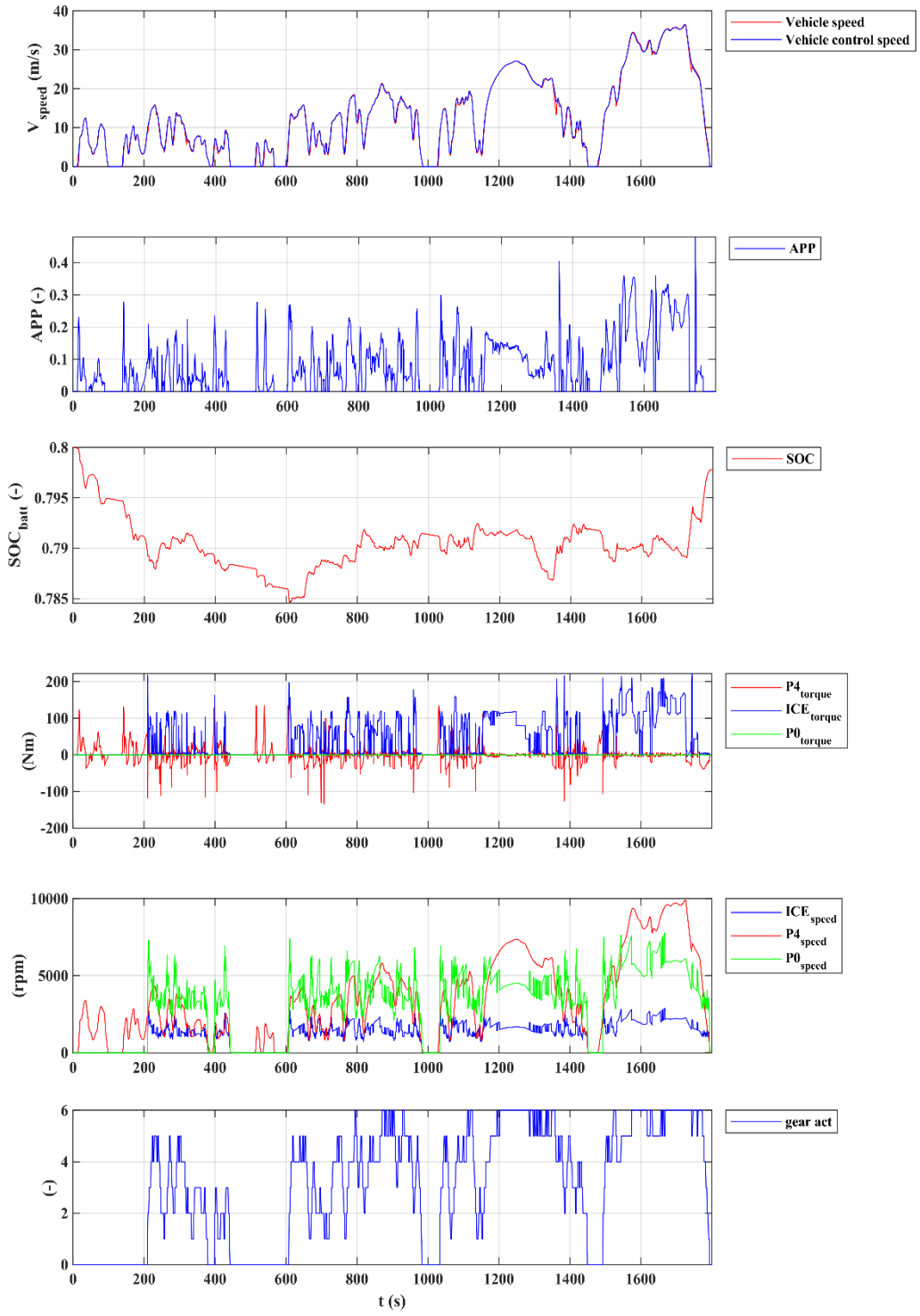

Figure 53: Simulation results of the electrified vehicle demonstrator along WLTP

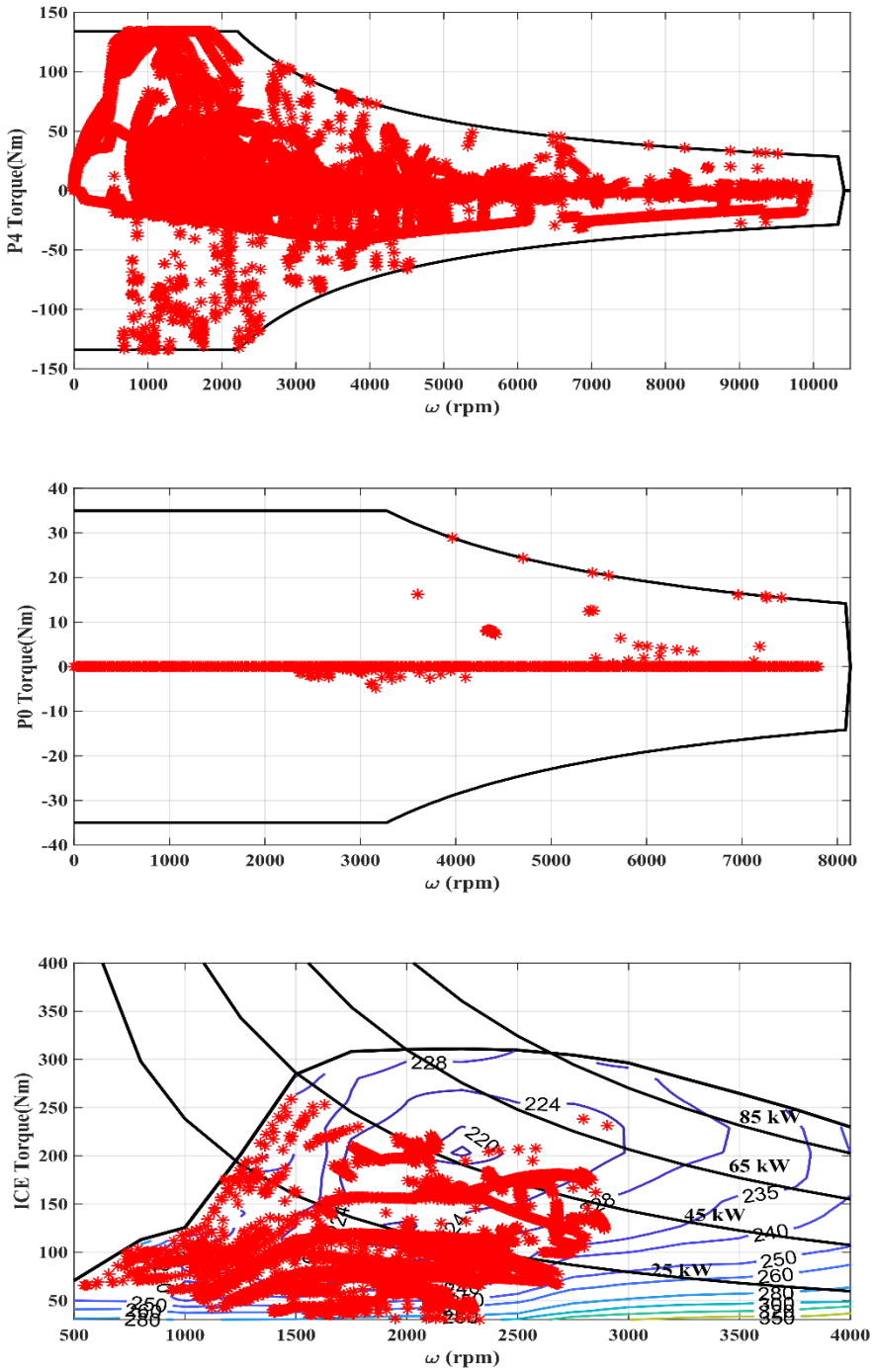

Figure 54: Operating points of a) P4 b) P0 and c) ICE of the electrified vehicle demonstrator along the WLTP

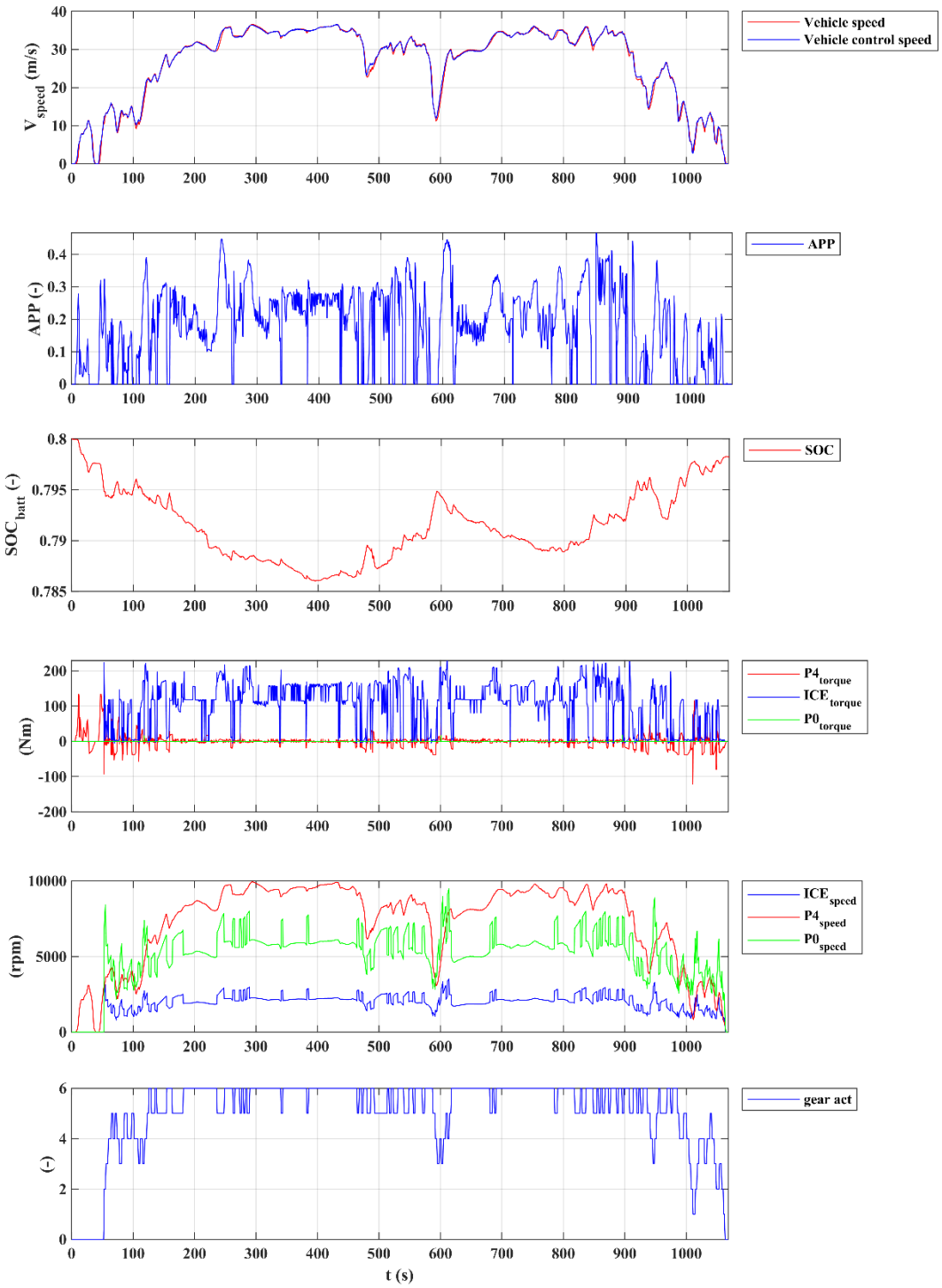

Figure 55: Simulation results of the electrified vehicle demonstrator along ARTEMIS motorway

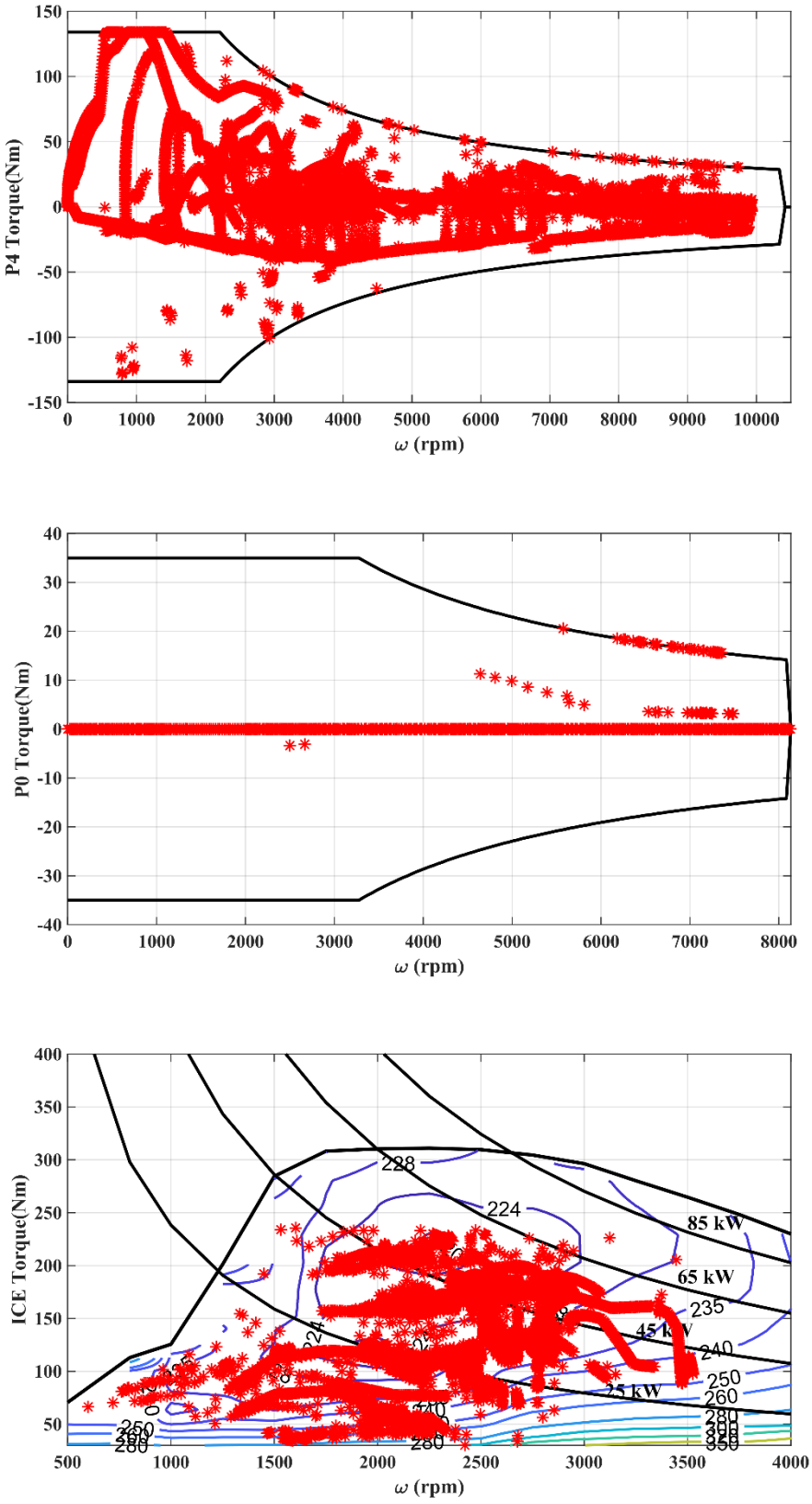

Figure 57: Operating points of a) P4 b) P0 and c) ICE of the electrified vehicle demonstrator along the Artemis motorway cycle

Figure 54- Figure 59 present the time histories of the main vehicle variables along the driving cycles as well as the ICE and motor characteristics together with the operating points. Fig. 54, Fig. 56 and Fig.58 are structured such that:

a) Show the target and the actual vehicle longitudinal speed;
b) Reports the APP signal from the AMESim driver model;
c) Reports the *SOC* profile;
d) Reports the torque provided according to EMS implemented in Matlab/Simulink
e) Shows the engaged AT gear.

In all cycles the SOC trajectory over time stays in the neighbourhoods of the 80%, which is the reference state of charge (SOC_{ref}). This is indeed helped by the high battery capacity, hence the SOC constraints are fulfilled, and the vehicle is charge sustaining. This aspect is also emphasised on the example of driving cycle performed for four repetitions. This is because the value of s is updated at each time step based on the SOC feedback and its deviation from the desired SOC value.

Figure 55, 57 and 58 present the operating points of the ICE, plotted on the efficiency map, and the operating points of the P4 and P0 motors. Thanks to ECMS the ICE operating points are moved towards highest efficiency area to reduce the fuel consumption as shown in the tables with the results. Moreover, the bottom area with lower efficiency would be very poor and the small power request is satisfied by the P4 EM. In fact, it can be noted in the plots how the internal combustion engine is off during the parts on the cycle where low wheel torque is required. This is caused by the moving average filter, which sends a signal to the controller to check if the optimal torque request to the ICE, form the ECMS, is lower than 60 Nm, and switches off the engine accordingly.

During vehicle deceleration the motor operates as a generator and energy is recuperated into the battery. In figure 59 for example is possible to see how the operating points follow the regeneration curve only in some point, this happen due to the limitation done to the regeneration. During the part of the cycle with low torque request, the P4 can provide wheel torque autonomously if the battery state of charge allows it. Eventually, it is interesting to notice the accelerator pedal position trend that means a good behaviour of the driveability map

Table 17: Simulation result comparison along the NEDC

Vehicle model	EMS	Duration (s)	FC (l/100km)	CO_2 (g/km)	SOC_{in} (-)	SOC_{fin} (-)	FC% (%)
Baseline	N/A	1200	6.24	165.1	-	-	-
Electrified in ICE mode	N/A	1200	5.34	141.2	-	-	-14.4%
Electrified	ECMS	1200	4.04	107.0	0.80	0.793	-35.2%

Table 18: Simulation result comparison along the WLTP

Vehicle model	EMS	Duration (s)	FC (l/100km)	CO_2 (g/km)	SOC_{in} (-)	SOC_{fin} (-)	FC% (%)
Baseline	N/A	1800	6.0	159.0	-	-	-
Electrified in ICE mode	N/A	1800	5.82	154.1	-	-	-3.00%
Electrified	ECMS	1800	4.94	130.6	0.80	0.798	-17.8%

Table 19: Simulation result comparison along the Artemis motorway

Vehicle model	EMS	Duration (s)	FC (l/100km)	CO_2 (g/km)	SOC_{in} (-)	SOC_{fin} (-)	FC% (%)
Baseline	N/A	1800	6.26	165.6	-	-	-
Electrified in ICE mode	N/A	1800	6.25	160.1	-	-	-1.6%
Electrified	ECMS	1800	6.06	160.3	0.80	0.798	-3.19%

The simulation results of the different drivetrains are summarised in Table 17 ,18 and Table 19. The obtained fuel consumption (FC) and the corresponding CO_2 emissions are reported; the initial and final battery state of charge are reported as well as the percentage of fuel consumption reduction (FC%) with respect to the original vehicle, which has been obtained as:

$$FC\% = \frac{FC_{vehicle\ model} - FC_{Baseline}}{FC_{Baseline}} * 100$$

Since state of charge final value sometimes is different from the initial value a compensation formula is considered [28]:

$$\Delta fuel = \frac{\Delta SOC * Q_{batt} * \overline{V_{batt}} * \overline{BSFC}}{1000 * \rho} \quad (62)$$

Where:

- $\Delta fuel =$ is the equivalent fuel consumption $[l]$
- ΔSOC= is the variation of battery SOC between the initial and final values
- Q_{batt}= is the capacity of battery $[Ah]$
- $\overline{V_{batt}} =$ is the average value of battery bus voltage during drive cycles [V]
- $\overline{BSFC}$= is the average efficiency value of the engine $[g/kWh]$

ρ = is the density of gasoline $[g/l]$

The following values were considered in this study:

- $\rho = 840 \ g/l$
- $Q_{batt} = 242 \ Ah$
- $\Delta SOC, \overline{V_{batt}}$ and $\overline{BSFC}$ have been acquired by AMESim depending on the cycle.

Based on this consideration the previous table have been updated. In Tab.20 the different vehicles with their respective characteristic are presented

Table 20: Comparison between vehicles used during the simulations

Vehicle model	Weight (kg)	S&S	Gearshift strategy	EMS
Baseline (2.0L)	1696	Yes	Standard	N/A
Electrified in ICE mode (1.6L)	1647	Yes	Custom 2	N/A
Electrified (1.6L)	1647	Yes	Custom 2	A-ECMS

Table 21: Simulation results comparison along NEDC, considering the SOC compensation formula

Vehicle model	Duration (s)	FC (l/100km)	CO_2 (g/km)	SOC_{in}	SOC_{fin}	$FC_{battery}$ (l/100km)	FC_{tot} (l/100km)	FC %
Baseline (2.0L)	1200	6.24	165.1	-	-	-	6.24	-
Electrified in ICE mode (1.6L)	1200	5.34	141.2	-	-	-	5.34	-14.4%
Electrified (1.6L)	1200	4.04	107.4	0.8	0.793	0.142	4.19	-32.8%

Table 22: Simulation results comparison along WLTP, considering the SOC compensation formula

Vehicle model	Duration (s)	FC (l/100km)	CO_2 (g/km)	SOC_{in}	SOC_{fin}	$FC_{battery}$ (l/100km)	FC_{tot} (l/100km)	FC %
Baseline (2.0L)	1800	6.00	159.0	-	-	-	6.00	-
Electrified in ICE mode (1.6L)	1800	5.82	154.1	-	-	-	5.82	-3%
Electrified (1.6L)	1800	4.94	130.7	0.8	0.797	0.042	4.98	-17%

Table 23: Simulation results comparison along ARTEMIS motorway, considering the SOC compensation formula

Vehicle model	Duration (s)	FC (l/100km)	CO_2 (g/km)	SOC_{in}	SOC_{fin}	$FC_{battery}$ (l/100km)	FC_{tot} (l/100km)	FC %
Baseline (2.0L)	1068	6.26	165.6	-	-	-	6.26	-
Electrified in ICE mode (1.6L)	1068	6.25	165.4	-	-	-	6.25	-0.15%
Electrified (1.6L)	1068	6.06	160.3	0.8	0.798	0.026	6.09	-2.7%

6.4 Comparison A-ECMS controller with off-line gearshift map and online gearshift logic with actual gearbox efficiency

Chosen parameters regarding the controller with online gearbox strategy and actual efficiency, thanks to the previous tuning, some simulations have been performed in order to compare the behaviour of the two controllers. This analysis tries to focus on the importance of the actual gearbox efficiency, that in the other controller was neglected. For this reason, ICE operating points for each gear have been displayed on the engine efficiency map. In the next figure results obtained along the WLTP are shown. Through the upgrade of the efficiencies look-up table in the controller the aim is to move the engine operating points towards areas characterized by higher efficiency value, indeed the strategy knows instantly how much the energy loss through the transmission is, so it can make the best decision to compensate this.

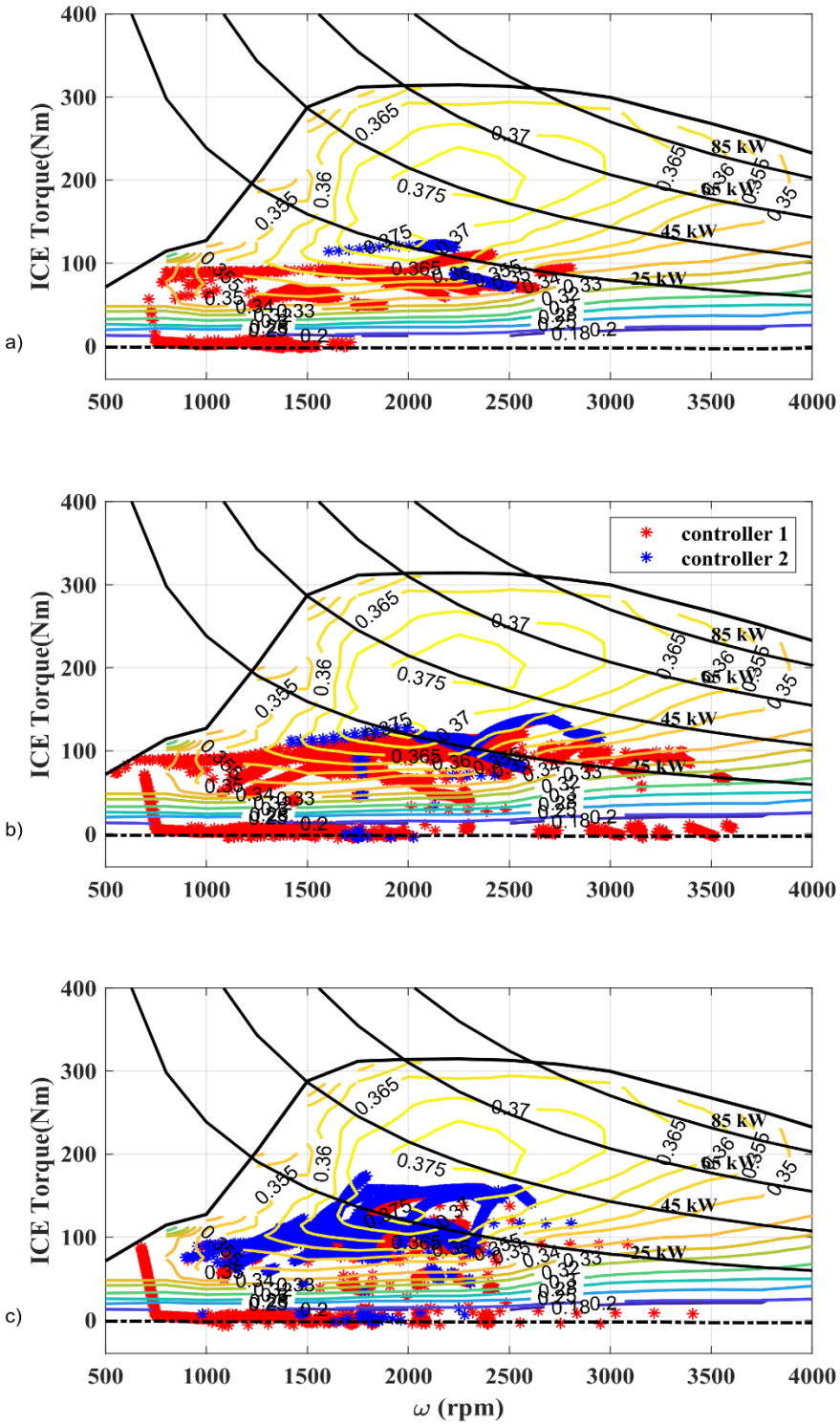

Figure 58:Operating points of a) 1st gear b) 2nd gear c) 3rd gear along WLTP

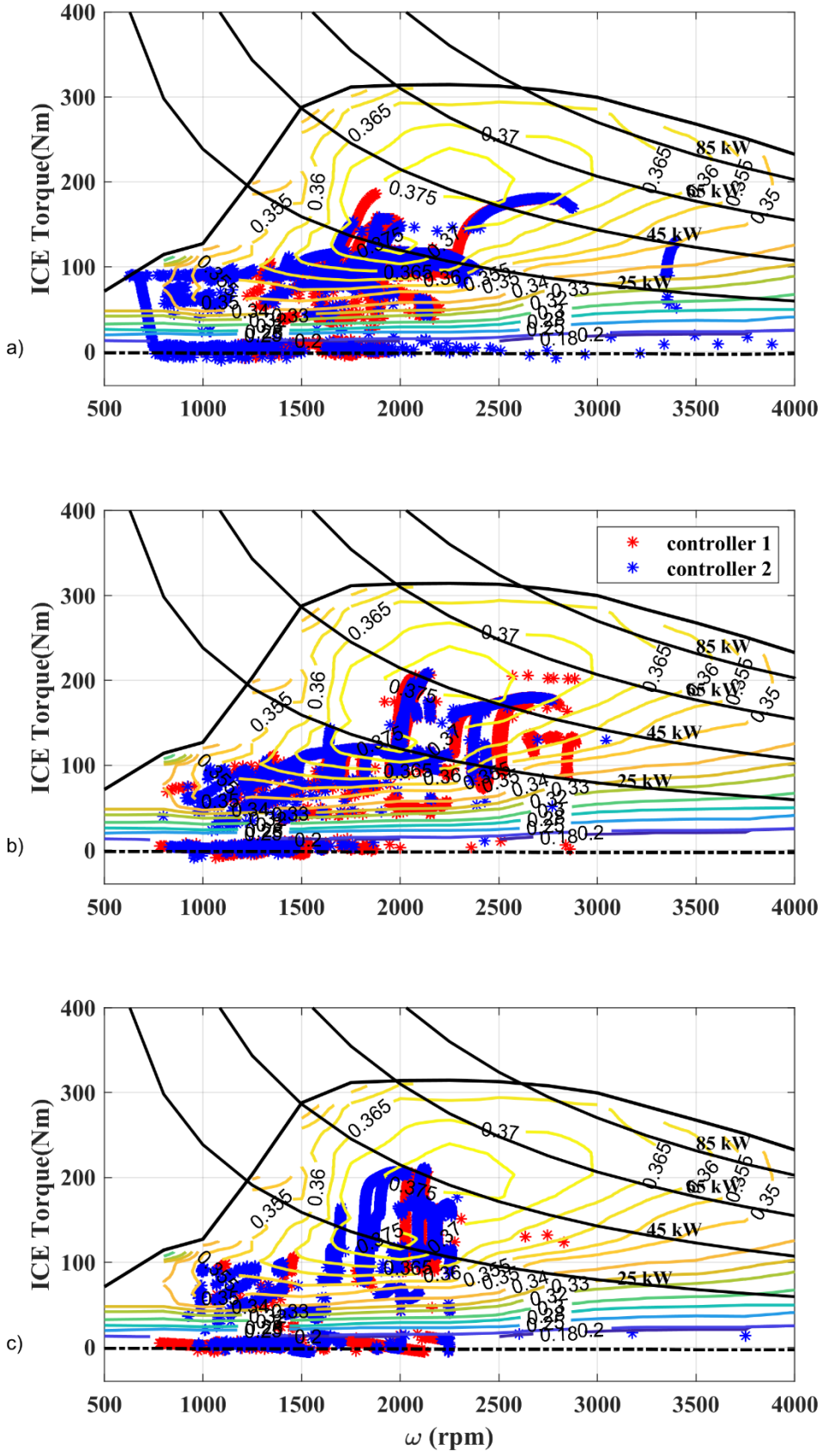

Figure 59: Operating points of a) 4th gear b) 5th gear c) 6th gear along WLTP

Fig.60 and Fig.61 shows that the controller 2 leads benefits in terms of efficiency mainly for the 1st, 2nd and 3rd gear where the engine operating points moves where the efficiency is higher. On the contrary the behaviour of the other gears is essentially the same for the two controllers. In fact, concerning the 5th and 6th gears the benefits of the controller 2 are linked to the reduction of fluctuations at high speed, as evidenced by the increase mean time of engagement for these two gears. Any way the advantages are highlighted by the mean values of efficiency for the engine and for the transmission along the drive mission.

Table 24:Efficiency comparison between the two controllers along WLTP

Controller	$\overline{\eta}_{ICE}$	$\overline{\eta}_{AT}$	$\overline{\eta}_{tot}$
Controller 1	0.346	0.74	0.255
Controller 2	0.353	0.75	0.265

Table 25: Efficiency comparison between the two controllers along NEDC

Controller	$\overline{\eta}_{ICE}$	$\overline{\eta}_{AT}$	$\overline{\eta}_{tot}$
Controller 1	0.345	0.745	0.257
Controller 2	0.35	0.745	0.265

Table 26: Efficiency comparison between the two controllers along ARTEMIS motorway

Controller	$\overline{\eta}_{ICE}$	$\overline{\eta}_{AT}$	$\overline{\eta}_{tot}$
Controller 1	0.360	0.783	0.286
Controller 2	0.361	0.779	0.287

In above tables results for other driving cycles are provided. Anyway, other simulations have been done to investigate the two controller's behaviour especially in terms of fuel consumption and driveability. Therefore, in the following plots the main variables of the vehicle are shown.

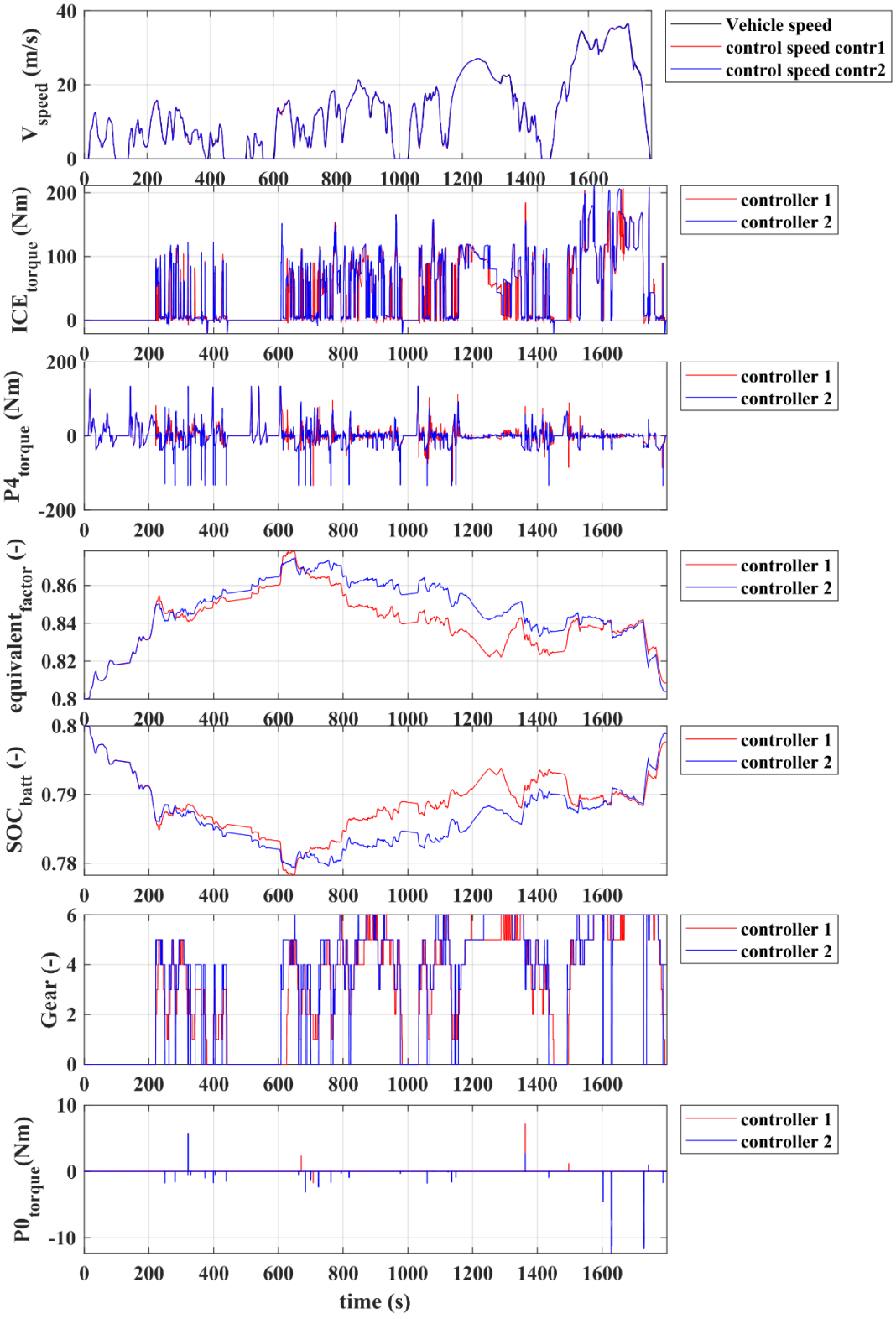

Figure 60: Comparison between two controllers along WLTP

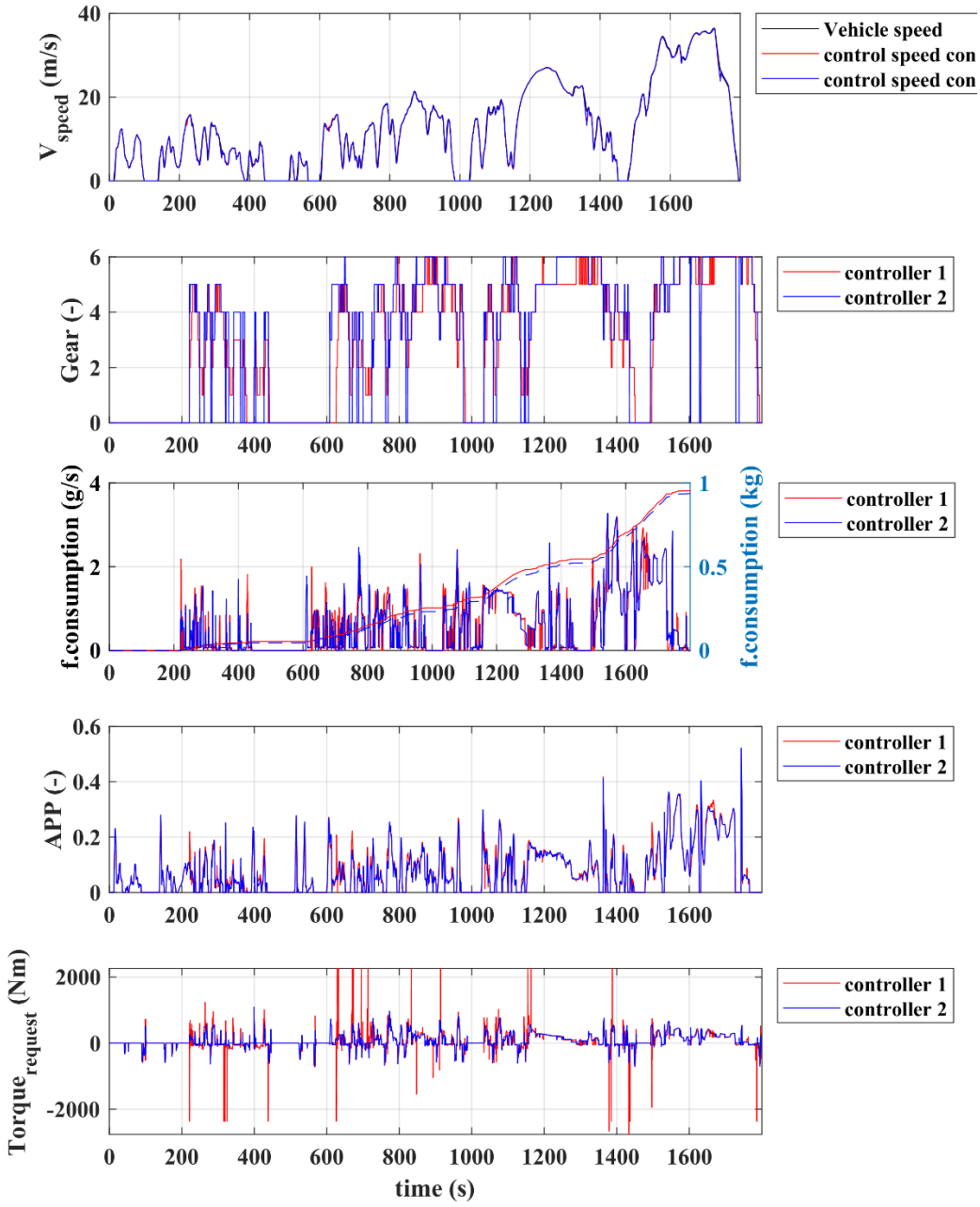

Figure 61: Comparison between two controllers along WLTP

Fig 60 and Fig 61 show how the two controllers have the same behaviour in terms of APP, vehicle speed tracking and concerning the battery state of charge. Indeed, in both situations the strategy is charge sustaining, thus the SOC remains around the reference value and at the end of cycle recovers the initial value. The differences regarding especially the fuel consumption. So, in Fig.61 the actual fuel consumption and total fuel consumption are shown, which reveal that there is a reduction in terms of fuel consumption in the controller with gearshift logic and efficiency as will be shown in the following tables. This difference has been

investigated also through the evaluation of the total energy used by the engine and two motors.

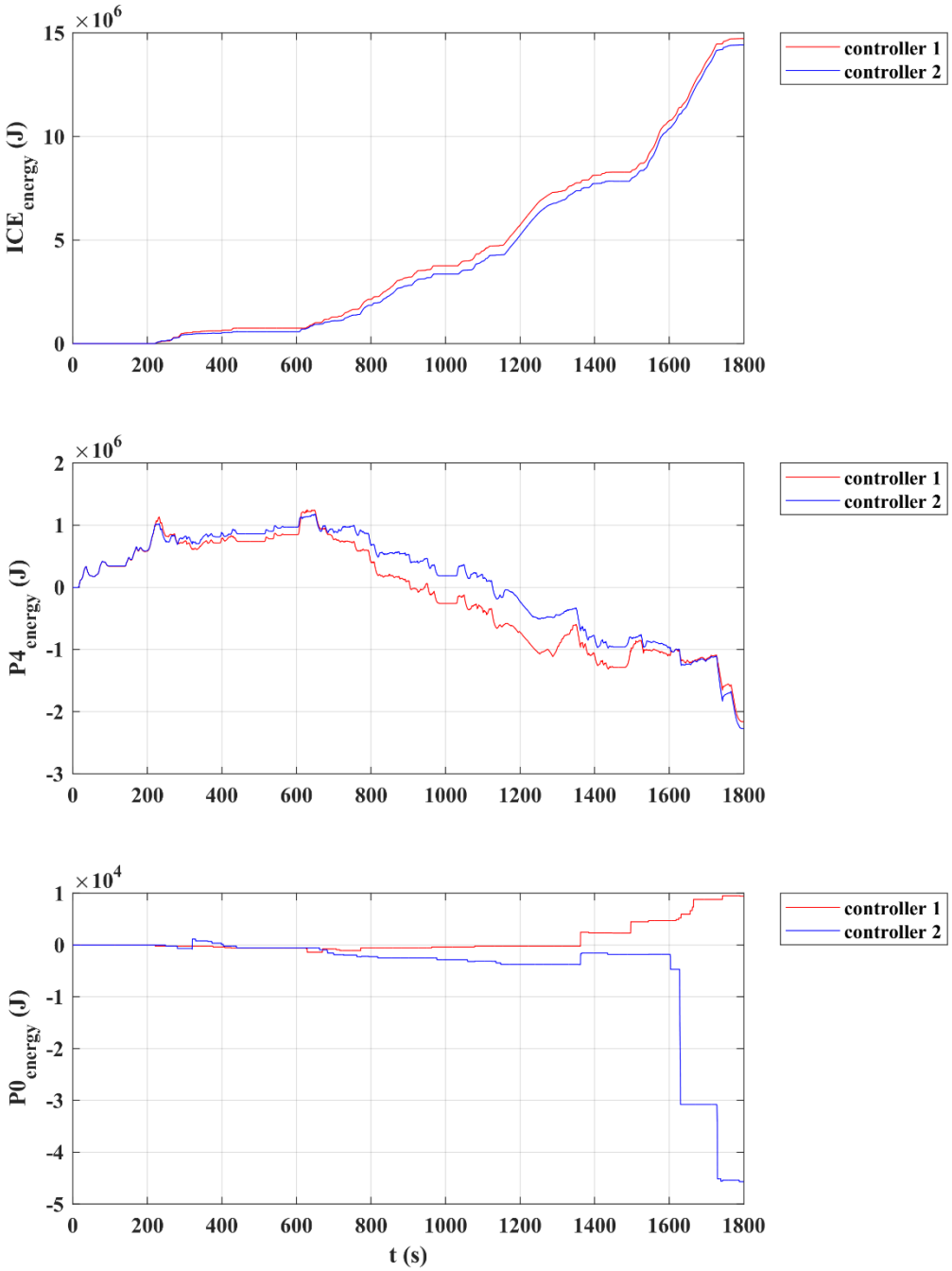

Figure 62:Energy comparison between two controllers

This figure confirms what said before, focusing on ICE energy the fact that in controller 2 the energy spent to complete the same drive mission is lower means that the engine consumed less. Other difference between the two controllers is linked to the gear trend because of the two different strategy used. Despite the number of gearshifts is still high because the strategy is developed to achieve the

fuel economy along WLTP there is a reduction in this number mainly because the lack of fluctuation between the 5th and 6th gear. This is underline in the next plot where the range between 1240 and 1360 s.

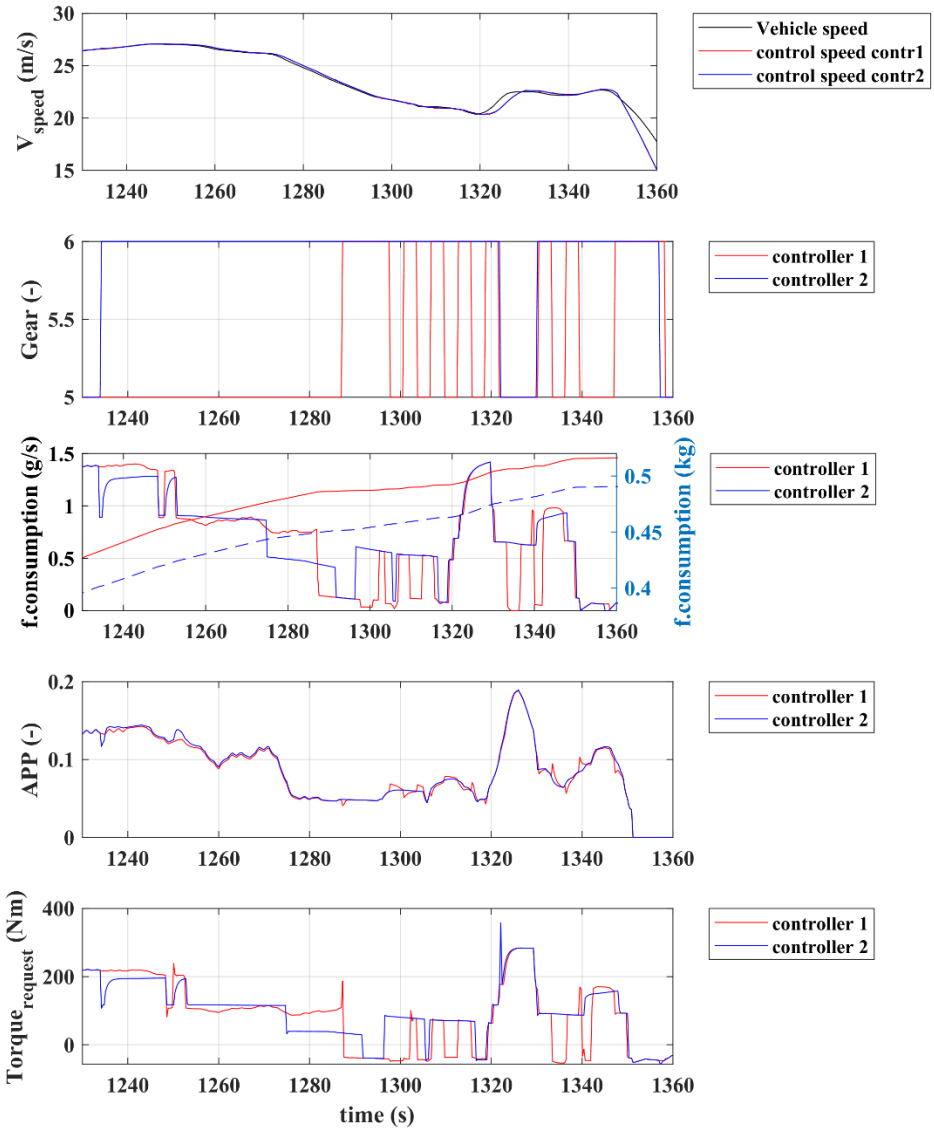

Figure 63:Magnified view of gearshift fluctuations along WLTP

In Fig.63 the reduction of fluctuations at high speed is evident, this is possible to notice also by the increase of mean engaged time per 5th and 6th gear. It is interesting to notice this advantage also in the NEDC cycle. In this case the reduction of fluctuations concerns the upshifts and downshifts between 5th and 4th gear. This analysis has been done considering the range between 900 and 970 s

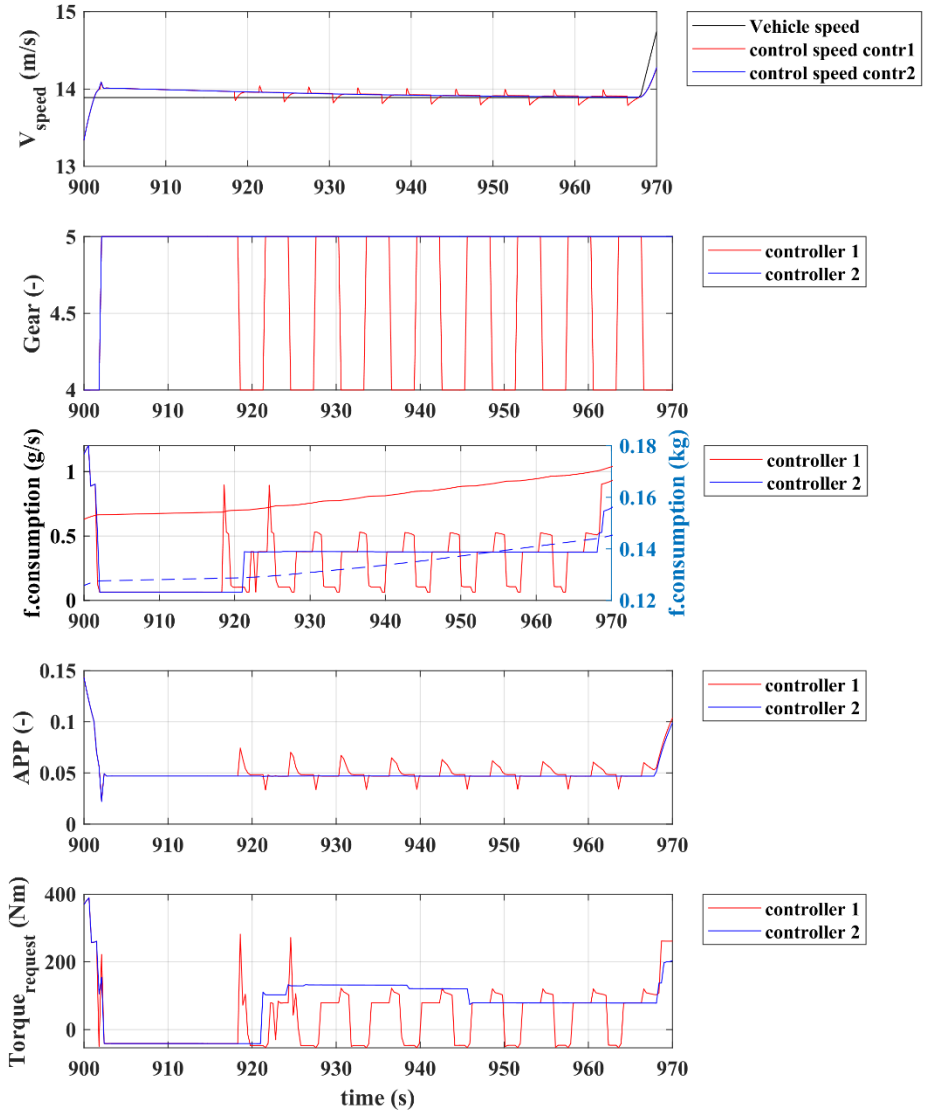

Figure 64: Magnified view of gearshift fluctuations along NEDC

In the figure above all fluctuations caused by the fluctuations of torque request and accelerator pedal position are deleted in the controller with online gearshift logic. All these considerations are summarized in next tables where the two controllers are compared for different driving cycles.

Table 27: Comparison between electrified vehicles with different controllers

Vehicle model	Weight (kg)	S&S	Gearshift strategy	EMS
Electrified (1.6L)	1647	Yes	Gearshift map	A-ECMS
Electrified (1.6L)	1647	Yes	Online logic	A-ECMS+efficiency

Table 28: Simulation results comparison along different driving cycles, considering the SOC compensation formula

Cycle	EMS	Duration (s)	FC (l/100km)	CO2 (g/km)	SOCin (-)	SOCfin (-)	$FC_{battery}$ (l/100km)	FC_{tot} (l/100km)	FC% (%)
WLTP	Controller 1	1800	4.94	130.65	0.80	0.797	0.042	4.98	-
WLTP	Controller 2	1800	4.86	128.5	0.80	0.798	0.021	4.88	-2.07%
NEDC	Controller 1	1200	4.04	107.4	0.80	0.793	0.142	4.19	-
NEDC	Controller 2	1200	3.95	104.5	0.80	0.793	0.140	4.09	-2.38%
JC08	Controller 1	1204	3.42	90.6	0.80	0.782	0.605	4.03	-
JC08	Controller 2	1204	3.35	82.9	0.80	0.781	0.772	3.91	-4.03%
FTP75	Controller 1	1877	4.39	116.2	0.80	0.787	0.260	4.65	-
FTP75	Controller 2	1877	3.90	103.1	0.80	0.780	0.485	4.57	-1.75%
ARTEMIS urban	Controller 1	993	3.41	90.2	0.80	0.781	0.900	4.79	-
ARTEMIS urban	Controller 2	993	4.39	119.5	0.80	0.778	1.04	4.46	-6.86%
ARTEMIS rural	Controller 1	1082	4.52	116.8	0.80	0.794	0.149	4.67	-
ARTEMIS rural	Controller 2	1082	4.42	120.1	0.80	0.793	0.179	4.59	-1.54%
ARTEMIS HW 130	Controller 1	1068	6.06	160.3	0.80	0.798	0.026	6.09	-
ARTEMIS HW 130	Controller 2	1068	6.00	158.8	0.80	0.795	0.074	6.08	-0.11%
US06	Controller 1	600	5.87	155.2	0.80	0.791	0.275	6.14	-
US06	Controller 2	600	5.91	156.5	0.80	0.795	0.131	6.05	-1.54%

Table 28 shows how in all driving cycles performed there is a reduction in terms of fuel consumption.

6.5 Acceleration test

The acceleration performance of the vehicle with the implemented EMS has been evaluated in terms of 0 – 100 km/h, 40-100 km/h, 80-120 km/h and 0-1000 m acceleration times, for a 100% APP signal. The time histories of the relevant vehicle variables are reported in Fig. 45 and Fig. 46. The results are summarised in Table 29. The results on the hybrid vehicle are the same for the two controllers, since the performance depends by the power installed on vehicle.

Table 29: Simulation results on acceleration tests for the different vehicle drivetrains.

Vehicle model	0 – 100 km/h (s)	40 – 100 km/h (s)	80 – 120 km/h (s)	0 – 1000 m (s)
Baseline	9.0	6.3	6.7	30.02
Electrified in ICE mode	9.9	7.5	7.3	31.1
Electrified	7.3	5.6	5.5	28.72

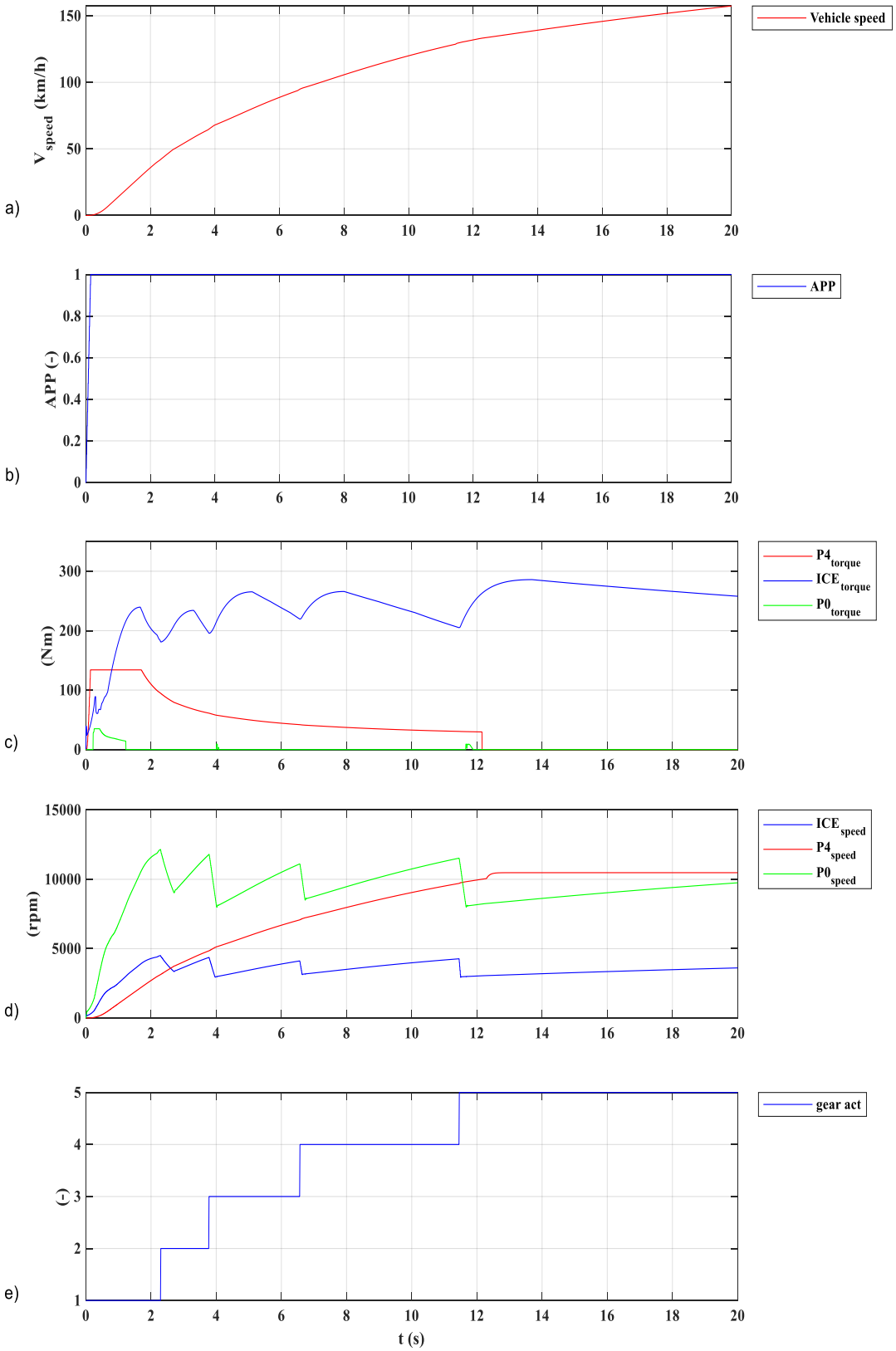

Figure 65: Acceleration test of the electrified vehicle demonstrator

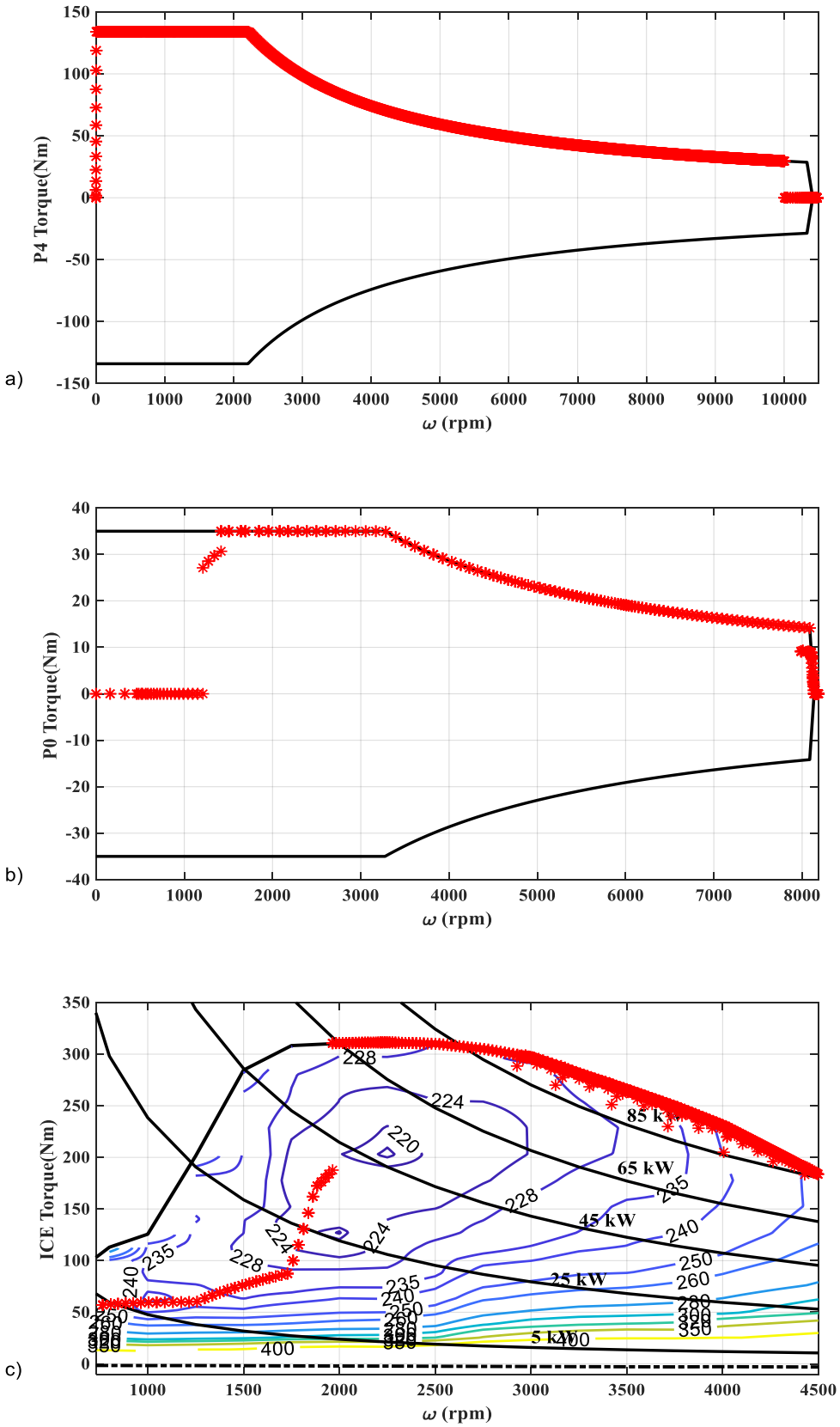

Figure 66: Operating points of a) P4 b) P0 and c) ICE of the electrified vehicle demonstrator on the accelerations test

The images above show how all the power available is exploit since for ICE, P4 and P0 all the operating points are on the upper limits of their characteristics.

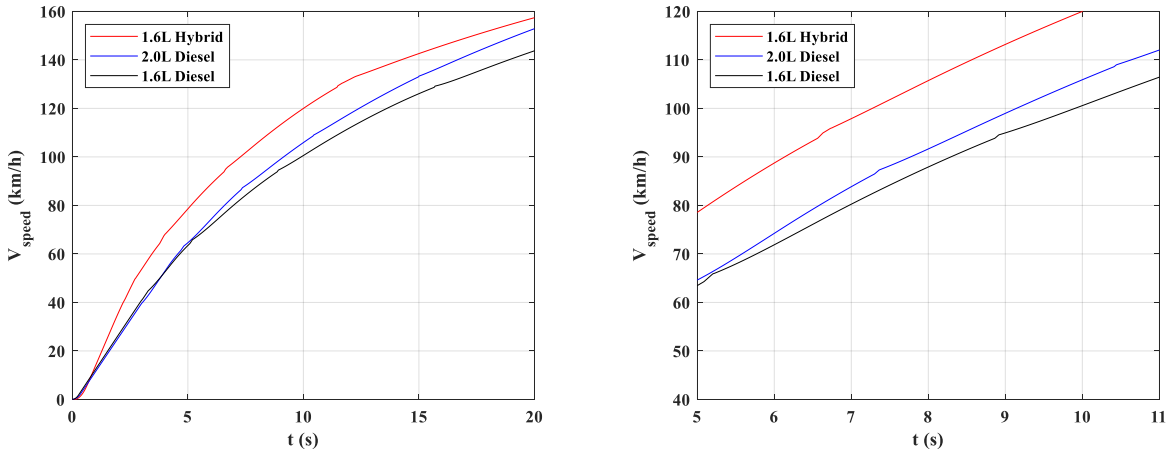

Figure 67: Comparison among different vehicles on 0 – 100 km/h acceleration test: a) time history of the vehicle speed; b) magnified view of the vehicle speed.

Table 29 summarizes the simulation results obtained by the vehicle equipped with the different drivetrains for the four manoeuvres. The best performance is obtained by the electrified vehicle demonstrator. Its acceleration time are: 7.3 s, 5.6 s, 5.5 s and 28.72 s on 0-100 km/h, 40-100 km/h, 80-120 km/h, and 0-1000 m tests. On the contrary, the electrified vehicle demonstrator in the ICE mode presents the worst performance among the three drivelines because of the lower power of the engine. These results show an improvement of the longitudinal vehicle acceleration performance of the hybrid drivetrain with a consisted reduction of the time needed to reach the target value. The improvement is of 18.8%, 12.5%, 17.91% and 4.33%.

6.6 Fully electric tests

The fully electric vehicle (FEV) mode completes the set of simulations of the hybridised vehicle. More specifically, simulations were run with the vehicle demonstrator model along two driving cycles (NEDC and WLTP) as well as at constant speed, considering only the P4 electric motor providing traction power. Table 30 shows the simulation results for the FEV on the NEDC and WLTP. The fully electric vehicle autonomy is as high as 78 km on the NEDC, while it decreases to 64 km on the WLTP. This is caused by the higher power request profile of the WLTP. In the high-speed parts of the driving cycles the vehicle in fully electric mode is not able to perfectly track the speed profile because of the torque limitation of the P4 electric motor. Table 31 contains the simulations results of the electrified

vehicle at constant speed manoeuvres (10, 20, 40, 60, and 80 km/h). As expected, the electric autonomy decreases with vehicle speed and it ranges between the approx. 61 km and 183 km for the higher and lower target speed respectively.

Table 30: Simulation results of the electric vehicle in fully electric mode

Driving cycle	SOC_{in} (-)	Specific battery consumption (kWh/km)	FEV autonomy (km)
NEDC	1	0.148	78
WLTP	1	0.180	64

Table 31: Simulation results of the electric vehicle in fully electric mode at constant vehicle speed

Constant speed (km/h)	SOC_{in} (-)	Specific battery consumption (kWh/km)	FEV autonomy (km)
10	1	0.063	183
20	1	0.081	144
40	1	0.120	101
60	1	0.152	76
80	1	0.190	61

7. Conclusions

The beginning of this work focuses on an update of a previous model with the integration of stop/start strategy and varying gearbox efficiencies. Successively, it discusses the development of the powertrain manager in charge of the optimal coordination of the hybrid electric vehicle components. Emphasis has been given to the optimal torque split between the internal combustion engine and the electrical components. The downsized baseline vehicle has been equipped with a motor generator unit in P0 position and with an electric motor in P4 position that can provide traction to the rear axle. In order to obtain a reduction in terms of fuel consumption of the hybridized drivetrain, the adaptive equivalent consumption minimisation strategy (A-ECMS) has been proposed, since it has real-time capabilities. Its performance has been assessed through a co-simulation platform realised through the integration of the vehicle model implemented on AMESim and Simulink model containing the energy management algorithm. In addition, two controllers with energy management strategy have been proposed. On the one hand, the first one is characterized by a gearshift logic based on an off-line optimal gearshift map, while on the other, in the second one an online gearshift logic is implemented that, according also to the information concerning the actual gearbox efficiency, can instantly choose the gear engaged by the transmission in order to have minimum brake specific fuel consumption (BSFC).

Different simulation scenarios have been utilised in co-simulation to assess the controller' performance. Based on the simulations run on the WLTP, the beneficial effects of energy management strategy combined with ICE downsizing and the hybridization of the baseline vehicle are demonstrated with a reduction that varies between 3.00% with the electrified vehicle in ICE mode and off-line gearshift map optimization and approx. 17.8% and 18.7% with the hybrid driveline equipped with controller 1 and controller 2 respectively. The improvement in terms of fuel economy is achieved through the online gearshift logic with actual efficiency that every time considers the actual power loss by the transmission thanks to six look-up table implemented in the controller. As highlighted by previous plots, the controller tries to move ICE operating points toward higher efficiency. It interesting to underline how the updated controller shows a reduction in terms of fuel economy in all driving cycle tested. Furthermore, for low speed cycles, the newly found

reduction in gears fluctuations guarantees an improvement concerning the vehicle driveability.

The energy management strategy has been tested along acceleration tests to assess the acceleration performance of the electrified vehicle demonstrator. The test shows that the best performances are obtained thanks to the two electric motors, since they provide the hybrid vehicle with a better acceleration. Indeed, there is an improvement of 18.8%, 12.5%, 17.91% and 4.33% in comparison with the baseline vehicle for the four manoeuvres done. Instead, as expected, the electrified vehicle in ICE mode.

A complete overview of the vehicle's performance has been achieved through simulation runs in fully electric mode that show that specific energy consumption of the battery is approx. 0.15 kWh/km and 0.18kWh/km on NEDC and WLTP respectively. This means that the estimated autonomy of the battery ranges between 64 and 78 km depending on the selected driving cycle.

On the whole, the main goal of this work has been the reduction of fuel consumption. Nevertheless, some issues might be identified in regard to the actual vehicle's driveability, especially concerning the high number of gearshifts that occur along a drive mission, which could make the implementation of this controller more difficult on a real vehicle. For that reason, the driver could be subjected to frequent fluctuations. Therefore, the development of a filter to add could be a good prosecution of this work

8. Riferimenti

[1] K. Ç. Bayindir, M. A. Gözüküçük, and A. Teke, "A comprehensive overview of hybrid electric vehicle: Powertrain configurations,powertrain control techniques and electronic control units," *Elsevier,* p. 9, 2011.

[2] D. Doni, «Development and implementation in Amesim of the Model Predictvie Control for the energy management of a HEV,» 2014.

[3] I. R. Leikarnes, «Modelling and Simulating a Hybrid Electric Vehicle,» June 2017.

[4] H. Borhan, A. Vahidi, A. M. Phillips, M. L. Kuang, I. V. Kolmanovsky e S. Di Cairano, «MPC-Based Energy Management of a Power-Split Hybrid Electric Vehicle,» *IEEE,* 2012.

[5] E. Galvagno, D. Morina, A. Sorniotti e M. Velardocchia, «Drivability analysis of through-the-road-parallel hybrid vehicles,» *Meccanica,* 2013.

[6] G. Rizzo, M. Sorrentino e I. Arsie, «Optimal Design and Dynamic Simulation of a Hybrid Solar Vehicle,» *SAE international,* 2006.

[7] Y. Jun, B. C. Jeon e W. Youn, «Equivalent Consumption Minimization Strategy for Mild Hybrid Electric Vehicles with a Belt Driven Motor,» *SAE international,* 2017.

[8] K. T. Chau e Y. S. Wong, «Overview of power management in hybrid electric vehicles,» *Elsevier,* 2002.

[9] L. Serrao, S. Onori e G. Rizzoni, «A Comparative Analysis of Energy Management Strategies for Hybrid Electric Vehicles,» *ASME,* p. 9, 2011.

[10] A. Sciarretta e L. Guzzella, «Control of Hybrid Electric Vehicles,» *IEEE,* 2007.

[11] M. Koot, J. Kessels, B. de Jager, W. Heemels, P. van den Bosch e M. Steinbuch, «Energy Management Strategies for Vehicular Electric Power Systems,» *IEEE,* 2005.

[12] C.-C. Lin, H. Peng, J. W. Grizzle e J.-M. Kang, «Power Management Strategy for a Parallel Hybrid Electric Truck,» *IEEE,* 2003.

[13] B. Asadi e A. Vahidi, «Predictive Cruise Control: Utilizing Upcoming Traffic Signal Information for Improving Fuel Economy and Reducing Trip Time,» *IEEE.*

[14] T. Hofman e M. Steinbuch, «Rule-based energy management strategies for hybrid vehicles,» *Elsevier,* 2007.

[15] Y. Yang, X. Hu, H. Pei e Z. Peng, «Comparison of power-split and parallel hybrid powertrain architectures with a single electric machine: Dynamic programming approach,» *ELSEVIER.*

[16] C. Musardo e B. Staccia, «ENERGY MANAGEMENT STRATEGIES FOR HYBRID ELECTRIC VEHICLES,» 2003.

[17] C. Musardo, G. Rizzoni, Y. Guezennec e B. Staccia, «A-ECMS: An Adaptive Algorithm for Hybrid Electric Vehicle Energy Management,» *Elsevier,* 2005.

[18] «Comparison of NIMH and Li-ion Batteries in Automotive Applications,» *IEEE,* 2008.

[19] L. Zeng e Z. Zhao, «An Optimized Energy Management Strategy of 48V Mild Hybrid Electrical Vehicle to Reduce Fuel Consumption,» *DEStech Transactions on Materials Science and Engineering,* 2016.

[20] A. Abdellahi, S. K. Rahimian, B. Blizanac e B. Sisk, «Exploring the Opportunity Space For High-Power Li-Ion Batteries in Next-Generation 48V Mild Hybrid Electric in Next-Generation 48V Mild Hybrid Electric,» *SAE international,* 2017.

[21] K. Adachi, Y. Ochi, S. Segawa e A. Higashimata, «Slip Control for a Lock-up Clutch with a Robust Control Method,» in *SICE Annual Conference in Sapporo*, 2004.

[22] R. Di Palo, «Gearshift Strategies for Through The Road Paralle Hybrid Electric Vehicle».

[23] L. Guzzella e A. Sciarretta, Vehicle Propulsion Systems, Springer.

[24] D. F. Opila, X. Wang, R. McGee, R. B. Gillespie, J. A. Cook e J. W. Grizzle, «An Energy Management Controller to Optimally Trade Off Fuel Economy and Drivability for Hybrid Vehicles,» *IEEE,* 2012.

[25] «Optimization of Gear Shifting and Torque Split forImproved Fuel Efficiency and Drivability of HEVs,» *SAE international,* 2013.

[26] D. F. Opila, D. Aswani, R. McGee, A. J. Cook e J. W. Grizzle, «Incorporating Drivability Metrics into Optimal Energy Management Strategies for Hybrid Vehicles,» *IEEE,* 2008.

[27] P. Pisu, K. Koprubasi e G. Rizzoni, «Energy Management and Drivability Control Problems for Hybrid Electric Vehicles,» *IEEE,* 2005.

[28] Y. Liu, J. Li, M. Ye, D. Qin, Y. Zhang e Z. Lei, «Optimal Energy Management Strategy for a Plug-in Hybrid Electric Vehicle Based on Road Grade Information,» *Energies,* 2017.

[29] Z. Lu, J. Song, H. Yuan e L. Shen, «MPC-Based Torque Distribution Strategy for Energy Management of Power-Split Hybrid Electric Vehicles,» *IEEE,* 2013.